FLOW PATTERN AND RESIDENCE TIME DISTRIBUTION OF STEEL MELT FLOWING IN A TUNDISH THROUGH PHYSICAL MODELING

A Thesis Submitted
in Partial Fulfilment of the Requirements
for the Degree of
DOCTOR OF PHILOSOPHY

by

SARBJIT SINGH

to the

DEPARTMENT OF MATERIALS AND METALLURGICAL ENGINEERING
INDIAN INSTITUTE OF TECHNOLOGY KANPUR

November, 1994

THIS THESIS IS DEDICATED TO

MY PARENTS,

for their sacrificial love.

MY WIFE,

for her constant encouragement and support.

MME - 1994-D-SIN-FLO

CERTIFICATE

It is certified that the work contained in the thesis entitled **"FLOW PATTERN AND RESIDENCE TIME DISTRIBUTION OF STEEL MELT FLOWING IN A TUNDISH THROUGH PHYSICAL MODELING"** by **Mr. Sarbjit Singh** has been carried out under my supervision and that this work has not been submitted elsewhere for a degree.

Dr. S. C. Koria
Professor
Department of Materials and Metallurgical Engineering
Indian Institute of Technology Kanpur
KANPUR - 208016, IMDIA

ACKNOWLEDGMENTS

I would like to express my sincere thanks to Professor Satish C. Koria for his guidance and supervision of this research work. His enthusiasm has been a source of great inspiration throughout the course of this project. His patience and efforts during the completion of this thesis are immensely appreciated.

I also wish to extend my appreciation to Professors A. Gosh, S.P. Mehrotra, R.C. Sharma, R.K. Dube and S.P. Gupta of the department, and Dr. V. Tare of Dept. of Civil Engineering for their encouragement and kind suggestions throughout the course of this work.

I am grateful to Mr. Jagir Singh(Dept. of Electrical Engineering), Mr. Raj Pal(Dept. of Aeronautical Engineering) and Mr. Abhilash Trivedi(P.C. Maintenance Cell) for their assistance with the development of a data acquisition and control system for carrying out the experimental measurements in the present work.

Many thanks must also go to the technical staff of the department and Central Workshop of the institute . Their contributions through the equipment construction phases of the project were invaluable.

I would like to thank many postgraduate students of the department with whom I worked for their friendship. In particular, I deeply appreciate the help of Mr. Anil Srivastava, Ms. Vidya and Mr.Srinivas K. Rao during the final preparation of the thesis.

The typing of this manuscript was most capably and in relatively short time performed by Mr. Yash Pal Gupta. My special thanks are also due to Mr. V.P. Gupta for useful discussion on designing of the conductivity probes and for tracing the figures compiled in this thesis.

I sincerely wish to convey my respect and appreciation for the efforts of my parents who made it possible for me to pursue this career. Words are insufficient to describe my gratitude towards them.

I also wish to express my appreciation to my wife Harvinder for her patience, understanding and support during the period of my candidature. I am thankful to my other family members also who directly or indirectly contributed towards the completion of this thesis.

At last I am grateful to Indian Institute of Technology, Kanpur for the financial support in the form of scholarship and to the National Mission for Iron and Steel, Government of India for the sponsorship of this project.

LIST OF CONTENTS

LIST OF FIGURES

LIST OF TABLES

NOMENCLATURE

$a_o a_1 a_2 a_3$	Coefficients in Eqs. 6.4 and 6.10
A, A′, B	Pre-exponents in Eqs. 6.5, 6.6 and 6.11
C_i	Dimensionless tracer concentration
c_i	Tracer concentration (g/l)
d	Pipe diameter (mm or m)
d_h	Height of the dam (mm or m)
d_p	Position of the dam (mm or m)
D	Dam
F	Test statistic value
FMs	Flow Modifiers
FP	Flow pattern
Fr	Froude number
Fr′	Modified Froude number
g	Acceleration due to gravity (ms^{-2})
H	Bath height (mm or m)
h,i,j,k,m,n,p	Exponents in Eqs. 6.10 and 6.11
l	Half length of the tundish (mm or m)
l_{ie}	Half inlet-exit distance (mm or m)
l'	Length of the eddy (mm or m)
l'_d	Characteristic length of small eddies, for which dissipation of energy by viscous force is maximum (mm or m)
l'_e	Characteristic length of medium size, energy containing eddies (mm or m)

l'_k	Characteristic length of smallest eddy, for which local Reynolds number is unity (mm or m)
$L = 2l$	Length of the tundish (mm or m)
L_C	Characteristic length (mm or m)
$L_{C,M'}$ $L_{C,P}$	Characteristic length parameter in model and prototype (mm or m)
L_{ie}	Distance between inlet and exit streams (mm or m)
M_e	Mass of tracer exited (g)
M_i	Initial mass of tracer (g)
M_r	Mass of tracer remaining in the tundish (g)
Mo	Morton number
NFM	No Flow Modifier
O	Open stream
$\dot{Q}$	Volumetric flow rate ($l\text{min}^{-1}$)
R_e	Reynolds number
RTD	Residence time distribution
s^2	Variance of RTD (s^2)
S	Submerged stream
SD	Slotted dam
t	Time (s)
t_i	Instantaneous time (s)
$\bar{t}$	Theoretical residence time (s)
t_{min}	Minimum time taken by tracer to arrive at the exit (minimum residence time) (s)
t_{peak}	Time taken by tracer to attain peak value of concentration at exit (Peak residence time) (s)
t_{mean}	Mean residence time (s)
$(t)_{NFM'}$ $(t)_{FM}$	Time parameter without and with flow modifiers (s)

u	Characteristic velocity (m/s^{-1})
u_m	Mean velocity of inlet stream, ms^{-1}
u_{ag}	Average velocity (m/s^{-1})
u_{max}	Maximum velocity on the horizontal plane (m/s^{-1})
$\bar{u}'_d$	Time averaged fluctuating component of velocity associated with eddies of length l'_d (ms^{-1})
$\bar{u}'_e$	Time averaged fluctuating component of velocity associated with eddies of length l'_e (s^{-1})
$\bar{u}'_k$	Time averaged fluctuating component of velocity associated with eddies of length l'_k (ms^{-1})
V	Volume of liquid inside tundish (m^3)
V_d	Dead volume (m^3)
V_m	Mixed volume (m^3)
V_p	Plug volume (m^3)
V_{sc}	Short circuited volume (m^3)
v_d, v_{dp}, v_m, v_{sc}	Fractional dead, dispersed plug, mixed and short circuited volumes
w	Weir
w_h	Height of weir (mm or m)
w_p	Position of weir (mm or m)
w+D	Weir+Dam
W	Width of tundish (mm or m)
We	Weber number
x_h	Dimensionless dam height
x_p	Dimensionless dam position

Greek Letters

α	Dimensionless width (W/L)
α_s	Fractional depth of submergence of shroud

β	Dimensionless height (H/L)
ε	Modifying factor
ε_{min}	Modifying factor for minimum residence time $(t_{min})_{FM}/(t_{min})_{NFM}$
ε_{mean}	Modifying factor for mean residence time $(t_{mean})_{FM}/(t_{min})_{NFM}$
ε_{peak}	Modifying factor for peak residence time $(t_{peak})_{FM}/(t_{peak})_{NFM}$
ε_S	Modifying factor for variance $(S^2)_{FM}/(S^2)_{NFM}$
η_h	Dimensionless weir height w_h/H
η_p	Dimensionless position of weir from inlet stream w_p/L
μ	Viscosity (kg $m^{-1}s^{-1}$)
ν	Kinematic viscosity (m^2s^{-1})
ρ_g & ρ_l	Density of gas and liquid (kg m^{-3})
σ	Surface tension of liquid (Nm^{-1})
σ^2	Dimensionless variance $S^2/\bar{t}^2$
τ_i	Dimensionless time $t_i/\bar{t}$
τ_{mean}	Dimensionless mean residence time t_{mean} / $\bar{t}$
τ_{min}	Dimensionless minimum residence time $t_{min}/\bar{t}$
τ_{peak}	Dimensionless peak residence time $t_{peak}/\bar{t}$
τ_R	Relative ratio parameter in Eq. 6.18
ϕ	Dimensionless inlet-exit distance L_{ie} /L
φ, φ_c, ψ, ψ_c	Relative ratio parameter in Eqs. 6.19 and 6.20
Ω	Conductivity in (Ohm^{-1})
Ω_{ag}	Average conductivity (Ohm^{-1})

ABSTRACT

The flow pattern and residence time distribution produced by submerged, open and argon shrouded molten steel stream in a tundish are investigated by a water model using the stimulus tracer response technique. Flow pattern is studied by methylene blue and following its dispersion within the tundish visually and by time elapsed and video photography. Residence time distribution is determined by recording continuously the conductivity of potassium chloride tracer at the exit of the tundish. Several parameters are varied; these are tundish width, inlet-exit distance, bath height, inlet Froude number, type of inlet streams slag cover, number of outlets and size, number and configuration of weir, dam, slotted dam and their combination.

It is found that wider tundishes produce short circuiting than narrower tundishes at all design and operating parameters for submerged stream pouring. In open stream pouring (unshrouded or shrouded) no short circuiting is observed. The effect of flow modifiers, among other factors, is found to depend on the type of pouring and dimensions, type and configuration. For submerged stream, weir of all sizes is found to produce short circuiting, whereas dam alone or in combination with weir eliminated short circuiting. For open stream, weir is found to restrict the turbulence of the inlet stream within the inlet region. The empirical correlations are developed to determine the residence times and variance of the fluid flowing in a tundish without and

with flow modifiers. The plausibility of the correlations is discussed in terms of momentum transfer for turbulent flow. Lastly, the applications of the correlations are discussed in terms of their ability to determine the residence times and variance of molten steel flowing in a tundish of a typical continuous caster.

CHAPTER - 1

INTRODUCTION

In recent years considerable efforts are being made to distribute several metallurgical treatments, which once concentrated in the primary steelmaking furnaces (converter, open hearth furnace and electric arc furnace), among specialised vessels from the blast furnace runner to the continuous caster. Table 1.1 is prepared to show the current trend in the distribution of metallurgical treatments among various metallurgical vessels[1-7]. For example, accurate temperature control, fine tuning of microalloying additions (such as boron, niobium, titanium etc.), calcium induced inclusion modification etc. are the final treatments, the effectiveness of each of which is easily impaired by long treatment and waiting times before casting[1-7].

These metallurgical treatments, if performed close to the solidification of steel, will prove to be the most effective, both in terms of the efficiency of the treatment and retaining the induced steel quality in the cast product.

In the chain of vessels handling molten steel, tundish is the last refractory lined vessel which handles molten steel prior to solidification and thus, offers an opportunity to perform metallurgical treatments. This objective requires to examine on one hand, the requirements of tundish for the continuous casting machine and on the other hand, the flow field and residence time

Table 1.1 : Current Trends in the Distribution of Metallurgical Treatments Among Various Steel Processing Reactors

Reactors ⟶ / Treatment ↓	Blast Furnace Runner	Torpedo Car	Ladle	Tundish
Desiliconization	Y	Y	Y	N
Desulphurization	N	Y	Y	N
Dephosphorization	N	Y	Y	N
Deoxidation	N	N	Y	N
Hydrogen & Nitrogen Removal	N	N	Y	N
Inclusion Modification	N	N	Y	Y
Inclusion Separation	N	N	Y	Y
Composition Trimming	N	N	Y	Y
Microalloying	N	N	Y	Y
Temperature Control	N	N	Y	Y

Y = Yes
N = No

requirements for metallurgical treatments.

The term 'tundish' as applied in continuous casting refers to an intermediate vessel placed between the ladle and the mold to supply and distribute molten steel to different molds. Fig. 1.1 shows the position of the tundish in a continuous casting machine[8]. The dimensions of the tundish depends on the size and shape (i.e. slab or billet/bloom) of the cast product and the number of molds, which may vary from single to as high as six. Depending on the combination of the aforementioned parameters the tundish length varies from 2.5m to 9.5m, width from 0.6m to 1.2m and bath height from 0.5m to 1.2m[5]. The commonly used shapes are rectangular with inclined or vertical walls, however, other shapes like T, trapezoidal, V, delta and T are also employed in some specific situations[4-6,9].

During the process of continuous casting, molten steel from the ladle enters the tundish from one end and after attaining a particular bath height leaves the other end in presence of a slag cover constantly and continuously.

For most of the casting period the molten steel bath height is maintained at a constant value. Between the ladle change-over period, bath height decreases. The former is termed as steady state and the later as unsteady state casting period.

The inlet stream is either submerged into the bath or falls through a submerged argon shrouded box[4-6]. In some cases the

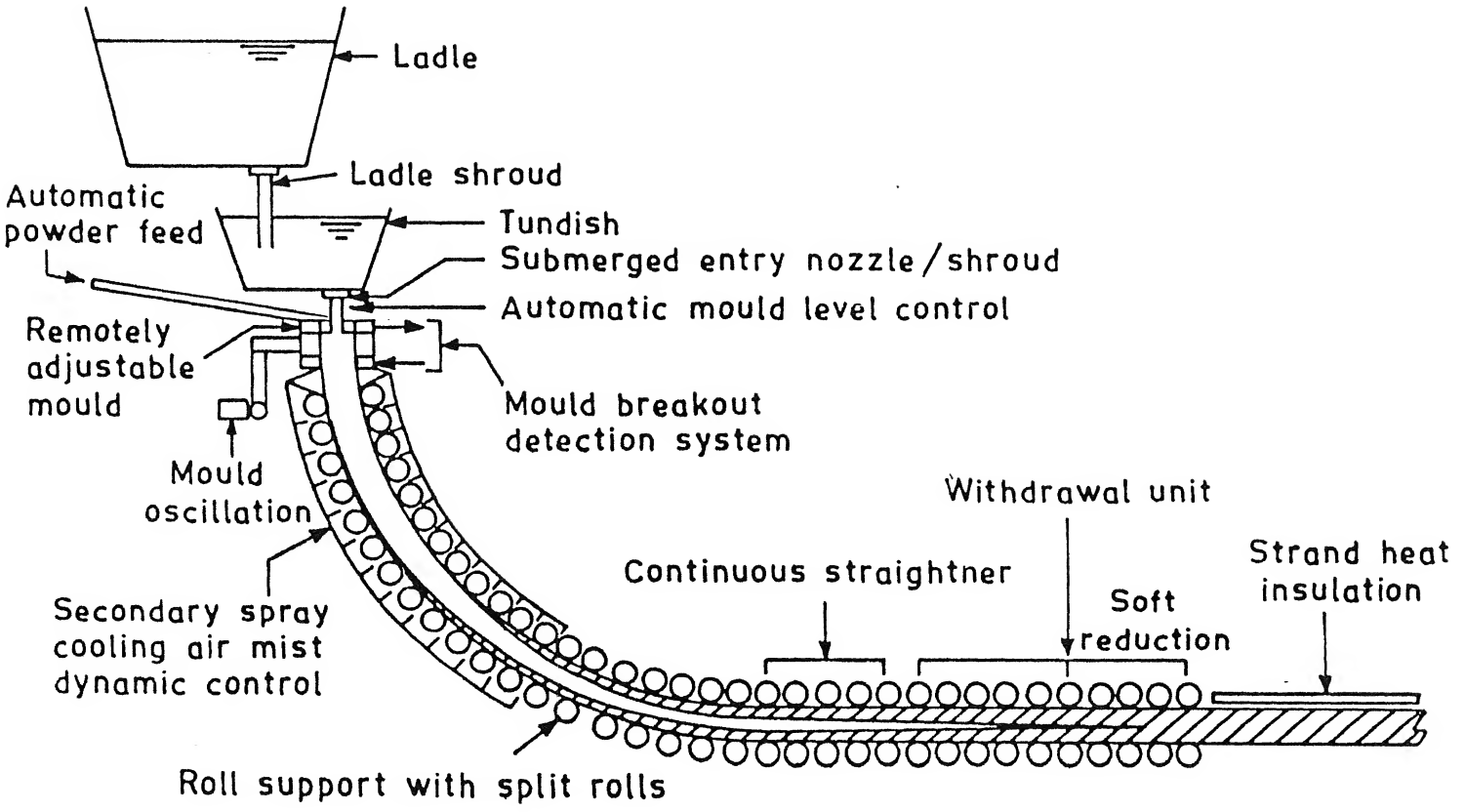

Fig.1.1: Position of tundish in a continuous casting machine.

inlet stream falls into the tundish through atmospheric air[4]. There are different configurations of the inlet-exit streams which depend mainly on the number of strands of the continuous casting machine. In a single strand casting machine, the inlet stream is on one side of the tundish and the exit one is on the other side[4-6]. Whereas in case of multi-strand machines, the inlet stream is at the centre of the tundish and the exit stream/(s) is/are located symmetrically on both sides of the inlet stream. In some cases the inlet stream is shifted away from the centre towards the width side of the tundish[9]. In other multi-strand machines, the inlet stream is on one side and the exit streams (more than one) are on other side of the tundish[10].

In the above method of transfer of molten steel from ladle to mold, the molten steel remains in the tundish for the time

$$\bar{t} = \frac{\text{Tundish Volume}}{\text{Volumetric Flow Rate}} \qquad (1.1)$$

which is known as the theoretical residence time. The availability of residence time just prior to solidification is the key concept to consider the use of tundish to perform the metallurgical treatments. Thus, tundish in addition to supply and distribute molten steel to mold (or molds), is considered to be an integral part of steel processing vessels. Based on the available informations on the use of tundish, a flow sheet (see Fig. 1.2) is prepared to show the role of tundish in the current philosophy of steelmaking[2-7,11-14]. It can be seen in the flow sheet that the role of the tundish is multi-faceted: it has to cater

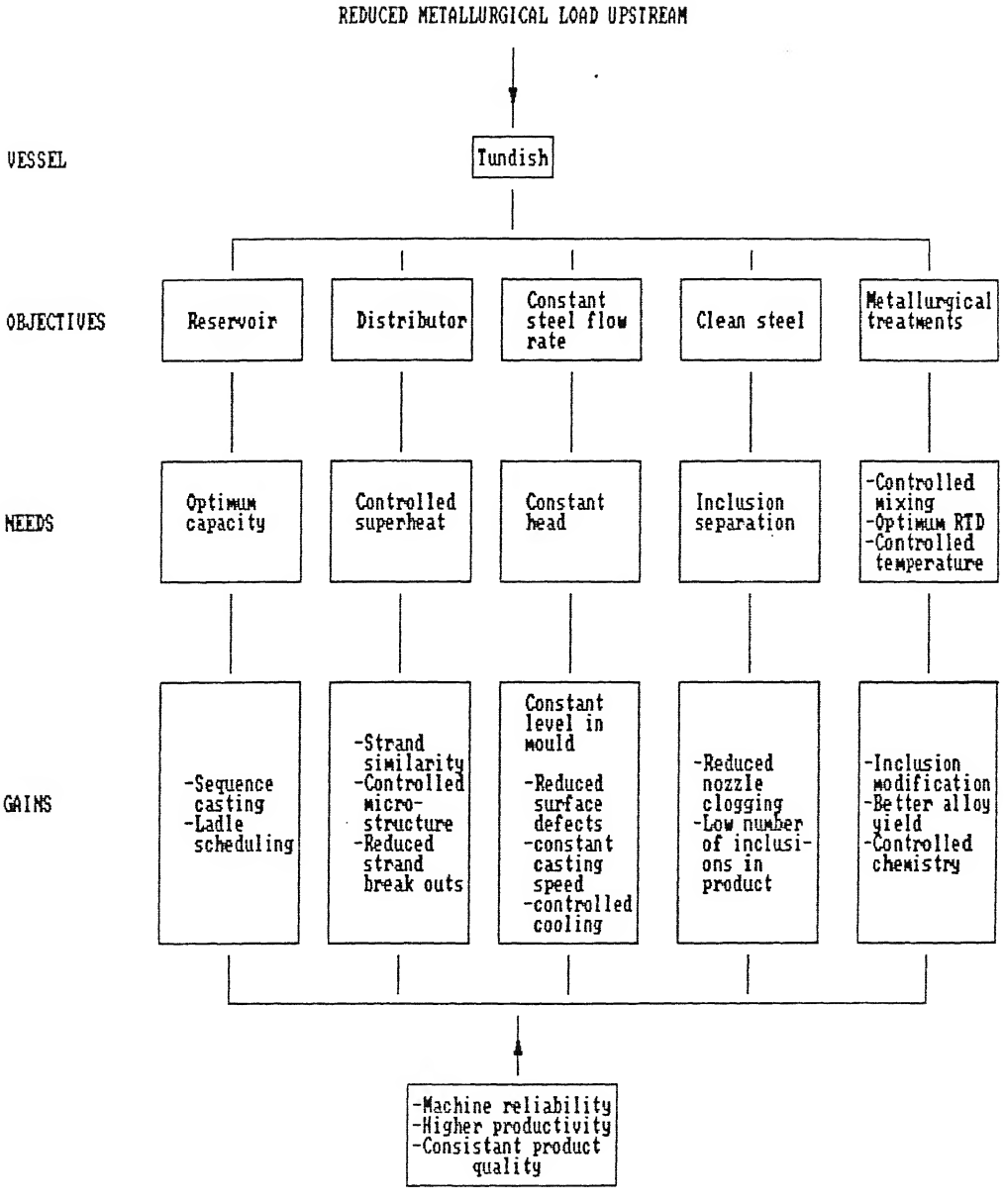

Fig.1.2: Process technological functions of tundish and accrued techno-economic benefits.

simultaneously the diversified needs of continuous caster (These needs are: to supply and distribute molten steel to different molds, to maintain constant flow rate and to provide steel during ladle change-over periods and the flow field and residence time controlled needs of metallurgical treatments).

Fluid flow studies have revealed that flow in the tundish is three dimensional with strong spatial variations[15-28]. Due to the spatial variations, the fluid flowing in the tundish can not be characterized by a single value of the residence time as calculated by Eq. 1.1, but there is a distribution of the residence time i.e. different volumes of fluid spend different times in the tundish. The efficiency of metallurgical treatments is closely linked with the nature of the fluid flow and residence time distribution. For example, inclusion flotation would require a surface directed flow and a narrow distribution of residence times, whereas alloy dissolution and distribution of the dissolved product would require intense mixing in the bath[1-4]. Thus, a knowledge of the nature of fluid flow and residence time distribution, among others, are the two important components in order to assess the suitability of a tundish to perform metallurgical treatments.

In the present thesis, the flow pattern and the residence time distribution of steel melt flowing in a tundish are studied in a physical model. The physical model is constructed by maintaining the geometrical and dynamical similarity with the industrial scale tundishes. Water is used as a flowing fluid.

The flow pattern and residence time distribution of water flowing in the model tundish are studied by a stimulus response technique[29]. The response of the suddenly imposed tracer concentration is recorded in terms of the concentration vs time plot on a microcomputer. Simultaneous to these measurements, the dispersion of the tracer is also filmed on a video tape. The video tapes are displayed on a colour monitor in order to derive the information on the nature of the flow by following the tracer dispersion as a function of time. The residence time distribution curve is characterized by the minimum, peak and mean residence time and the variance[8]. Correlations are obtained to calculate the residence times as a function of various tundish design and operating parameters. The results are presented and discussed.

About the organisation of the material, Chapter - 2 deals with the literature survey. In Chapter - 3, the principles of physical modeling are presented and the design details of the model tundish are given. The experimental set-up and the procedure to conduct the experiments are described in detail in Chapter-4. The results obtained are presented and discussed in Chapters-5 and 6. In Chapter-7 the applications of the results are presented in relation to the design of the tundishes. Conclusions and suggestions for further work are given in Chapter-8 and 9 respectively.

CHAPTER - 2

LITERATURE REVIEW

Tundishes in their original installations on the continuous casting machines were thought to act as supplier and distributor of molten steel to different molds during the process of continuous casting. With the growing concern to economize the steel processing route and to produce clean steels, there is an increasing trend in the steel industry to use tundish to perform some metallurgical treatments. Whether a tundish can be used to perform a metallurgical treatment or not would depend, among other factors, on the type of flow pattern and residence time distribution of steel melt flowing in it[1-5,11].Thus,it has become necessary to investigate the fluid flow behaviour in a tundish so that it, in addition to its basic functions can be made to accept the metallurgical load as and when the need arises.In this chapter the available literature on the tundish fluid flow behaviour is reviewed and presented.

2.1 METHODS OF FLUID FLOW STUDIES

The behaviour of steel melt flowing in a tundish is studied by a mathematical[5,10,14-28] and or a physical model[2,5,6,9,13,17,19,25-28,35-45]. In Table 2.1 details of tundishes are given which were employed by different investigators in their fluid flow studies. It can be seen that in all studies a tundish of specific caster is chosen to modify its design so as to

Table 2.1 : Details of tundishes employed for fluid flow studies

Source / Year	Tundish Design Parameters (Dimensions in Meters)								Operating Parameters				Type of Study
	Caster	Shape	N	W	H	L	L_{ie}	Stream	Q $m^3s^{-1}x10^3$	d (mm)	Fr	Scale Factor	
35 (1981)	Slab	R with IW	2	0.83	0.76	6.76	2.85	O.S.	16.67	54	111.0	1	W.M.
	Slab	R with IW	1	0.83	0.76	4.14	2.85	O.S.	8.33	54	27.0	1	W.M.
13 (1983)	Slab	V	2	-	-	-	-	-	-	-	-	-	W.M.
12 (1986)	Slab	R with IW	1	-	1.40	-	-	S.S.	-	-	-	0.4	W.M.
39 (1986)	Slab or Twin bloom	R with IW	2 o 4	0.80	1.0	8.00	2.54 or 3.14	S.S.	8.57	-	29.0	0.66	W.M.
33 (1986)	Slab	R with IW	2	0.90	1.2	8.0	3.12	S.S.	14.3	-	4.0	1	W.M., MM & actual
5, 16 (1986)	Slab	R with IW	2	0.65	0.75	6.79	2.85	S.S.	16.67	54	111.0	1	W.M., MM & actual
17 (1976)	Slab	R with VW	2	1.0	1.28	7.0	-	S.S.	28.00	-	15.9	1/6	W.M., MM
9 (1986)	-	R with IW		-	-	-	-	S.S.	-	-	-	0.15 or 0.25	W.M.
37 (1986)	Bloom	R with VW or through		0.7	1.0	2.08	-	S.S.	-	-	-	0.25 or 1	W.M.
	Billet	R with IW		0.9	0.84	3.96	-	S.S.	-	-	-	1	Actual Trial

Continued

Table 2.1 : Details of tundishes employed for fluid flow studies (Continued)

Source / Year	Tundish Design Parametrs (Dimensions in Meters)								Operating Parameters				Type of Study
	Caster	Shape	N	W	H	L	L_{ie}	Stream	Q $m^3s^{-1}x10^3$	D (mm)	Fr	Scale Factor	
19,38 (1986) (1987)	Slab	R with IW	2	0.92	0.81	7.92	3.56	O.S. or S.S.	-	-	5.63	0.33	W.M. & M.M.
14 (1986)	Slab	R with IW	1	-	-	-	-	O.S. or S.S.	-	-	-	1	W.M. & M.M.
2,46 (1987)	Bloom	T	3	-	-	4.48	-	S.S.	-	-	-	0.50	W.M.
18 (1987)	Slab	R with IW	2	0.70 or 1.20	0.7	7.0	3.25	S.S.	7.14	70	20	-	M.M.
5, 20 (1988)	Twin Slab	R with IW	2	0.90	1.20	8.00	2.50 & 3.68	S.S.	17.80	-	5.25	1	W.M. & M.M.
36 (1988)	Billet	T	4	0.46	0.71	3.42	-	S.S. O.S.	-	-	-	1	W.M.
		or Δ T	3	-	0.71	2.67	-	S.S.	-	-	-	1	W.M.
40,43 (1988)	Billet	R with IW	6	0.65	0.49	5.80	0.55 1.65 2.75	S.S. or S.S.	3.67	45	2.08	0.6	W.M.
22 (1990)	Slab	R with IW	1	0.84	1.0	4.00	5.5	-	-	-	-	0.33	W.M. & M.M.
10,42 (1990) (1991)	Slab or Bloom	R with IW & Step	1 o 3	0.79	1.1	4.70	2.48 3.20 3.90	S.S. or ASB	8.4 or 4.7	-	-	1	M.M. & W.M.

Continued

Table 2.1 : Details of tundishes employed for fluid flow studies (Continued)

Source / Year	Tundish Design Parameters (Dimensions in Meters)								Operatng Parameters				Type of Study
	Caster	Shape	N	W	H	L	L_{ie}	Stream	Q $m^3s^{-1}x10^3$	d (mm)	Fr	Scale Factor	
29 (1991)	Bloom	R with IW	1	-	-	-	-	S.S. or ASB	-	-	-	0.15	W.M.
44 (1991)	Slab	R with IW	1	1.10	1.10	3.45	-	S.S.	4.76	84	0.93	1	W.M.
21,23, 26-28 (1991)	Slab	R with IW or VW	1	0.34	0.40	1.30	1.25	S.S.	-	-	0.99, 3.98 or 15.93	-	-
34 (1991)	Slab	R with IW	2	-	-	-	-	S.S.	9.52 & 21.40	-	-	-	-
24 (1992)	Slab	R with IW	2	0.76	0.90	6.74	.00	S.S.	34.4	112	11.12	1	M.M.
25 (1992)	Slab	R with IW & VW	1	0.70	0.74	2.44	.95	S.S.	4.75	20	4.8	0.33	W.M.
21.26, 27,28 (1991) (1992)	Slab	R with VW	2	1.0	1.15	8.0	-	S.S.	11.94	100	2.35	-	M.M.
47 (1993)	-	R with IW	1	0.08 1.07 10.0	1.1	5.19	-	S.S.	-	-	-	Full (1) 0.25	W.M.& M.M.

Explanation:
R = Rectangular
IW = Inclined Wall
O.S. = Open Stream
S.S. = Submerged stream
ASB = Argon Shrouded Box
WM = Water model
MM = Mathematical model

accommodate the local steelmaking requirements.

In a mathematical model the fluid flow behaviour in the tundish is simulated by Navier-Stoke's equation for turbulent flow. Both water and steelmelt are considered as a fluid flowing in the tundish. Using K-ε model and with the appropriate empirical constants for turbulence dissipation, the Navier-Stoke's equation is solved to get spatial variation of the velocity of water and molten steel flowing in the tundish. It may be noted that the same empirical constants for turbulence dissipation were employed for water and molten steel flowing in respective tundishes. In references[5,19,22], the momentum and tracer dispersion equations are coupled to get a RTD-curve. The transient nature of the fluid flow and heat transfer of the melt in the tundish are also simulated[21,23,26-28].

In a physical model, water is used to simulate the behaviour of steel melt. A full or fractional scaled model is constructed by following the Froude number similarity. The flow pattern and residence time distribution (RTD) are studied by the tracer response technique. Few investigators have injected radioactive copper tracer to study behaviour of molten steel flowing in the tundish[29,37]. Large number of investigators have studied the fluid flow behaviour for submerged inlet stream pouring condition[2,5,9,10,12,14,16-29,33,34,36-40,46]. Very few have studied for open-inlet stream condition[6,10,14,29,35,36,38,40-42].

2.2 FLOW PATTERN

The term flow pattern is used to describe the path adopted by the fluid while flowing from inlet to the exit of the tundish. It is studied by a mathematical model and expressed in terms of velocity plots in different xyz - planes for water and steel melt flowing in a tundish. Some investigators have studied the flow pattern by flow visualization technique by injecting colored tracer into a physical model.

It is reported that the flow of the liquid in the tundish is three dimensional with strong spatial variations[5,10,14,16-22,24,26-28,33,38,42,46]. The flow produced by the submerged inlet stream of water in the tundish is found to be identical to that of steel melt flowing isothermally and under steady state conditions[26,27]. The flow consists of : The entering jet hits the bottom of the tundish and then flows downward or sideways toward the wall of the tundish. This liquid then moves up the tundish side walls to the free surface, partly moving downstream in the direction of the exit and the rest recirculating back toward the incoming jet. The velocities drop significantly with the increasing distance from the incoming jet. The above type of flow produces different proportions of volumes of plug, mixed, dead and short circuited.

The flow is found to be highly turbulent near the inlet region of the tundish.

Due to the flow of the steel melt toward the exit at steady state, a small drop in temperature of the order of 2-3°C is reported in a mathematical model study[21,28]. Due to this temperature differential, there is a strong recirculation of the melt along the bottom of the tundish from the outlet toward the incoming melt stream[21,28]. This back flow of the melt along the bottom of the tundish is absent in the isothermal case[21,29].

The effect of Flow Modifiers (hereafter FMs) on the flow pattern is studied and the following are reported:

i) Weir alone is not found to alter the flow pattern when compared with No Flow Modifier (NFM). However, it helps retaining slag within the inlet region.

ii) Dam alone or in combination with weir, or slotted dam alters the flow pattern when compared with that of without FMs in the following ways:

   a) it restricts the turbulence of the inlet stream within the inlet region on account of which the flow downstream the dam becomes more uniform.

   b) it creates surface directed flow.

The flow pattern produced by the open stream pouring is mostly studied by the flow visualisation technique[6,10,14,29,35,36,38,40,42]. Gas entrainment leads to

extensive turbulence and buoyancy driven upward flow in the pouring pad region. The liquid stream loses its downward momentum on entering the tundish and reverses to the free surface. This flow pattern is valid for the single strand and in one half of the two strand casting tundish; in the later, the flow pattern in one half ofthe tundish is found to be identical to that of the other half.

For argon shrouded open stream, the shroud diameter and its submergence control the amount of gas that escapes from the shroud region and thereby changes the relative magnitudes of the flow currents along the surface and the tundish floor[10,29,42].

The effect of size and configuration of the FMs on the flow pattern is studied[6,35,38,40]. Weir is found to restrict the effect of rising air bubbles within the inlet region which resulted in elimination of surface wave motion and confinement of turbulence of the inlet stream within the inlet region.

2.3 RESIDENCE TIME DISTRIBUTION

The response of the tracer is measured at the exit of the tundish in a physical model[5,6,9,13,17,20,25-28,35-45]. From the tracer response curve, the residence time distribution of water flowing in the tundish is determined without and with FMs. All investigators reported that there is a distribution of residence times. In each case, RTD-curve is characterised by the minimum,

peak and mean residence times. Since in most of the investigations, the tundish of a particular caster with the specific design and operating conditions is modeled, a critical assessment of the residence times could not be made. However, their values are used in developing empirical correlations in the present study and as such they are given in Chapter - 6.

2.4 OBJECTIVES OF THE STUDY

In the present study, the flow pattern and residence time distribution of molten steel flowing in a tundish are studied by a water model. The following objectives are set forth:

i) To study the effect of wide range of tundish design and operating parameters on the flow pattern and RTD for submerged and open stream pouring conditions without and with FMs.

ii) To provide a basis of comparison of the results of the different investigators on residence times. For this purpose appropriate correlations are planned to be developed without and with FMs.

iii) To explore the possibility of providing a guideline (within the limitations of the physical model) for the selection of dimensions of a tundish for a new continuous caster installations.

iv) To provide a basis of selection of FM.

CHAPTER - 3

MODEL SIMULATION

In the present thesis, the flow pattern and RTD of molten steel flowing isothermally in a tundish without and/or under the protection of slag cover is studied in a physical model for submerged, open and argon shrouded inlet streams. Water was used to model the flow of steel, primarily because of the similarity in kinematic viscosity, ease of handling and availability. A thermocole sheet was employed to model the influence of tundish slag cover on molten steel flow dynamics. The model tundish in the present thesis does not belong to a particular continuous caster. In such a situation, a physical model of the tundish fluid flow system was constructed by following the similitude criteria. This chapter describes the similitude criteria employed to obtain the dimensional and operating parameters to construct and operate the model tundish.

3.1 SIMILITUDE CRITERIA

3.1.1 Geometric

For the geometric similarity, shape and various linear dimensions were considered. As pointed out in introduction that the most widely employed shape of the tundish is rectangular with vertical or inclined walls, the model tundish shape was kept rectangular. The geometric similarity was achieved by keeping the

corresponding ratios of linear dimensions in the model similar to that of the prototype. These ratios are:

$$\left(\frac{W}{L_c}\right)_M = \left(\frac{W}{L_c}\right)_P \tag{3.1}$$

$$\left(\frac{H}{L_c}\right)_M = \left(\frac{H}{L_c}\right)_P \tag{3.2}$$

$$\left(\frac{L_{ie}}{L_c}\right)_M = \left(\frac{L_{ie}}{L_c}\right)_P \tag{3.3}$$

With the help of the expressions (3.1) to (3.3) and the values of $\left(\frac{W}{L_c}\right)_P$, $\left(\frac{H}{L_c}\right)_P$ and $\left(\frac{L_{ie}}{L_c}\right)_P$, other dimensions of the model tundish were obtained by considering 1m base length of the tundish.

3.1.2 Dynamic

The dynamic similarity was observed by considering the forces which determine the behaviour of molten steel flowing in the tundish; these are: inertial, gravitational, viscous and surface tension[6]. The ratio of these forces constitute the following dimensionless numbers[6]:

$$\text{Froude No (Fr)} = \frac{u^2}{gL_c} = \frac{\text{inertia force}}{\text{gravitational force}} \tag{3.4}$$

$$\text{Reynolds No (Re)} = \frac{uL_c}{\nu} = \frac{\text{inertia force}}{\text{viscous force}} \tag{3.5}$$

$$\text{Weber No. (We)} = \frac{\rho u^2 L_c}{\sigma} = \frac{\text{inertia force}}{\text{surface tension force}} \qquad (3.6)$$

$$\text{Morton No (Mo)} = \frac{g\,\mu^4}{\rho_L \sigma^3} = \frac{\text{gravitational force x viscous force}}{\text{surface tension force}} \qquad (3.7)$$

For the liquid stream without any air entrainment, i.e. for submerged stream, falling into the bulk, the gravity and the inertial forces are predominant for the simulation of inlet stream of the model with the prototype[35]. The penetration of the stream into the liquid pool occurs as inertial force overcomes surface tension force, thereby Weber number becomes important criterion for similitude[35]. Once the stream and liquid pool become one continuous phase, fluid propagation inside the tundish depends on viscous and inertial forces (or the Reynolds number) and the wave motion on the bath surface depends on inertial and gravitational force (or the Froude number)[35].

For the heterogeneous stream (gas + liquid as in open stream pouring or in case of argon shrouded inlet stream) the Morton number similarity was observed. The similarity in case of flow behaviour of heterogeneous stream was observed by considering the modified Froude number, defined as[35].

$$Fr' = \frac{\rho_g u^2}{(\rho_L - \rho_g) g L_c} \qquad (3.8)$$

By Eqs. 3.4 ad 3.8, we get

$$Fr' = \frac{\rho_g u^2}{\rho_L - \rho_g} Fr \qquad (3.9)$$

In order to calculate above numbers, the diameter of the shroud was taken as characteristic length and mean velocity of inlet stream as characteristic velocity, which is defined as

$$u_m = \frac{4Q}{\pi d^2} \qquad (3.10)$$

Substituting (3.10) into (3.4) to (3.6), we get

$$Fr = \frac{16Q^2}{\pi^2 g d^5} \qquad (3.11)$$

$$Re = \frac{4Q}{\pi \nu d} \qquad (3.12)$$

$$We = \frac{16 \rho Q^2}{\pi^2 \sigma d^3} \qquad (3.13)$$

The dynamic similarity between the model and the prototype requires the equality of the above numbers[5,6], i.e.,

$$\left.\begin{aligned} &Fr_M = Fr_P,\ Re_M = Re_P;\ We_M = We_P \\ &Fr'_M = Fr'_P \quad \text{and} \quad Mo_M = Mo_P \end{aligned}\right\} \qquad (3.14)$$

The values of the physical constants which were used to calculate the above numbers, are given in Table 3.1.

Table 3.1 : Physical Properties of Water at 20°C and Steel at 1600°C

Physical Property	Water (20°C)	Steel (1600°C)
Viscosity, μ, $Kgm^{-1}s^{-1}$	$1x10^{-3}$	$6.4x10^{-3}$
Density, ρ, Kgm^{-3}	1000	7014
Kinematic Viscosity, $\nu=\mu/\rho$, m^2s^{-1}	$1x10^{-6}$	$0.912x10^{-6}$
Surface Tension σ, Nm^{-1}	$73.05x10^{-3}$	$1600x10^{-3}$

Using the available values of Q and d of the industrial scale tundishes employed on single or two strand casting machines, all the numbers are calculated by expressions 3.7, 3.9 and 3.11 to 3.13. The range of calculated values of dimensionless numbers are given in the Table 3.2.

In order to be able to calculate above numbers for the present model, d and Q must be selected. It has been shown by many investigators that the Froude number similarity between the model and the prototype is sufficient to describe the fluid flow behaviour in the tundish[5,6,17]. As such, the inlet flow rate and diameter of inlet shroud were chosen in such a way so that the Froude number similarity is maintained between the model and the prototype, and the other numbers remain as close to each other as possible. The calculated values of all the dimensionless numbers are given in the Table 3.2.

3.2 ACHIEVEMENT OF SIMILARITY

It can be seen in Table 3.2 that the geometric similarity parameters lay within the range of industrial tundishes. However, there is a partial similarity with reference to the parameters representing magnitude of forces in the model and the prototype. Froude number in the model lay within the range of industrial tundishes. Since the Froude number similarity is maintained (i.e. $Fr_M = Fr_P$), the dissimilarity in the other dimensionless numbers

Table 3.2 : Comparison of Characteristic Parameters of Indusrial tundishes with the Present Model

Type of Similarity	Parameter	Industrial Tundishes	Model Tundish
Geometric	L	2.5 - 9.5m	1m
	W/L^*	0.15 - 0.29	0.072 - 0.31
	H/L^*	0.18 - 0.36	0.12 - 0.34
	L_{ie}/L^*	0.68 - 0.92	0.68 - 0.88
	Shape	Rectangular with vertical or inclined walls	Rectangular with vertical or inclined walls
Dynamic	Fr	0.45 - 111	0.74 - 40.77
	Re	1.1×10^{5} - 4.2×10^{5}	0.9×10^{4} - 2×10^{4}
	We	0.74×10^{3} - 13.9×10^{3}	0.5×10^{2} - 5.33×10^{2}
	Mo	5.73×10^{-13}	2.52×10^{-11}
	Fr'	1.1×10^{-4} - 2.8×10^{-2}	8.6×10^{-4} - 4.7×10^{-2}

* For two strand casting tundish and symmetrically placed inlet shroud, only half the tundish length is considered.

using water as a model fluid is due to the following relationships obtained by Eqs. 3.9 and 3.11 to 3.13.

$$\frac{Re_M}{Re_P} = \left[\frac{L_{C,M}}{L_{C,P}}\right]^{3/2} \tag{3.15}$$

$$\frac{We_M}{We_P} = 3.13 \left[\frac{L_{C,M}}{L_{C,P}}\right]^{2} \tag{3.16}$$

$$\frac{Fr'_M}{Fr'_P} = 4.7 \tag{3.17}$$

The ratio $L_{C,M}/L_{C,P}$ is a scale factor. In case $Fr_M = Fr_P$,, Re_M can only be equal to Re_P when $L_{C,M} = L_{C,P}$ according to Eq. 3.15. In that case $We_M = 3.13\ We_P$. The dissimilarity in the Weber number is not considered to influence the flow similitude since in both cases the value of the number indicates the dominant effect of inertial force in comparison to the surface tension force. The influence of the inertial force is already incorporated in the Froude and the Reynolds numbers. Reynolds number in the model is lower by an order of magnitude than that of prototype, but both the values lay within the turbulent region. The effect of Reynolds number on the fluid flow is discussed in Chapter - 6.

CHAPTER - 4

EXPERIMENTAL

In this chapter, the experimental set-up and the procedure are described to study the flow pattern and residence time distribution of water flowing in the tundish for submerged, open and argon shrouded inlet streams.

4.1 SET-UP

Fig. 4.1 shows the schematic view of the experimental set-up along with the instrumentation. The unfilled arrows indicate the flow of electronic signals to coordinate the various stages of an experiment. These stages are: actuation of tracer injection circuit and collection of data. The set-up consists of a model tundish, water supply, tracer injection and tracer-response measurement system.

4.1.1 Model Tundish

The schematic view of the model tundish is shown in Fig. 4.2. It was fabricated from a 10mm thick perspex glass sheet and was rectangular in cross-section with east and west walls inclined at an angle of 105° from the horizontal. The base dimensions were 1000mm x 310mm and height was 365mm. The maximum capacity was to

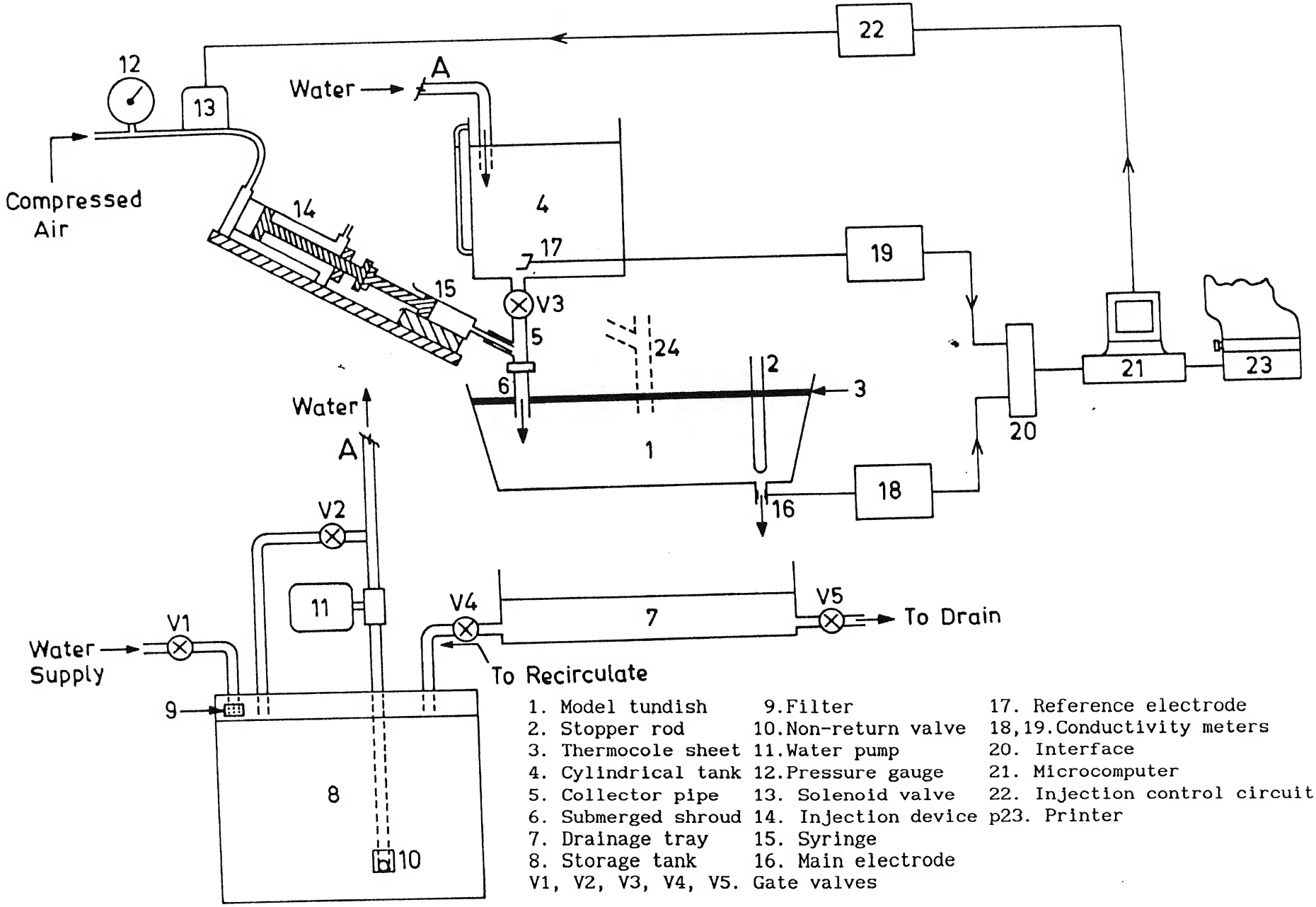

Fig.4.1: Experimental set-up for tundish fluid flow studies.

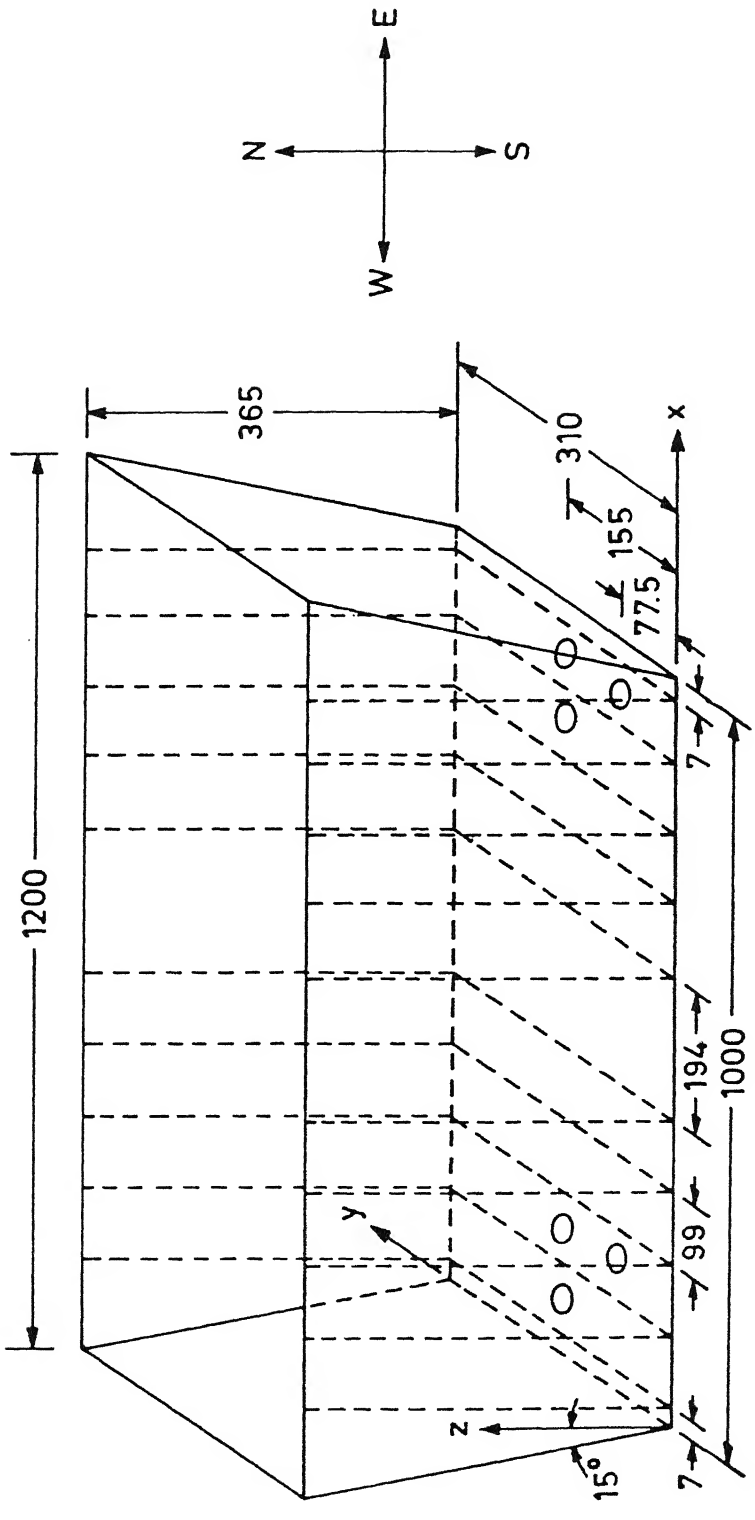

Fig.4.2: Details of perspex model tundish design.

hold 0.124 m^3 of water. Holes of diameter 14.3mm were made on the tundish base at the centre of the width and at the centre of the half width as shown in the figure.Smaller diameter opening of size 10mm was obtained by inserting perspex glass ring into the 14.3mm hole as and when the need arose. The holes were plugged according to the need of the experiment.

Grooves of size 4mm x 4mm were engraved at the various distances on the base and north and south walls of the tundish in order to make the east and west walls vertical and to insert flow modifiers. Dam, weir and slotted dam were used as flow modifiers. Dam and weir of different heights were fabricated from 4mm perspex glass sheet. The slotted dam was made by using a 7mm thick perspex glass sheet. Fig. 4.3 shows the schematic view of the slotted dam. Thirty two holes of 10mm diameter were drilled at an inclination of 30° from the horizontal. The holes were arranged in eight rows and four columns as shown in the figure.

4.1.2 Water Supply

Water supply in all experiments was obtained from a $1m^3$ water storage tank. From the storage tank, water was transferred into a $0.5m^3$ capacity cylindrical vessel which was placed 400mm above the tundish. A 4mm ID glass tube was mounted outside the vessel to indicate the water level. The water level in the cylindrical vessel was maintained constant during the experiment. At the bottom of the vessel a gate valve (V3 in Fig. 4.1) with a 250mm long pipe (hereafter termed as collector pipe) was provided to

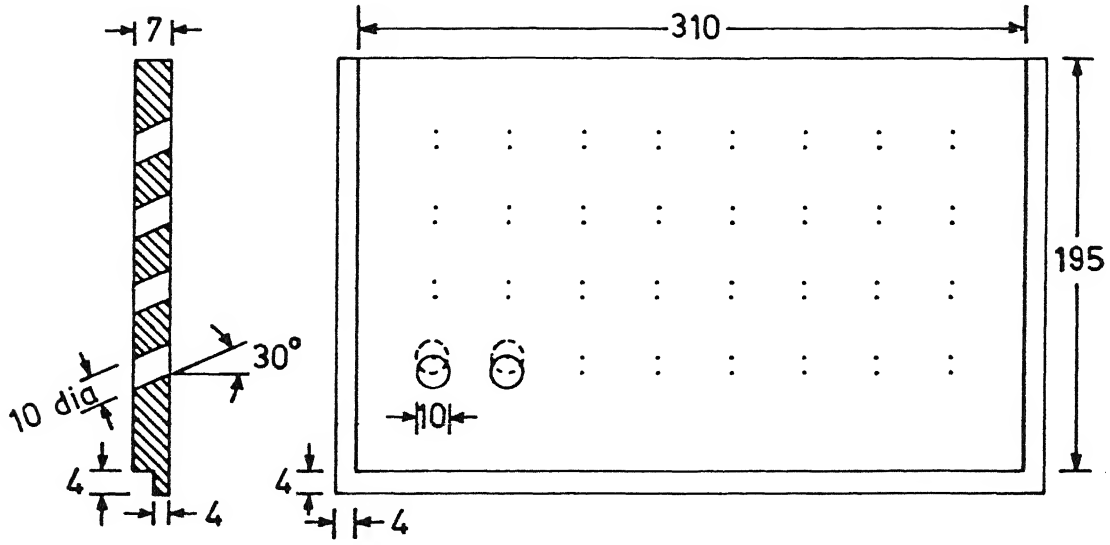

Fig.4.3: Design of slotted dam.

control the water flow rate into the tundish.

Water was supplied into the tundish either through a steel pipe or through an air chamber (both were submerged in the tundish water bath) or through atmospheric air. The air chamber simulates the argon shrouded inlet stream. The steel pipe or air chamber was attached to the collector pipe. Fig 4.4 shows the schematic view of the air chamber. The air chamber was fabricated from a glass cylinder, one end of which was sealed with a circular perspex glass sheet and the other end was left open. On the perspex sheet holes were drilled for in and outflow of air into the glass chamber. A steel pipe was fitted at the centre of the sheet and was connected to the collector pipe during experiments.

The flow rate of water through the tundish exit was controlled by a stopper rod. It was fabricated from an aluminium rod, one end of which was made conical and the other end was threaded. Fig. 4.5 shows the stopper rod along with the dimensions. The aluminium rod was inserted into a perspex glass plate, which was mounted on the north and south walls of the tundish. The threaded end of the aluminium rod was rotated into an internally threaded perspex glass disc fixed above the perspex plate as shown in the figure. In order to control the flow rate of water through the tundish exit, the aluminium rod was rotated clockwise or anticlockwise.

The water from the tundish exit was recirculated or drained via a tray placed below the tundish as shown in Fig. 4.1. The recirculation or drainage of water was achieved by gate valves (V4

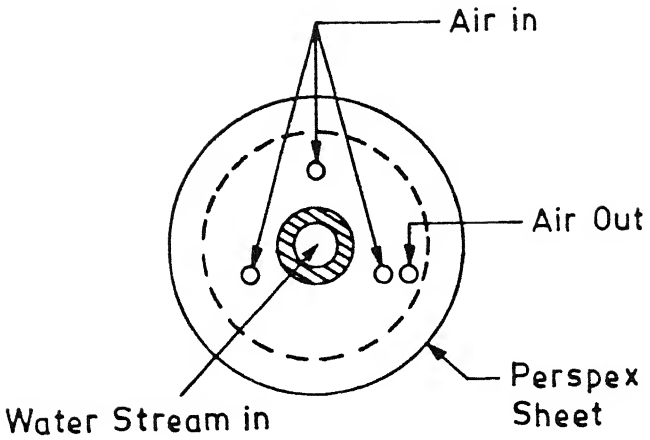

Top View

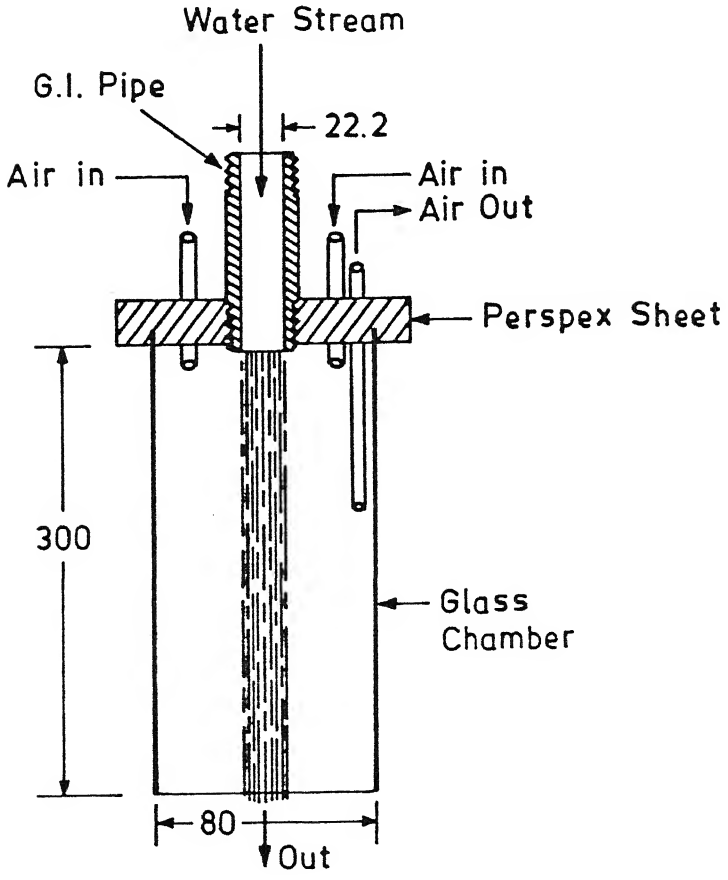

Front View

Fig.4.4: Design of an air chamber to simulate argon shrouded inlet stream.

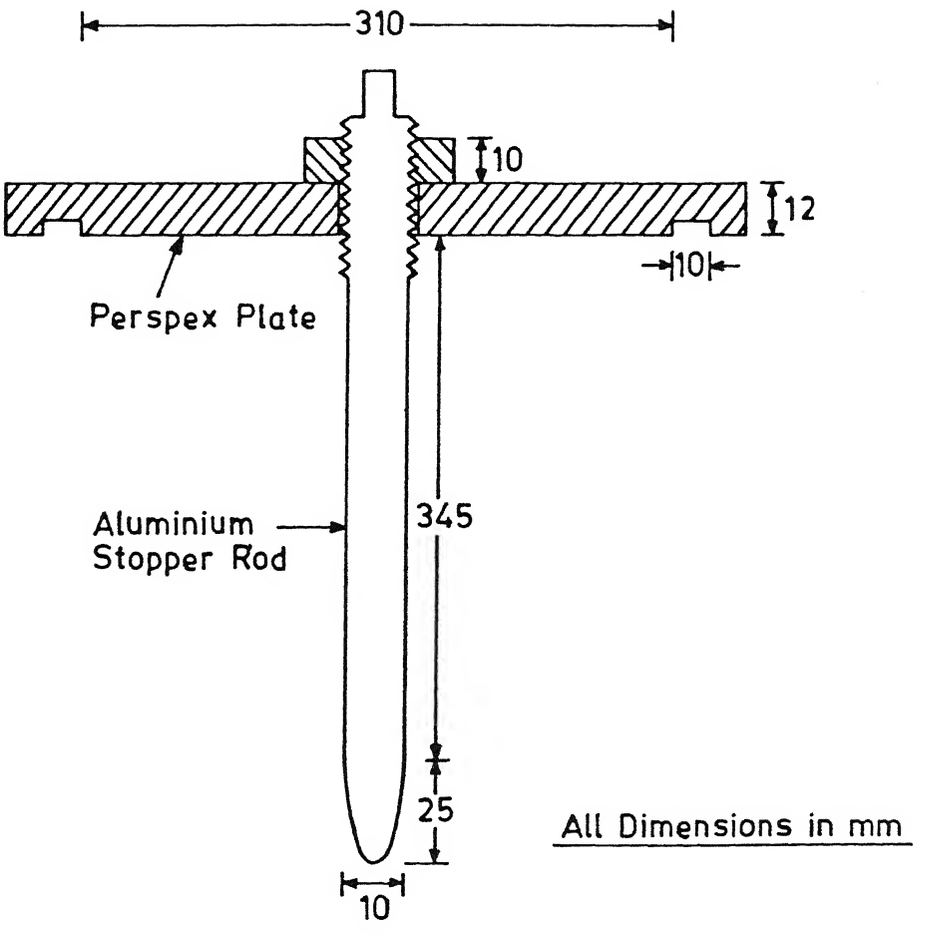

Fig.4.5: Design of stopper rod to control water flow rate.

and V5), provided near the base of the tray.

4.1.3 Tracer

Methylene blue and potassium chloride (KCl) were used as tracers in the present study. Methylene blue was used for identification of flow pattern and KCl for residence time distribution. Both tracers were injected into the inlet stream in the form of a pulse input and their response was measured within and at the exit of the tundish.

4.1.3.1 *Injection Device*

Tracer injection was done by a plastic syringe, which was placed in between the collector pipe and a pneumatically operated cylinder-piston assembly, which was mounted on a steel plate, as shown in Fig. 4.1. The needle of the syringe was kept inserted into the brass tube of the collector pipe as shown in the figure. Air supply to the cylinder was controlled by a solenoid valve.

4.1.3.2 *Measurement Techniques*

In experiments, tracer dispersion within the tundish and the concentration variation at the exit were measured to study flow pattern (FP) and residence time distribution (RTD). In the following, the techniques for FP and RTD are described separately.

(A) *Flow pattern*

Flow pattern was studied by visual observations and by time lapsed and cine photography. For photography, the tundish was illuminated uniformally from back side of the north wall of tundish with the help of halogen lamps. The time lapsed photographs were taken by using the Camera, Minolta-7000. Shutter speed and aperture were fixed as 1/60s and f/4 respectively. The cine photography was done by using a video camera of National Panasonic make. Video tapes were displayed on the colour monitor to study the flow pattern.

(B) *Residence Time Distribution*

RTD study was made by measuring conductivity of water continuously at the tundish exit. For this purpose a differential conductivity circuit was developed as shown in Fig. 4.1. The circuit utilizes two probes, one placed at the tundish exit (main probe) and other placed in the cylindrical vessel (reference probe). These probes were connected to two separate conductivity meters. The conductivity meters were capable of measuring conductivity values ranging from 0 to 200 mMho.

i) *Design of Probes*

Fig. 4.6(a) shows the design of the main probe. It consists of a hollow perspex glass cylinder, on one end of which two square shape platinum foils were fixed diametrically opposite to each other. The other end of the cylinder was threaded in order to fix

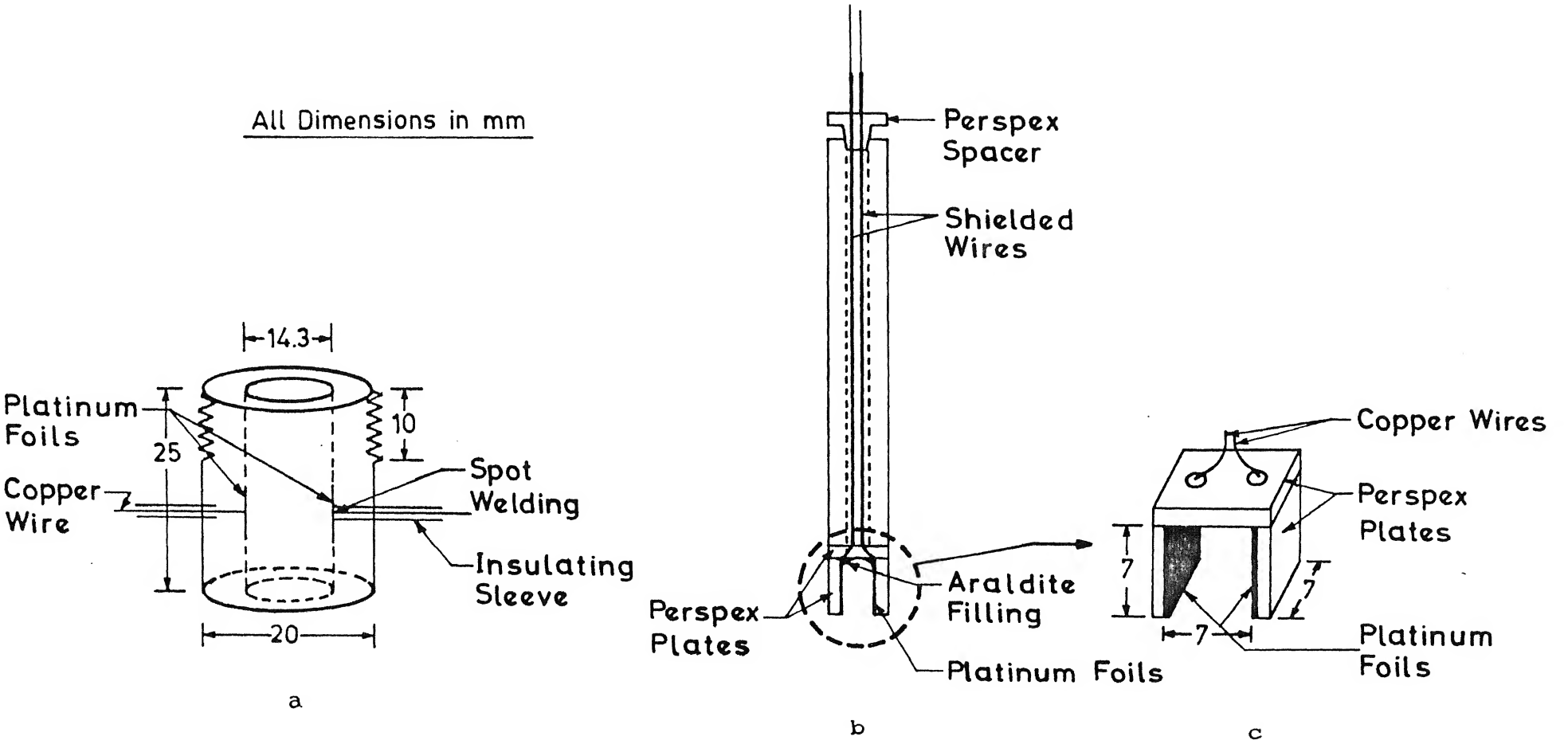

Fig.4.6: Design of conductivity probes for fluid flow studies.

it below the hole in the tundish base. A copper wire was spot welded on the centre of the surface of each platinum foil as shown in the figure.

The design of reference probe is shown in Fig. 4.6(b). Two platinum foils were fixed on two separate perspex glass plates. Both of these plates were further fixed, vertically and parallel to each other, on to another perspex plate, as shown in Fig. 4.6(c). These perspex plates carrying the platinum foils were joined to the lower end of a brass tube and the spot welded copper wires (with insulating sleeves) were taken out from the upper end. A perspex glass spacer was fixed at the top end of the brass tube to avoid any pull to the copper wires.

ii) *Preparation of Probes*

In order to eliminate the polarization effects caused by the alternating current, the platinum foils were coated with a layer of finely divided platinum black. This was carried out by electrolysis of a solution containing one percent platinum chloride and 0.02 percent of lead acetate.

The following procedure was adopted for platinization:

- The old coating was stripped off with the aqua regia and rinsed with distilled water.

- A solution containing 10mg platinum chloride and 0.1mg lead

acetate in 30ml of distilled water was prepared.

- The probe with platinum foils was immersed in the above solution and D.C. current of density $2x10^{-4}Amm^{-2}$ was passed for 10 minutes in one direction and then reversed for the same period.

- The foils were rinsed in distilled water and immersed in 5% solution of H_2SO_4. The current of the same density as mentioned above was passed for 10 minutes in one direction and for another 10 minutes in reverse direction.

- The foils were rinsed in distilled water and the probe was ready for use.

When the probes were not in use, their platinum foils were kept immersed in distilled water.

4.1.4 Data Acquisition System

The data on variation of tracer concentration with time were acquired to study RTD. The data acquisition systems comprised of a tracer injection cricuit and on-line data recording equipment.

4.1.4.1. *Tracer Injection Circuit*

Fig. 4.7 shows the electronic circuit developed to actuate

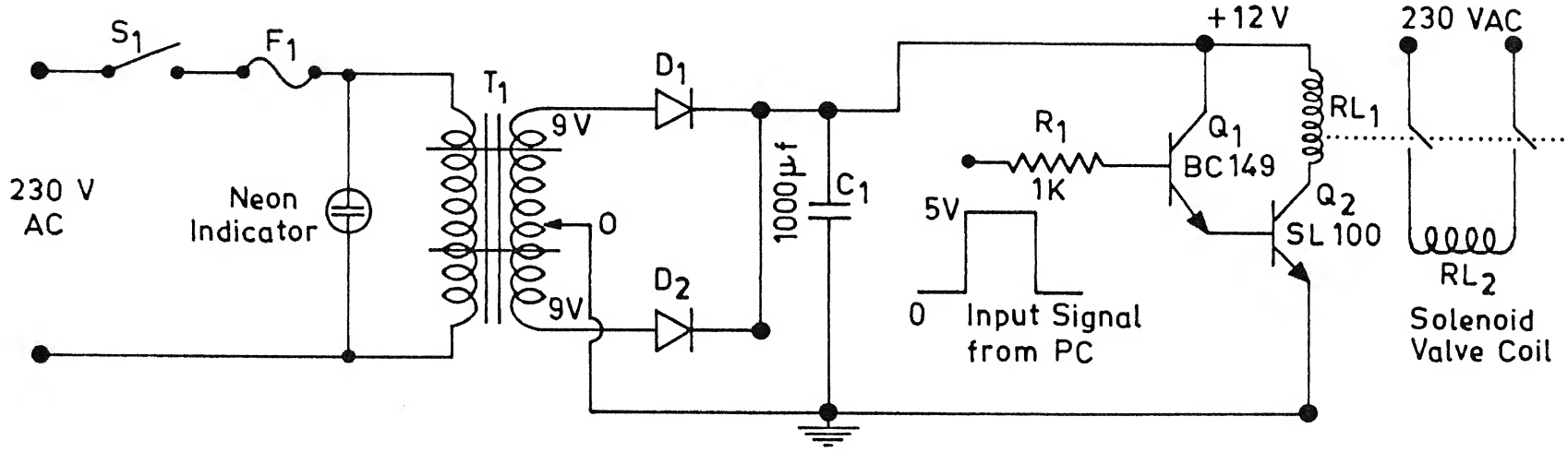

Components : Switch S_1, Fuse F_1, Transformer T_1, Neon Indicator, Diodes D_1 and D_2, Capacitor C_1, Transistors Q_1 and Q_2, 12V Relay RL_1, 230V(AC) Relay RL_2

Fig.4.7: Electronic circuit to actuate the solenoid valve for tracer injection.

the solenoid valve of the tracer injection device. This circuit was triggered by a signal (5V) from the printer port of the IBM-PC/XT, microcomputer. As soon as the signal was given from the microcomputer, the transistors Q_1 and Q_2 started conducting and the current flow through the circuit energized the relay RL_1. This made the normally open contacts of the 12V relay to close, which allowed the 230V A.C. supply to energize the coil of the solenoid valve. As soon as the signal from micro-computer was stopped, the current stopped flowing in the circuit and relay RL_1 was de-energized. This made the closed contacts of the relay to open and 230V A.C. supply to solenoid valve was disconnected. Thus one cycle of tracer injection was over and the system was again ready for the next cycle of injection.

4.1.4.2. *Data Recording Equipment*

The signals generated by the probes were recorded continuously with the help of a digital converter (ADC) card, PCL-213 (Dynalog Micro-Systems) and a micro-computer, IBM-PC/XT (HCL, Bombay). There were 16 input channels available on the ADC card. The maximum sampling rate of the card was 7.5 samples per second. There was an in-built filter circuit for rejecting the input noise. The analog input voltage range was 0 to ±40.96mV. The provision was there for amplifier gain selection of 1, 10 or 100. The millivolt signals from conductivity meters of main probe and of reference probe were fed separately to the two analog channels of ADC card, i.e. channel number zero and 2 respectively.

4.1.4.3 *Software*

A computer program was written to integrate and coordinate the process of tracer injection and data recording. Fig. 4.8 shows the flow chart of the program. The computer program is given in Appendix - 1. Main sections of this program are tracer injection, channel selection and sampling (i.e. analog to digital conversions), and data storage into data files.

The input values given at the start of program were sampling rate (i.e. SMPRT = 240 samples per minute), trial sampling duration (TRSMD) and experimental sampling duration (EXSMD). Trial sampling duration decided the time for which the analog to digital conversions were to be made before tracer injection and experimental sampling duration decided the time for which conversions were made after the tracer injection. These conversions were made in timer triggering mode. Counters were, therefore, loaded at this stage to synchronize the process of conversions. The next step after this was channel selection and sampling. The program for this was written in such a way that in every 15 seconds, 56 samples were taken from the signal at channel number zero and next four samples from the signal at channel number 2. Therefore, most of the samples were taken from channel number zero (receiving the signal from main probe) in order to record the fast change in conductivity as compared to that on channel number 2 (receiving the signal from reference probe).

The tracer injection commands of the program were used to trigger the tracer injection circuit by supplying a 5V D.C. signal

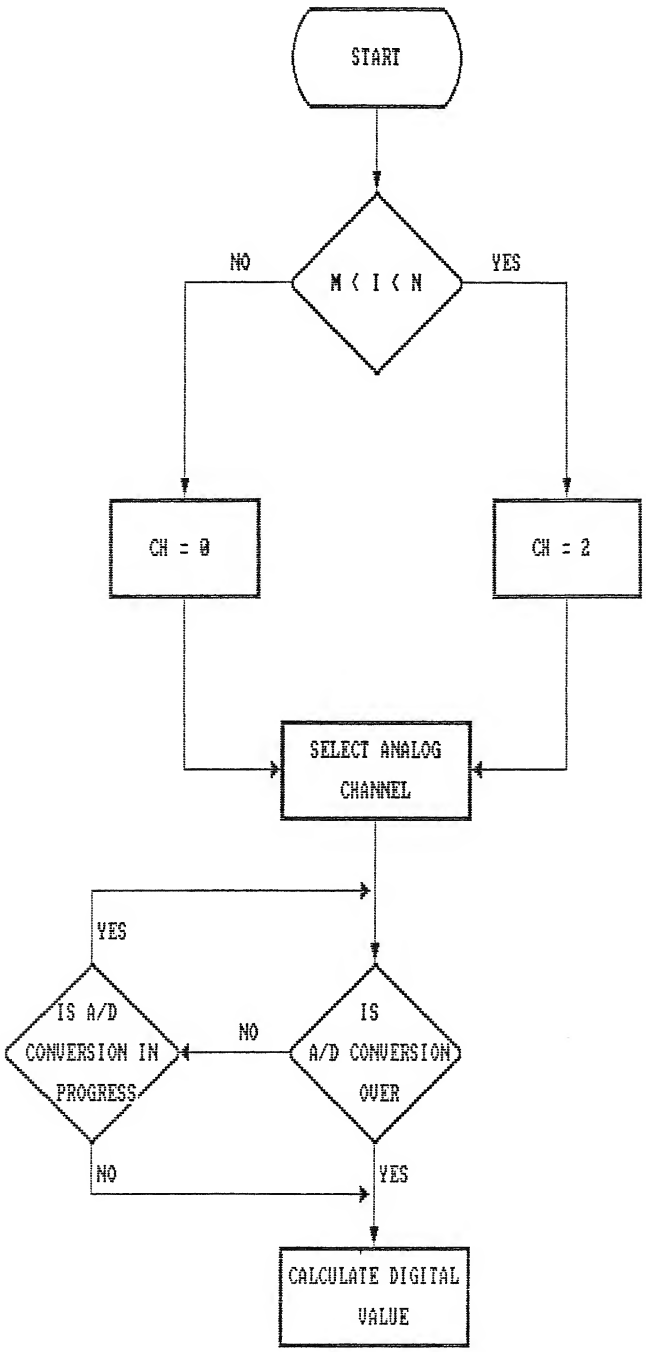

.... continued on page 43

Fig. 4.8: Algorithm to coordinate the process of tracer injection, data acquisition and the data processing

Fig. 4.8 continued .....

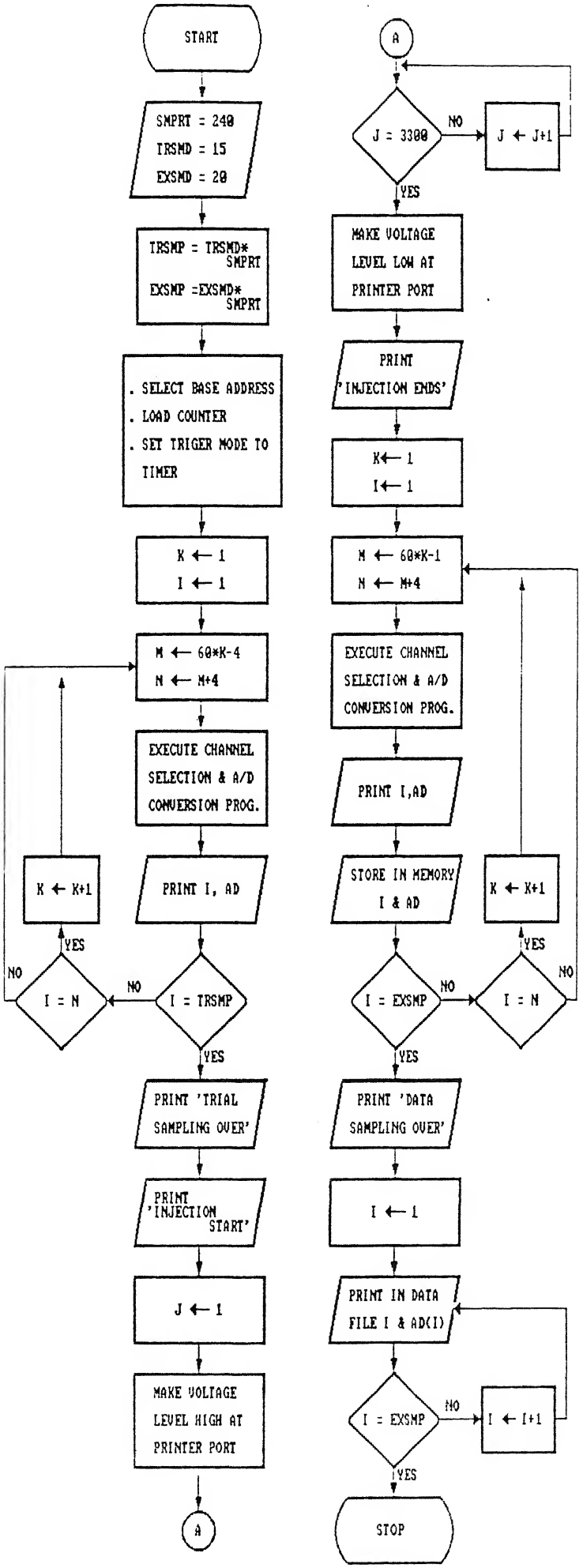

through the printer port of the computer. The time duration for this signal was fixed with the help of a Do-loop (i.e. by counting a number, J from 1 to any specified value). This time duration was kept slightly more than the time taken for complete tracer injection. After the tracer injection, the channel selection and sampling commands were again executed. After each conversion the value was stored in memory. After the experimental sampling duration, given at the start of the program, the digital values were transferred from computer memory to the data file.

4.2 CALIBRATION

4.2.1 Probe

The calibration of the probe along with it's conductivity meter was performed by using a 0.1N potassium chloride solution. The temperature of the solution was measured and it's conductivity value was noted from the reference. The probe was immersed into 0.1N solution and the cell constant knob was adjusted to match the conductivity value given by conductivity meter with the known conductivity value. The cell constant for both the probes was within the range 0.9 to 1.0. Whenever the platinum foils of probes were recoated with platinum black, the calibration was repeated.

4.2.2 Tracer Concentration

In the experiments, conductivity was measured. The

relationship between conductivity (Ω) and tracer concentration (c) was determined as follows:

The potassium chloride solutions of different concentrations $1x10^{-2}$, $2x10^{-2}$, $3x10^{-2}$, $4x10^{-2}$, $5x10^{-2}$ and $6x10^{-2}$ g/l were prepared by using tap water. The conductivity of these solutions was measured with main probe and that of tap water with reference probe. It was ensured that temperature of solutions and tap water was same during conductivity measurements. The conductivity of solutions due to potassium chloride (i.e. obtained by subtracting conductivity of tap water from the conductivity of potassium chloride solutions) was plotted against the concentration of solution as shown in Fig. 4.9. The following relationship was obtained by least square analysis.

$$c = 4.62x10^{2}\Omega \qquad (4.1)$$

Here c is in g/l and Ω is in ohm^{-1} cm^{-1}. The variation of temperature of water within the experimental range of 22 to 27°C, was found to have no effect on the above correlation.

4.3 PROCEDURE

A typical experiment was carried out in the following way: For RTD study, probes were fixed as shown in the Fig. 4.1. Depending upon whether FP or RTD study was to be done, 20ml solution of methylene blue (strength = 15g/l) or potassium chloride (strength = 200g/l) was filled into the plastic syringe.

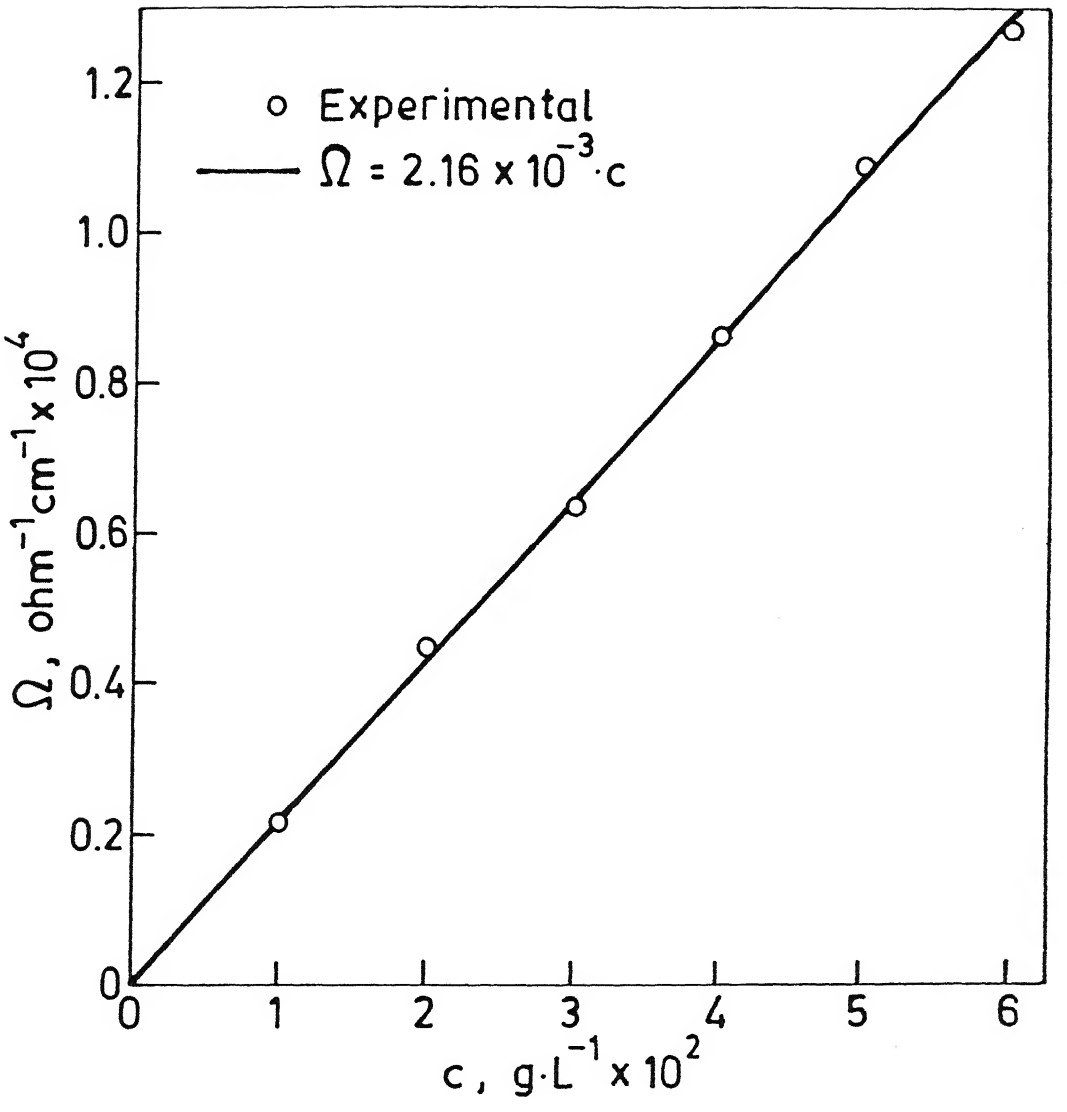

Fig.4.9: Calibration of conductivity probe.

The syringe filled with the tracer solution was placed in between the cylinder-piston assembly and collector pipe, with its needle inserted into the brass tube of collector pipe as shown in the Fig. 4.1. The head of the piston of cylinder-piston assembly was moved forward to make it just touch the plunger of the syringe.

In the storage tank water was filled upto the required level and taken into the overhead cylindrical vessel by running the water pump. The water from cylindrical vessel was further supplied to the tundish and recirculated via tray into the storage tank. Water levels in the cylindrical vessel (800mm) and in the tundish were maintained with the help of valves V2 and V3 respectively. After this the procedure was adopted according to the study (i.e. FP or RTD) to be made.

4.3.1 Flow Pattern

The recirculation of water was continued for 15 minutes to establish a steady state flow field in the tundish. Recirculation was then stopped and the tundish was operated in a flow through mode. The software program was run on the computer only for executing the tracer injection command. Tundish was illuminated to take photographs at a regular interval of time and/or to make video film.

4.3.2 Residence Time Distribution

The experimental sampling duration (i.e. EXSMD) in the

software program was fixed to 2.2 times the theoretical residence time of water flowing in the tundish. This was done to ensure the exit of most of the tracer through the tundish nozzle. The program was executed and recirculation was stopped and tundish was operated in a flow through mode. After the tracer injection, the experiment was continued for the time EXSMD, as discussed before. The conductivity value during the experiment was continuously getting displayed on the monitor of microcomputer.

On completion of the experiment, the water flow into and out of the tundish was stopped. The tundish water was stirred thoroughly to mix the tracer uniformly and the average conductivity of water was measured at the tundish exit. This value of conductivity was later used to determine the amount of tracer left in the tundish after the experiment.

4.4 EXPERIMENTAL VARIABLES

The behaviour of water flowing in the tundish was studied for a wide range of design and operating parameters. The experiments were performed with three different types of inlet streams: submerged, open and air shrouded stream . The different combinations of variables are characterised in Table 4.1 for experiments with tundishes without flow modifiers.

Several experiments are performed by using FMs. Weir, dam and slotted dam of different sizes and configurations were used in the present study for submerged and open stream pouring. All

Table 4.1 : Characterization of Combination of Tundish Design and Operating Parameters.

Run	Bath Dimensions (m)				Water Volume	Operating Parameters			
	L_t	L_b	W	H	$m^3 x10^{-3}$	L_{ie} (m)	Q $m^3 s^{-1} x10^{-4}$	h (m)	t (s)
ST1-1/OT1-1 & AT1-1	1.140	1.000	0.310	0.260	86.2	0.780	1.55	0.039	556
ST1-1D	1.140	1.000	0.310	0.260	86.2	0.780	1.55	0.221	556
ST1-1N	1.140	1.000	0.310	0.260	86.2	0.780	1.55	0.039	556
ST1-1S	1.140	1.000	0.310	0.260	86.2	0.780	1.55	0.039	556
ST1-2	1.140	1.000	0.310	0.340	114.9	0.780	1.55	0.039	742
ST1-3	1.140	1.000	0.310	0.180	61.4	0.780	1.55	0.039	377
ST1-4	1.140	1.000	0.310	0.260	80.6	0.780	1.55	0.039	520
ST1-5	1.140	1.000	0.310	0.260	86.2	0.680	1.55	0.039	556
ST1-6	1.140	1.000	0.310	0.260	86.2	0.880	1.55	0.039	556
ST1-7	1.140	1.000	0.310	0.260	86.2	0.780	2.33	0.039	370
ST1-8	1.140	1.000	0.310	0.260	86.2	0.680	3.22	0.039	268
ST1-9	1.140	1.000	0.310	0.260	86.2	0.780	3.22	0.039	268
ST1-10	1.140	1.000	0.310	0.260	86.2	0.880	3.22	0.039	268
ST1-11/ AT1-11	1.140	1.000	0.262	0.260	72.9	0.760	1.55	0.039	470
ST1-12/ AT1-12	1.140	1.000	0.215	0.260	59.8	0.780	1.55	0.039	386
ST1-13	1.140	1.000	0.187	0.260	52.0	0.780	1.55	0.039	336
ST1-14	1.140	1.000	0.167	0.260	46.5	0.780	1.55	0.039	300
ST1-15	1.140	1.000	0.150	0.260	41.7	0.780	1.55	0.039	269
ST1-16	1.182	1.000	0.150	0.340	55.6	0.780	1.55	0.039	359
ST1-17	1.096	1.000	0.150	0.180	28.3	0.780	1.55	0.039	183
ST1-18	1.140	1.000	0.150	0.260	41.7	0.680	1.55	0.039	269
ST1-19	1.140	1.000	0.150	0.260	41.7	0.880	1.55	0.039	269
ST1-20	1.140	1.000	0.135	0.260	37.6	0.780	1.55	0.039	242
ST1-21/ AT1-21	1.140	1.000	0.120	0.260	33.4	0.780	1.55	0.039	215
ST1-22	1.096	1.000	0.120	0.180	22.6	0.780	1.55	0.039	146
ST1-23	1.064	1.000	0.120	0.120	14.9	0.780	1.55	0.039	96
ST1-24	1.140	1.000	0.072	0.260	20.0	0.780	1.55	0.039	129
ST1-25	1.140	1.000	0.072	0.260	20.0	0.680	1.55	0.039	129
ST1-26	1.140	1.000	0.072	0.260	20.0	0.880	1.55	0.039	129
ST2-1	1.140	1.000	0.310	0.260	86.2	0.880	1.55	0.039	556
ST2-2	1.070	1.000	0.150	0.130	20.1	0.680	1.55	0.039	130
ST2-3	1.070	1.000	0.150	0.130	20.1	0.880	1.55	0.039	130
ST2-4	1.070	1.000	0.072	0.130	09.7	0.680	1.55	0.039	62
ST2-5	1.070	1.000	0.072	0.130	09.7	0.880	1.55	0.039	62

Explanation:

T stands for tundish
First digit after T : Number of outlets ; 1 single and 2 two
Second digit after T : Characterization number
S, O and A for submerged, open and air shrouded inlet stream
ST1-1N nozzle controlled exit flow. In others by stopper rod
ST1-1S Themocole sheet is used.

Table 4.2 : Characterization of type and Configuration of Flow Modifiers

Configuration	Type of Flow Modifier			
	Weir (w)		Dam (D)	
	w_p (m)	w_h (m)	d_p (m)	d_h (m)
W11	0.05	0.038		
W12	0.05	0.104		
W13	0.05	0.156		
W14	0.05	0.208		
W21	0.15	0.038		
W22	0.15	0.104		
W23	0.15	0.156		
W24	0.15	0.208		
W32	0.25	0.104		
W42	0.35	0.104		
W53	0.095	0.156		
D11			0.05	0.013
D12			0.05	0.038
D13			0.05	0.065
D14			0.05	0.091
D15			0.05	0.143
D16			0.05	0.190
D17			0.05	0.247
D21			0.15	0.013
D22			0.15	0.038
D23			0.15	0.065
D24			0.15	0.091
D25			0.15	0.143
D26			0.15	0.190
D27			0.15	0.247
D34			0.25	0.091
D44			0.35	0.091
D52			0.095	0.038
D54			0.095	0.091
D62			0.195	0.038
D64			0.195	0.091

Conttd...

Table 4.2 : Characterization of type and Configuration of Flow Modifiers (Conttd.)

Configuration	Type of Flow Modifier					
	Weir (w)		Dam (D)		Slotted dam (SD)	
	w_p (m)	w_h (m)	d_p (m)	d_h (m)	SD_p (m)	SD_h (m)
SD11					0.05	0.182
SD21					0.15	0.182
SD21D24			0.25	0.091	0.15	0.182
SD31D44			0.35	0.091	0.25	0.182
W12D21	0.05	0.104	0.15	0.013		
W12D22	0.05	0.104	0.15	0.038		
W12D23	0.05	0.104	0.15	0.065		
W12D24	0.05	0.104	0.15	0.091		
W12D25	0.05	0.104	0.15	0.143		
W12D26	0.05	0.104	0.15	0.190		
W12D27	0.05	0.104	0.15	0.247		
W13D21	0.05	0.156	0.15	0.013		
W13D22	0.05	0.156	0.15	0.038		
W13D24	0.05	0.156	0.15	0.091		
W13D23	0.05	0.156	0.15	0.143		
W11D24	0.05	0.038	0.15	0.091		
W14D24	0.05	0.208	0.15	0.091		
W22D34	0.15	0.104	0.25	0.091		
W32D44	0.25	0.104	0.35	0.091		
W12D24	0.054	0.104	0.158	0.091		
W32D44	0.25	0.104	0.35	0.091		
W53D64	0.095	0.156	0.195	0.091		

Explanation : First Word : Type of flow modifier e.g.
w = Weir, D = Dam, SD = Slotted dam
First digit : Position from inlet stream
Second digit : Height of FM

Example : W11 : Position of Weir is 0.05m and height 0.38m
W12D21 : It is weir+dam combination. Postion of weir is 0.05m and its height 0.104m and position of dam is 0.15m and its height is 0.013m. Both positions are measured from the inlet stream.

In the above way the other configuration numbers can be understood.

types and configurations of FMs are classified in Table 4.2.

4.5 ANALYSIS OF DATA

All the conductivity vs time data recorded by the data acquisition system were used to calculate the tracer concentration vs time, mass of the tracer out and to obtain a normalized RTD-curve. The mean residence time and variance are also determined. In Appendix - 2 the computer program is given which is used to calculate the above mentioned parameters. The procedure is described in the following:

4.5.1 Normalized RTD-Curve

The conductivity values were converted into concentration by Eq. 4.1. The dimensionless concentration and time were calculated by:

$$\text{Dimensionless concentration } C_i = \frac{c_i}{M_i} \times V \qquad (4.2)$$

and

$$\text{Dimensionless time } \tau_i = \frac{t_i}{\bar{t}} \qquad (4.3)$$

The dimensionless concentration was plotted against time and the curve so obtained is termed as RTD-curve. This curve is also known as C-Curve.

4.5.2 Mass Balance

In experiments, all the tracer did not come out of the tundish at the end of experiments, i.e., some amount of tracer remained always in the tundish. The mass balance of the tracer is given by

$$M_i = M_e + M_r \tag{4.4}$$

The mass of the tracer which exited the tundish during an experiment was determined by

$$M_e = \sum_{i=1}^{N} c_i \, \Delta t \tag{4.5}$$

Here N is the total number of readings of concentration c_i. All the experiments are performed for time duration 2.2 times theoretical residence time (theoretical residence time of all experiments is given in Table 4.1)and with 240 samples per minute, the value of N is $8.8x\bar{t}$. The value of Δt is 0.25s. With the above values, M_e is calculated. Mass of the tracer remaining in the tundish, i.e. M_r, is calculated by Eq. 4.1. Rewriting Eq. 4.1 in terms of gram of tracer, we get

$$M_r = 4.62x10^2 \, \Omega_{ag} V \tag{4.6}$$

By Eqs. 4.4, 4.5 and 4.6, the mass balance of the tracer was carried out. Table 4.3 shows the mass balance calculations for some runs. It can be seen that 92-97% of the total amount of

Table 4.3 : Mass balance of the tracer injected into the tundish

Run	d (mm)	M_e (g)	M_r (g)	$\left(\frac{(M_e+M_r)}{M_i}\right)$ x 100
ST1-1	22.2	3.706	0.163	96.72
ST1-1	10.0	3.654	0.187	96.02
OT1-1	-	3.605	0.159	94.10
AT1-1	-	3.515	0.183	92.45
ST1-1D	22.2	3.541	0.203	93.06
ST1-1N	22.2	3.638	0.147	94.62
ST1-1S	22.2	3.625	0.183	95.20
ST1-2	22.2	3.157	0.170	92.17
ST1-3	22.2	3.661	0.151	95.30
ST1-4	22.2	3.495	0.194	92.22
ST1-5	22.2	3.653	0.191	96.10
ST1-6	22.2	3.581	0.155	93.40
ST1-7	22.2	3.575	0.143	92.95
ST1-8	22.2	3.585	0.163	93.70
ST1-9	22.2	3.613	0.187	95.00
ST1-10	22.2	3.621	0.195	95.38
ST1-11	22.2	3.685	0.162	96.17
ST1-11	10.0	3.681	0.162	96.07
AT1-11	-	3.553	0.192	93.62
ST1-12	22.2	3.695	0.160	96.37
ST1-12	10.0	3.613	0.146	93.97
AT1-12	-	3.617	0.174	94.77
ST1-13	22.2	3.723	0.132	96.37
ST1-14	22.2	3.654	0.159	95.32
ST1-14	10.0	3.577	0.165	93.55
AT1-14	-	3.588	0.142	93.25
ST1-15	22.2	3.681	0.131	95.30
ST1-15	10.0	3.594	0.137	93.27
ST1-16	22.2	3.614	0.154	94.17
ST1-17	22.2	3.569	0.146	92.87
ST1-18	22.2	3.533	0.148	92.02
ST1-19	22.2	3.597	0.141	93.45
ST1-20	22.2	3.678	0.123	95.02
ST1-21	22.2	3.635	0.125	94.00
ST1-21	10.0	3.546	0.169	92.87
AT1-21	-	3.541	0.137	91.95
ST1-22	22.2	3.576	0.140	92.90
ST1-23	22.2	3.538	0.147	92.12
ST1-24	22.2	3.485	0.199	92.10
ST1-24	12.0	3.473	0.206	91.97
ST1-25	22.2	3.480	0.218	92.45
ST1-26	22.2	3.432	0.243	91.87
ST2-1	22.2	3.653	0.187	96.00
ST2-2	22.2	3.548	0.155	92.57
ST2-3	22.2	3.571	0.148	02.97
ST2-4	22.2	3.446	0.217	91.57
ST2-5	22.2	3.495	0.186	92.02

tracer injected could be recovered. Small percent loss of the tracer i.e. 3 to 8% is considered to lay within the range of tracer injection experiments.For other runs of the Table 4.2,the mass balance calculations yielded the same results as reported in the Table 4.3.

4.5.3 Mean Residence Time and Variance

These were calculated as follows:

$$t_{mean} = \frac{\sum_{i=1}^{N} t_i c_i \Delta t}{M_e} \qquad (4.7)$$

and

$$S^2 = \frac{\sum_{i=1}^{N} t_i^2 c_i \Delta t}{M_e} - t_{mean}^2 \qquad (4.8)$$

CHAPTER - 5

EXPERIMENTAL RESULTS

Several experiments were performed to record the mechanism and the variation of concentration of tracer dispersing into water flowing in a tundish without and with flow modifiers for a wide range of design and operating parameters as given in Tables 4.1 and 4.2. The different combinations of variables for a particular experiment are characterized in Table 4.1. Table 4.2 characterizes the different types of configurations of flow modifiers which were used in tundishes T1-1 to T1-26 and T2-1 to T2-5 of Table 4.1 for submerged (S) and open stream pouring (0 or A). Methylene blue was used to record the tracer dispersion by still and cine photography and for visual observations. Whereas potassium chloride was used to know the variation of concentration at the exit of the tundish by recording change in conductivity as a function of time. Several experiments were repeated under identical conditions and it has to mention here that in all cases the results were highly reproducible.

5.1 MECHANISM OF TRACER DISPERSION

Visual and photographic observations had shown that for the inlet stream submerged into water, width of the tundish was the principle parameter governing the tracer dispersion within the tundish. All other combinations of parameters as listed in Table

4.1 (ST1-1 to ST1-26 and ST2-1 to ST2-5) were found to disperse tracer according to the tundish width. Whereas for inlet stream falling through the atmospheric air or air chamber, tundish width was not found to be a significant parameter. Use of flow modifiers of all types and configurations of Table 4.2 were found to influence the tracer dispersion for both types of inlet streams i.e. submerged and open.

5.1.1 Submerged Stream Pouring

5.1.1.1 *Without Flow Modifiers*

Figs. 5.1 to 5.4 contain photographs at different time intervals to show the tracer dispersion in a 310 mm wide tundish for ST1-1, ST1-1D, ST1-2, ST1-4 and ST1-9 combinations. Whereas in Fig. 5.5 tracer dispersion is shown for ST2-1 combination.

Fig. 5.1 shows the tracer dispersion for the Froude number 0.74 (5.1A, ST1-1) and 3.17 (5.1B, ST1-9). The effect of bath height (ST1-12) and that of larger depth of submergence of inlet streams (ST1-1D) on the tracer dispersion are shown in Figs. 5.2 and 5.3. The tracer dispersion in a vertical wall tundish (ST1-4) is shown in Fig. 5.4. All other combinations, i.e. ST1-3 to ST1-8 and ST1-10 were found to behave in a similar way.

In all photographs of Figs. 5.1 to 5.5, we note that the flow is highly turbulent near the inlet region (see the rapid colour dispersion in photograph a of all figures). From the inlet region

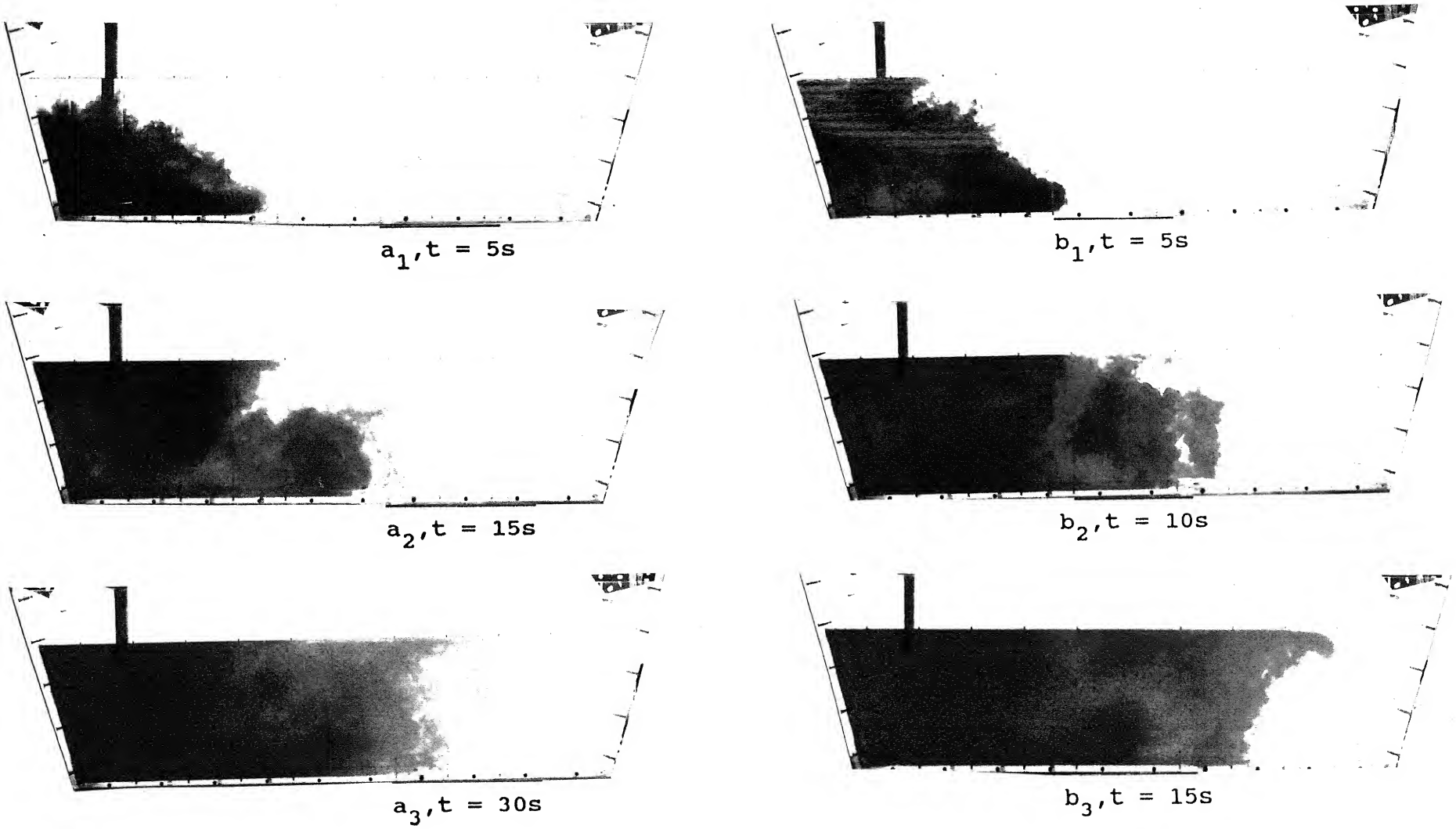

Fig. 5.1 : Effect of Froude number on the tracer dispersion in a 310mm wide tundish (A) Fr= 0.74 of ST1-1 & (B) Fr=3.17 of ST1-9

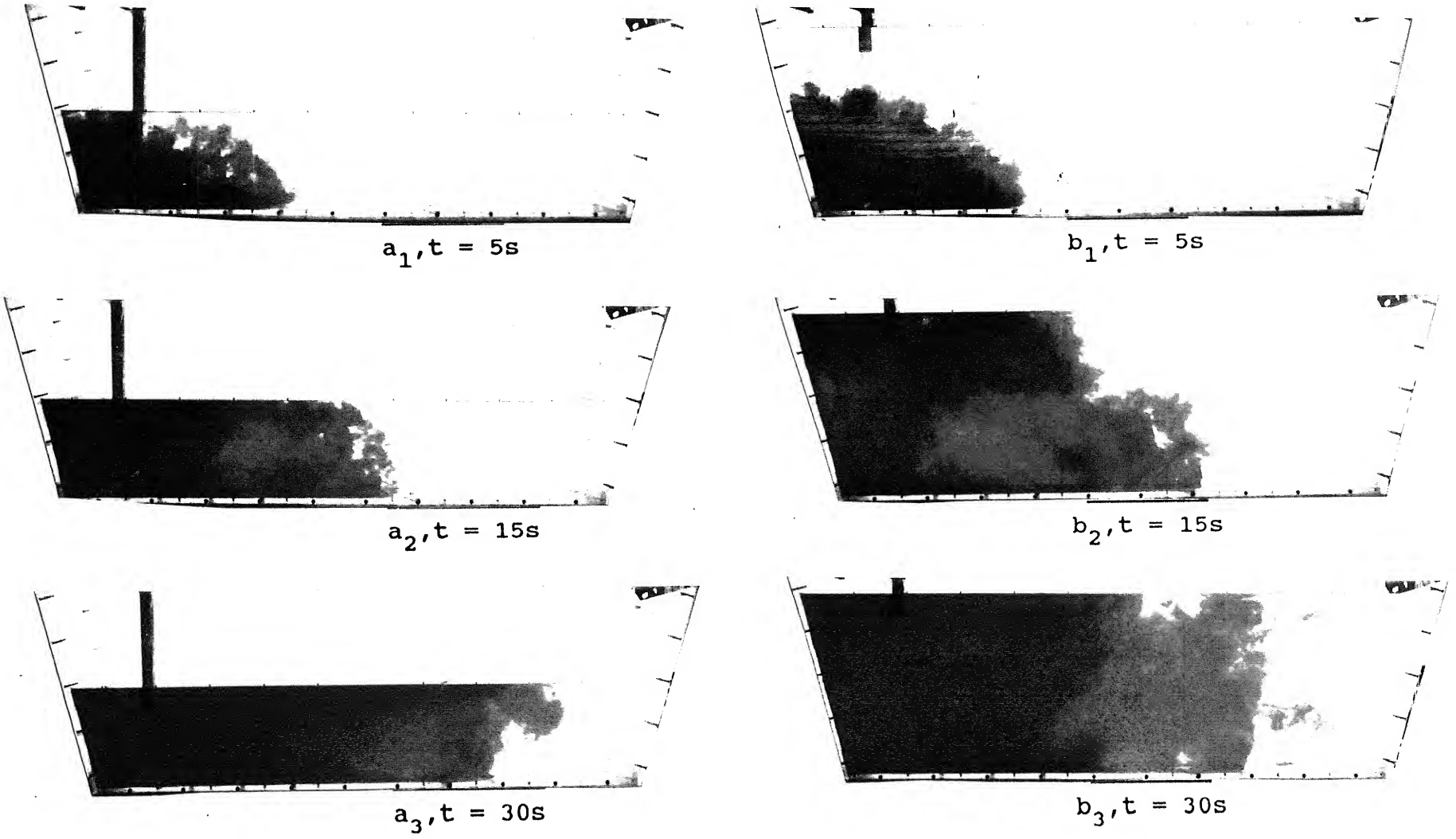

Fig. 5.2 : Effect of bath height on the tracer dispersion in (A) ST1-3, H= 180mm & (B) ST1-2, H=340mm

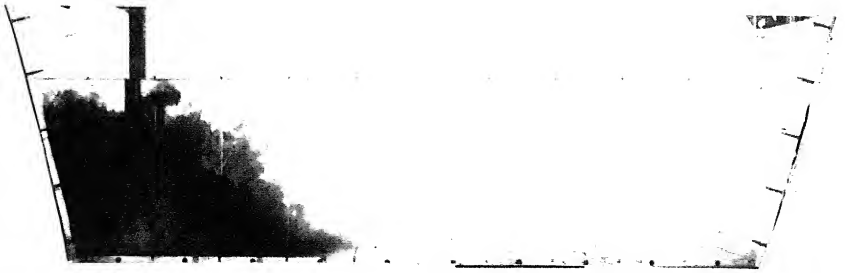

a_1, t = 5s

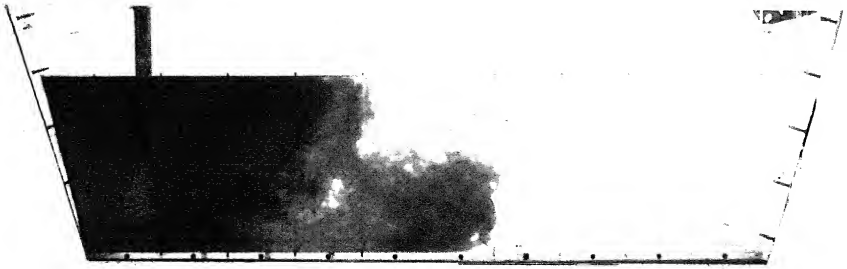

a_2, t = 15s

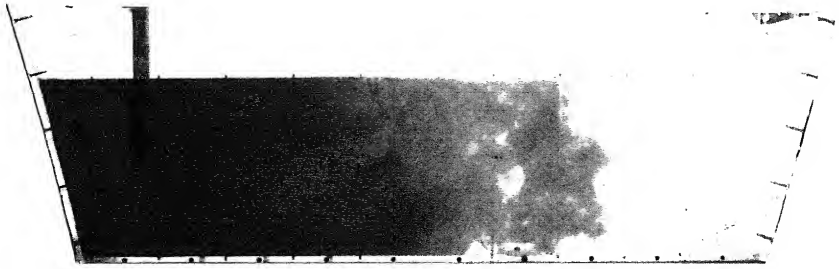

a_3, t = 30s

Fig. 5.3 : Tracer dispersion in ST1-1D tundish for shroud submergence depth = 0.22H

b_1, t = 5s

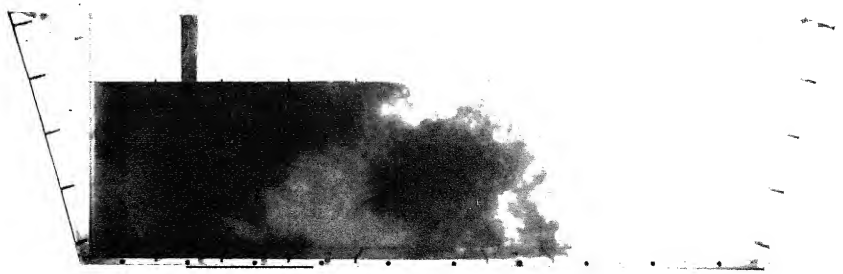

b_2, t = 15s

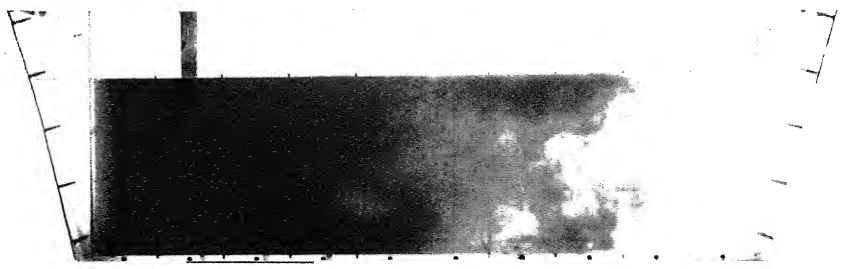

b_3, t = 30s

Fig. 5.4 : Tracer dispersion in a vertical wall ST1-4 tundish

the tracer disperses in all directions. It can further be seen in all photographs that a small portion of the tracer is advancing on the inlet-exit plane straight towards the exit whereas the rest portion of the tracer continues to disperse according to the flow field established in the tundish. The straight movement of the tracer is termed in the following 'short circuiting' of the fluid. In a two strand casting tundish (see Fig. 5.5) it can be seen that the said small portion of the tracer (see intense colour patch in photo a_1 of Fig. 5.5) is advancing straight to the exit on both sides of the inlet streams.

The display of the video taps had shown reversal of the tracer towards the inlet area and recycling of the tracer in the middle of the tundish.

It may further be seen in Fig. 5.5 that for the conditions of the two strand casting tundish, the mechanism of colour dispersion in one half of the tundish is similar to that of the other half which indicates that the flow is symmetrical. Also the rate of advancement and dispersion of colour are much faster than that of single strand casting tundish (compare Fig. 5.1 with 5.5). The faster dispersion of tracer is to be expected since in a two strand casting tundish the tracer disperses on both sides of the inlet stream in comparison to a single strand wherein major portion of the tracer disperses on one side of the inlet stream.

Visual observations had shown that decrease in width below a certain value influences the tracer dispersion. When the width was decreased to 167mm and then further to 72mm, i.e., ST1-14,

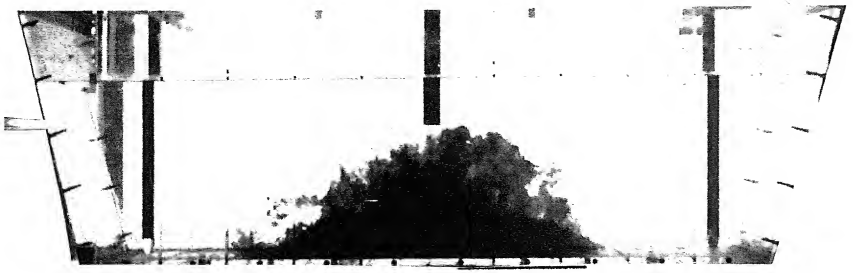

a_1, t = 4s

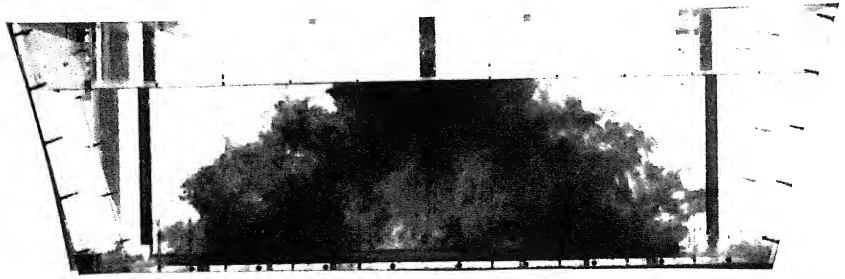

a_2, t = 8s

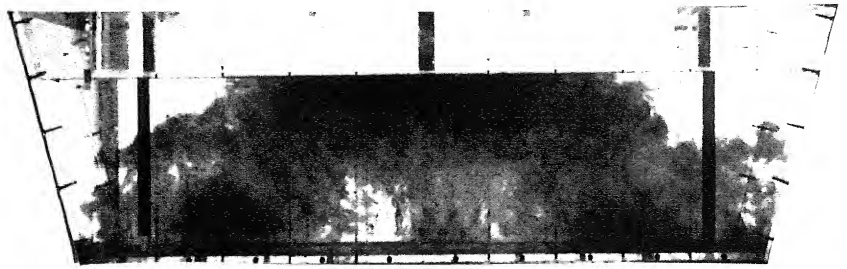

a_3, t = 12s

Fig. 5.5 : Tracer dispersion in a two strand tundish ST2-1

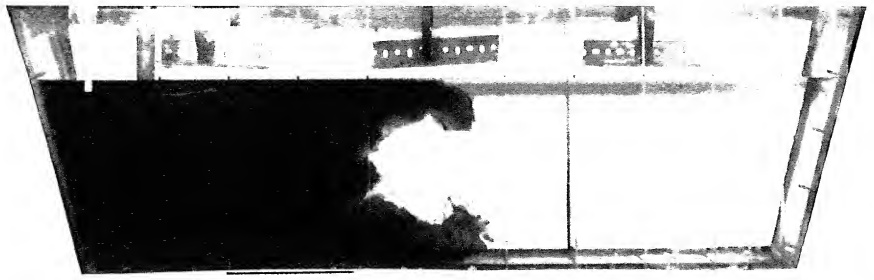

a_1, t = 15s

a_2, t = 30s

Fig. 5.6 : Tracer dispersion in ST1-14 tundish of 167 mm width

ST1-21 and ST1-24 combination, the straight movement of a portion of tracer was not observed towards the exit. For the inlet-exit stream configuration of two strand casting tundish i.e. in ST2 combinations the tracer dispersion was observed to be similar to that of ST1-14 or ST1-21 combination but at much reduced widths. Here when the width was decreased to 150mm the short circuiting was observed but when decreased to 72mm, no such short circuiting could be identified either visually or on the video tape.

As an example, Fig. 5.6 shows tracer dispersion at 15s and 30s for ST1-14 combination. As seen in the photographs, there is no preferential movement of the tracer on the inlet-exit plane as that obtained for 310mm wide tundish (compare Fig. 5.1 with 5.6).

The photographic study indicates clearly that in submerged pouring, tundish width is an important parameter.

5.1.1.2 *With Flow Modifiers*

As seen in photographs presented in section 5.1.1 that flow of the fluid in a relatively wide tundish (310mm width i.e. for combinations ST1-1 to ST1-10) is accompanied by short circuiting for submerged inlet stream conditions. This observation is made for single (ST1 combination) and as well as two strand casting (ST2 combination) arrangements of inlet-exit streams. Whereas narrow tundish (ST1-14, ST1-21 and ST1-24) did not show short circuiting of the fluid. Further, the flow of the fluid was found

to be highly turbulent particularly within the inlet region of the tundish. In case of two strand casting arrangement of inlet-exit stream, the flow of the fluid is more turbulent within the entire tundish than that of single strand casting tundish. Further, the fluid shows low tendency to flow towards the free surface.

Thus flow modifiers are employed to meet the following objectives:

i) To eliminate the short circuiting of the fluid.

ii) To create the surface directed flow.

iii) To confine turbulence intensity of the inlet stream within the inlet region so that flow field becomes relatively laminar in the rest of the tundish.

Different types and configurations of flow modifiers are employed in tundishes of combinations ST1-1 to ST1-26 and ST2-1 to ST2-5 for submerged pouring. The types and configurations of flow modifiers are already characterized in Table 4.2. In the following the effects of different types of FMs on tracer dispersion is described:

(A) *Influence of Weir*

Fig. 5.7 shows the influence of weir on the rate of advancement and dispersion of methylene blue in tundish of ST-1

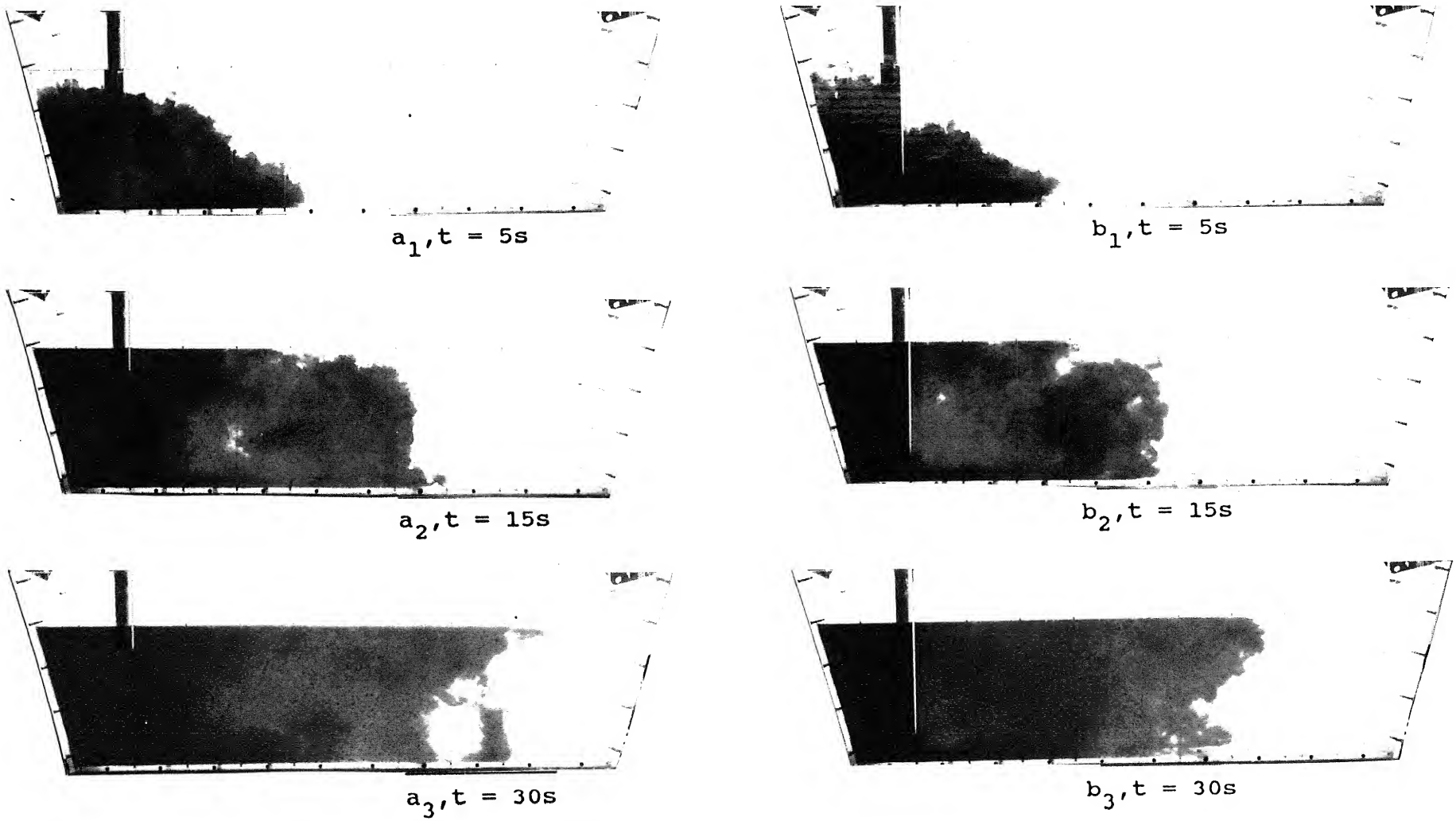

Fig. 5.7 : Influence of weir height on the tracer dispersion in ST1-1 tundish (A) W11 and (B) W14 configuration

combination for W11 (5.7A) and W14 (5.7B) configurations. Whereas in Fig. 5.8 the effect of position of weir is shown for W12 (5.8A) and W32 (5.8B) configurations.

In Fig. 5.9 the tracer dispersion is shown in ST2-1 tundish with W53 configuration placed on both sides of the inlet stream. The following observations are made:

i) Tracer dispersion in ST1-1 or ST2-1 with weir is essentially similar to those of without weir. Here also the straight movement of the tracer towards the nozzle exit is discernible on the horizontal plane near the bottom of the tundish (see photographs a_2 and b_2 of Figs. 5.7 and 5.8 and a_2 of 5.9). Thus, weir is not found to eliminate short circuiting in the tundish fluid flow system.

ii) The turbulence intensity of the inlet stream is not found to be restricted within the inlet region (see the rapid colour dispersion and its spread in the tundish in photographs 5.7 to 5.9) as a consequence of which the turbulence spreads in the rest of the tundish.

iii) Tracer dispersion in a two strand casting tundish is much faster than that of single strand one. For example in Fig. 5.9, the tracer reached the exit of east- and westside walls in 8s as compared to that of Fig. 5.8A where the tracer seems to appear in 30s at the exit.

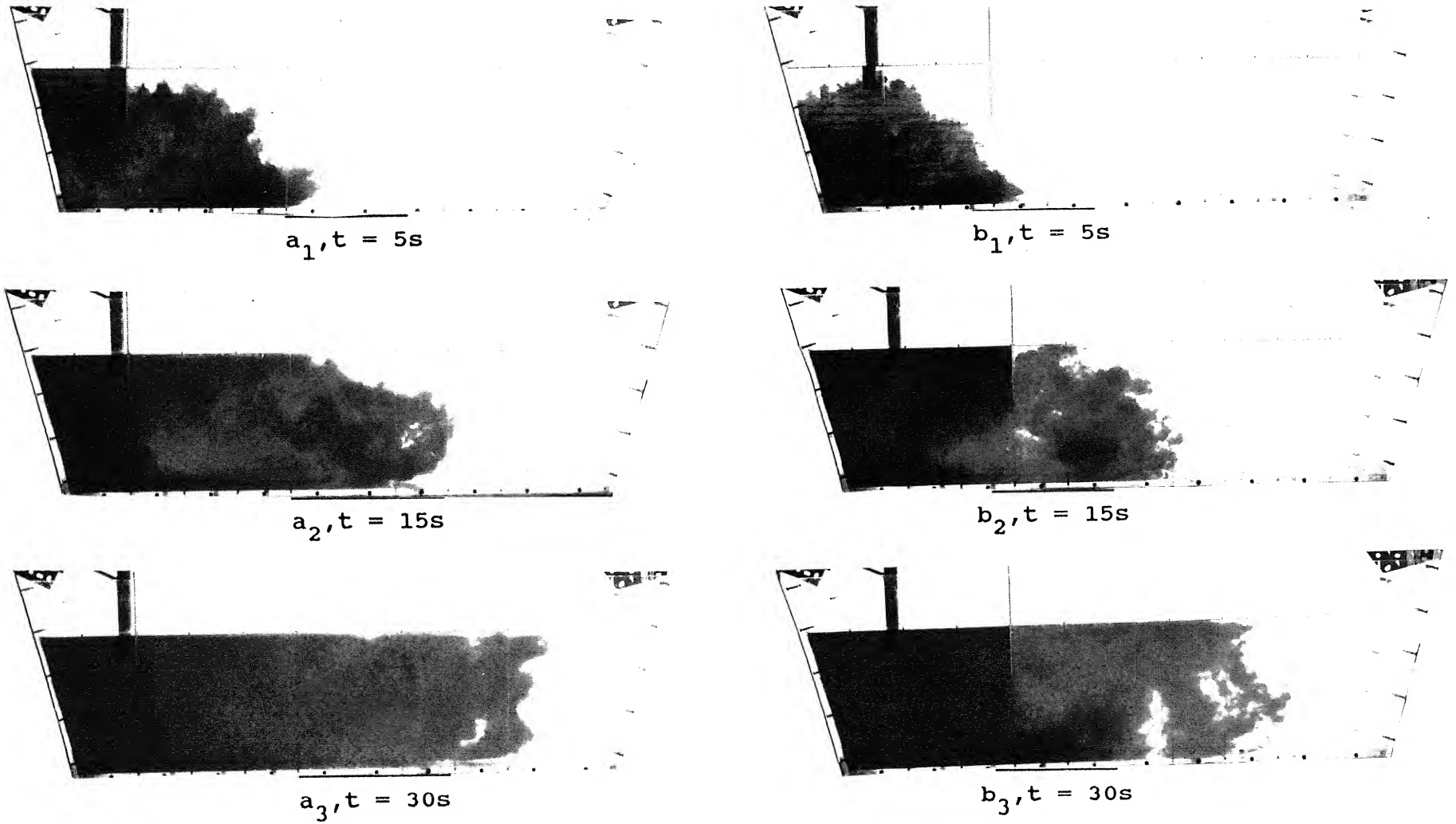

Fig. 5.8 : Influence of the position of the weir on the tracer dispersion in ST1-1 tundish (A) W12 and (B) W32 configuration

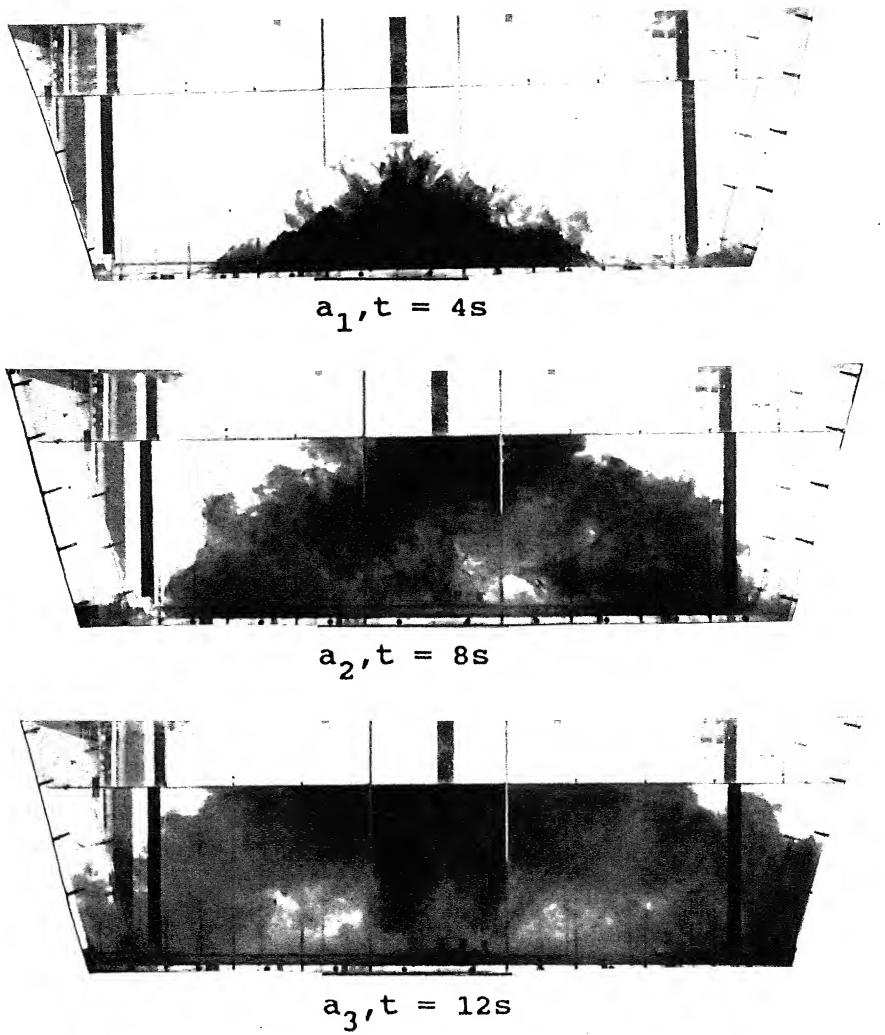

a_1, t = 4s

a_2, t = 8s

a_3, t = 12s

Fig. 5.9 : Tracer dispersion in a ST2-1 tundish for W53 configuration

(B) *Influence of Dam*

Figures 5.10 and 5.11 contain typical photographs of the tracer dispersion in presence of dam for ST1-1 tundish. Other tundishes of Table 4.1 showed the behaviour of tracer dispersion similar to those of above figures. Fig. 5.10 shows the effect of position of dam for D14 and D34 configurations. In Fig. 5.11 the effect of dam height is shown for D12 and D17.

We note that the tracer in the tundish downstream of the dam is visible only when water upstream of the dam gets coloured (see photos b_1 of Fig. 5.10). The region of the tundish upstream of the dam acts like a source of transfer of the kinetic energy of the inlet stream into the rest of the tundish in contrast to photographs in Figs. 5.1 to 5.6 in which energy is dissipated from the point of impingement of the inlet stream. Thus, the dam restricts the turbulence of the inlet stream within the inlet region as a consequence of which the fluid flow becomes uniform in the rest of the tundish. Placing dam more away from the inlet stream (see photo a_1 and a_2 and b_1 and b_2 of Fig. 5.10) increases the cross section of the region upstream the dam on account of which the inlet stream turbulence intensity gets dampened more which results in more uniform flow in the rest of the tundish.

The dam forces the water of the inlet stream to move towards free surface before it is transferred into the tundish on the downstream side of the dam. Over the top edge of the dam the fluid flows in all directions i.e. towards bottom, tundish nozzle exit and everywhere in the rest of the tundish. Thus, the

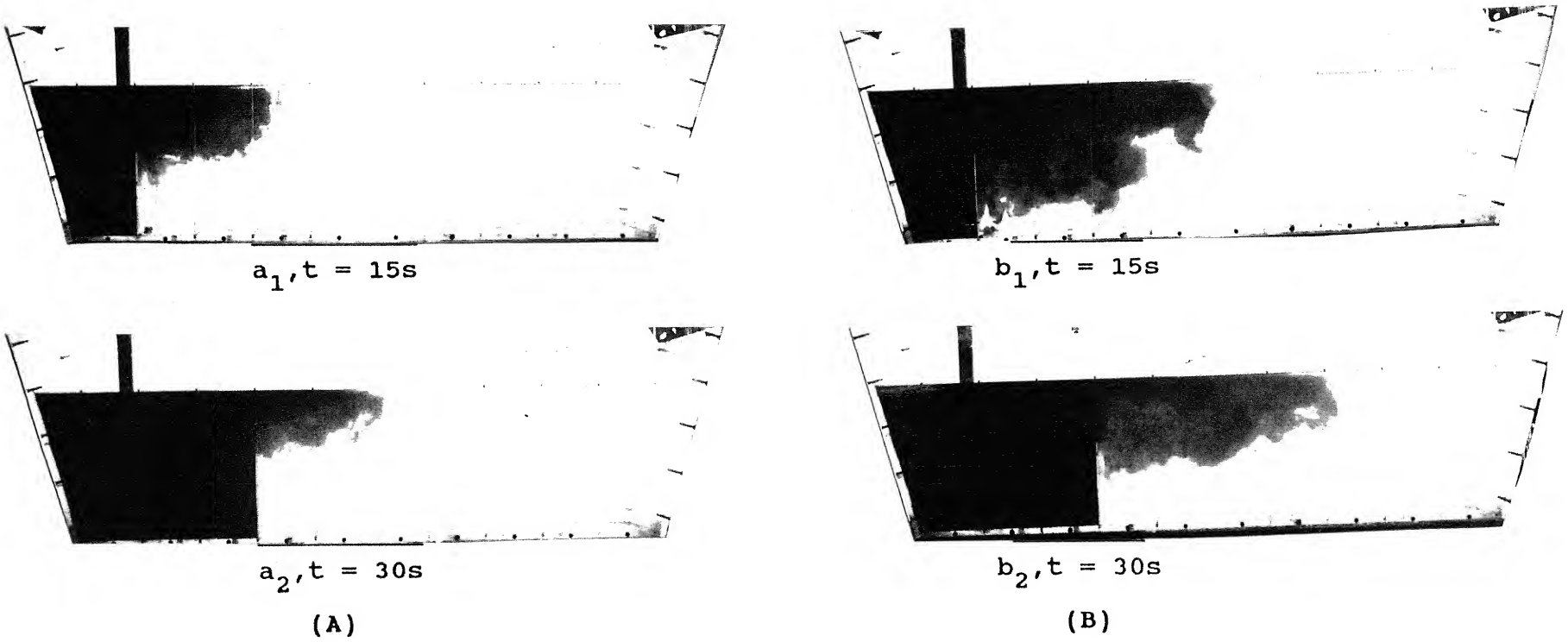

Fig. 5.10 : Influence of the position of the dam on the tracer dispersion in ST1-1 tundish (A) D14 and (B) D34 configuration

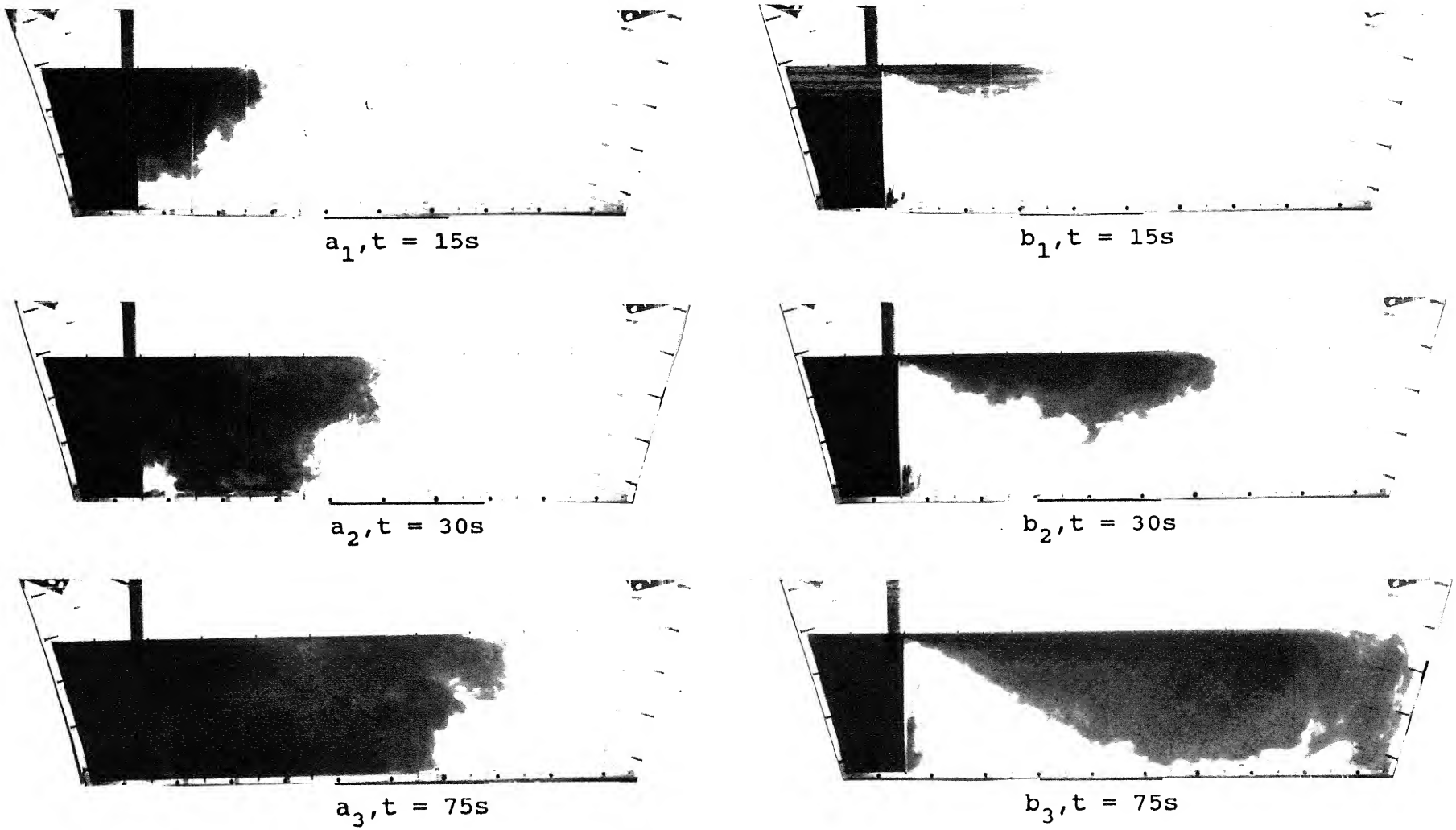

Fig. 5.11 : Influence of the height of the dam on the tracer dispersion in ST1-1 tundish (A) D12 and (B) D17 configuration

straight movement of the tracer towards the nozzle exit is eliminated completely which results in increase in tendency of the fluid to flow towards surface. Further the extent of this upward directed flow was found to depend on the height of dam (see photos a_1, a_2 and a_3 and b_1, b_2 and b_3 of Fig. 5.11). From the top surface layers, the fluid flows downwards in the z direction. From the type of photographs given in Figs. 5.10 and 5.11, the distance in the x direction from the dam over which the blue colour persists is measured at different intervals of time. Similarly, the distance in the z-direction from the top surface is measured. The ratio of these distances, i.e. x/z, is plotted in Fig. 5.12 as a function of dimensionless dam height for different times after the start of tracer injection. As can be seen, the ratio x/z increases as the dam height increases, which implies that the increase of the rate of movement of liquid at the top surface in the x direction is greater than in the z-direction.

The photographs of Fig. 5.11 show further that the increase of dam height increases the dead volume of liquid in the tundish (see the regions adjacent to the dams on the downstream side).

In Fig. 5.13, tracer dispersion is shown for ST2-1 tundish with D52 configuration. It can be seen in the photograph that the dam restricts the inlet stream turbulence within the inlet region. The flow downstream the dam is surface directed. It can be noted that the tracer is not able to arrive at the exit, even 24s after the start of tracer injection as compared to 8s in case of without dam (see photographs a_3 in Figs. 5.13 and 5.5). On the downstream side of the dam, it can be seen that near the dam the tracer is

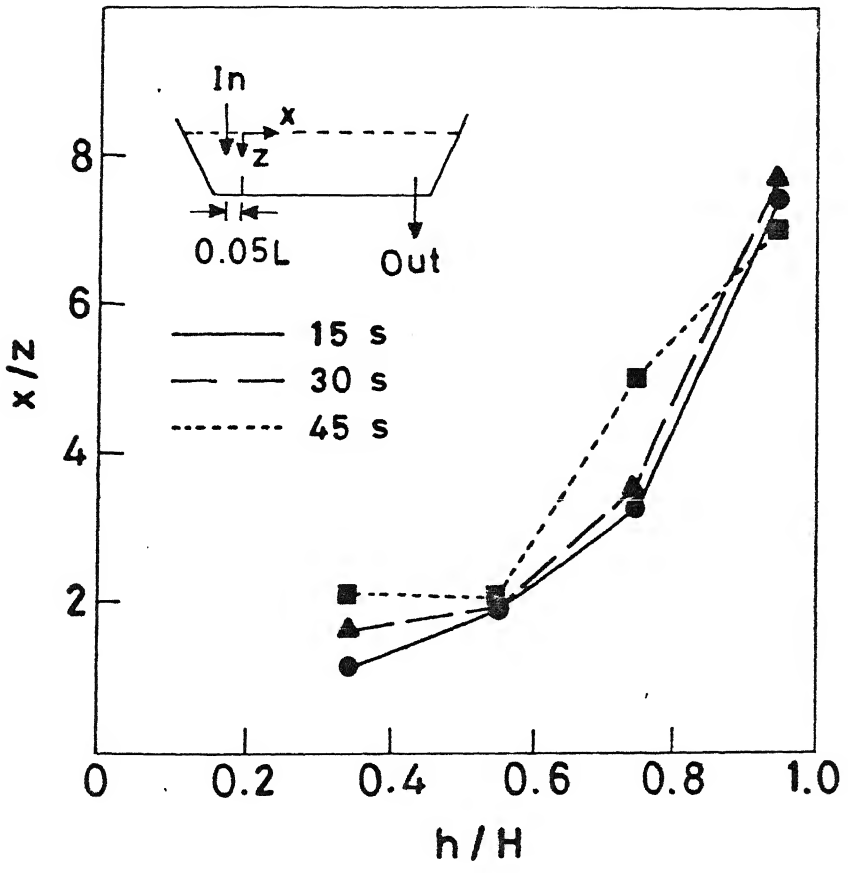

Fig.5.12: Ratio of the color advancement in x-direction to that in z-direction as a function of dam height at different times after the tracer injection.

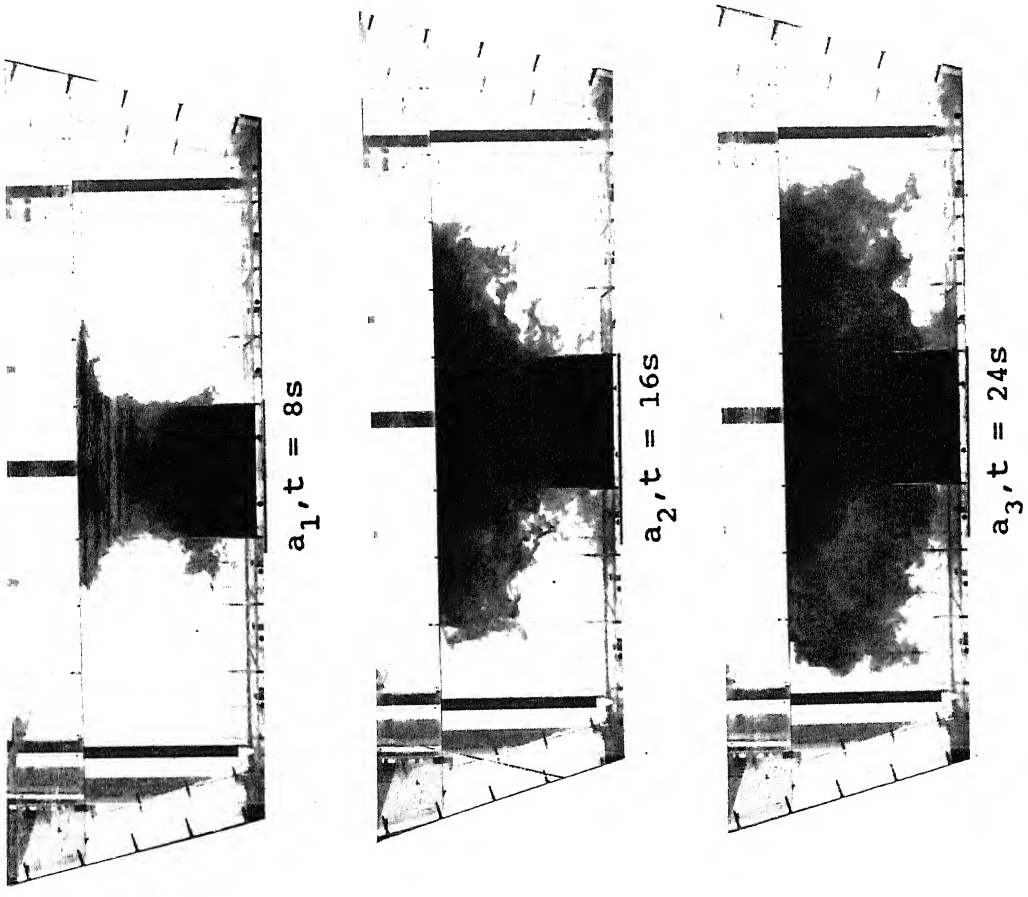

Fig. 5.13 : Tracer dispersion in a ST2-1 tundish for D53 configuration

taking long time to disperse (see photographs a_2 and a_3). It seems that the fluid velocities are lower in this region as compared to the rest of the tundish and this region can be termed as dead one in comparison to the other regions.

(C) *Influence of Combinations*

Several photographs were obtained by placing weir or slotted dam of different sizes in between inlet stream and dam in ST1 and ST2 tundishes. For the sake of illustration, Fig. 5.14 shows some photographs of tracer dispersion in ST1-1 tundish for W11D24 (a_1 and b_1), W12D26 (a_2 and b_2) and W12D24 (a_3 and b_3) weir + dam configurations. In Fig 5.15, tracer dispersion is shown in ST2-1 tundish with W53D64 weir + dam configuration. The following observations can be made from the photographs:

i) In both T1 and T2 tundishes the tracer dispersion is somewhat similar to that of dam alone (compare photographs 5.11 with 5.14 and 5.13 with 5.15).

ii) The surface directed component of the liquid and the surface velocity (i.e. on the xy-plane at Z = H) is observed to be somewhat greater for Weir + Dam than that for dam (compare the intensity and the region of the colour of the tracer downstream the dam in a, b, of the Fig 5.14 with a_1,a_2 or b_1,b_2 of Fig. 5.11).

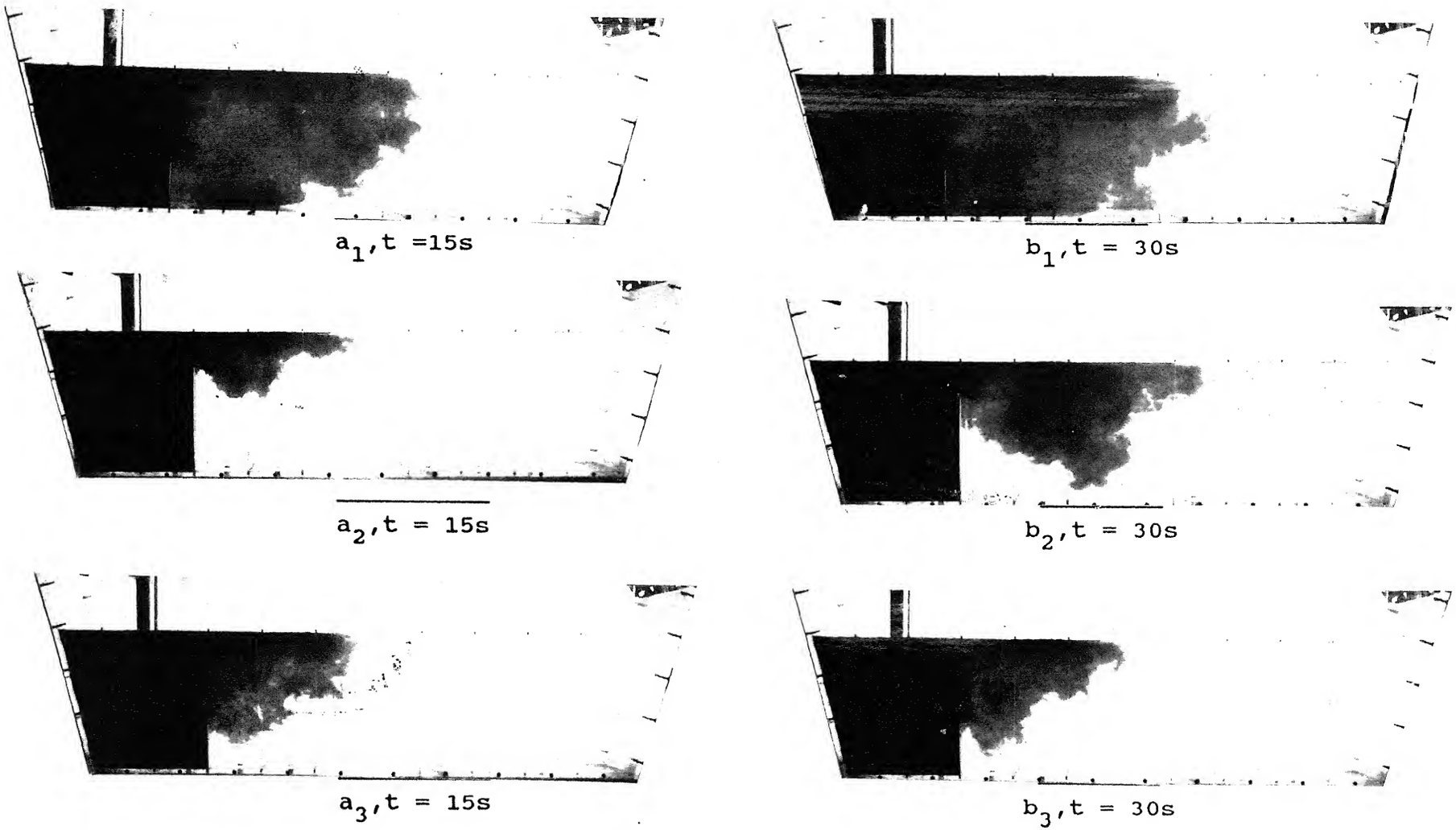

Fig. 5.14 : Tracer dispersion in ST1-1 tundish with weir+dam for different sizes of wier and dam a_1b_1 for W11D24, a_2b_2 for W12D26 and a_3b_3 for W12D24.

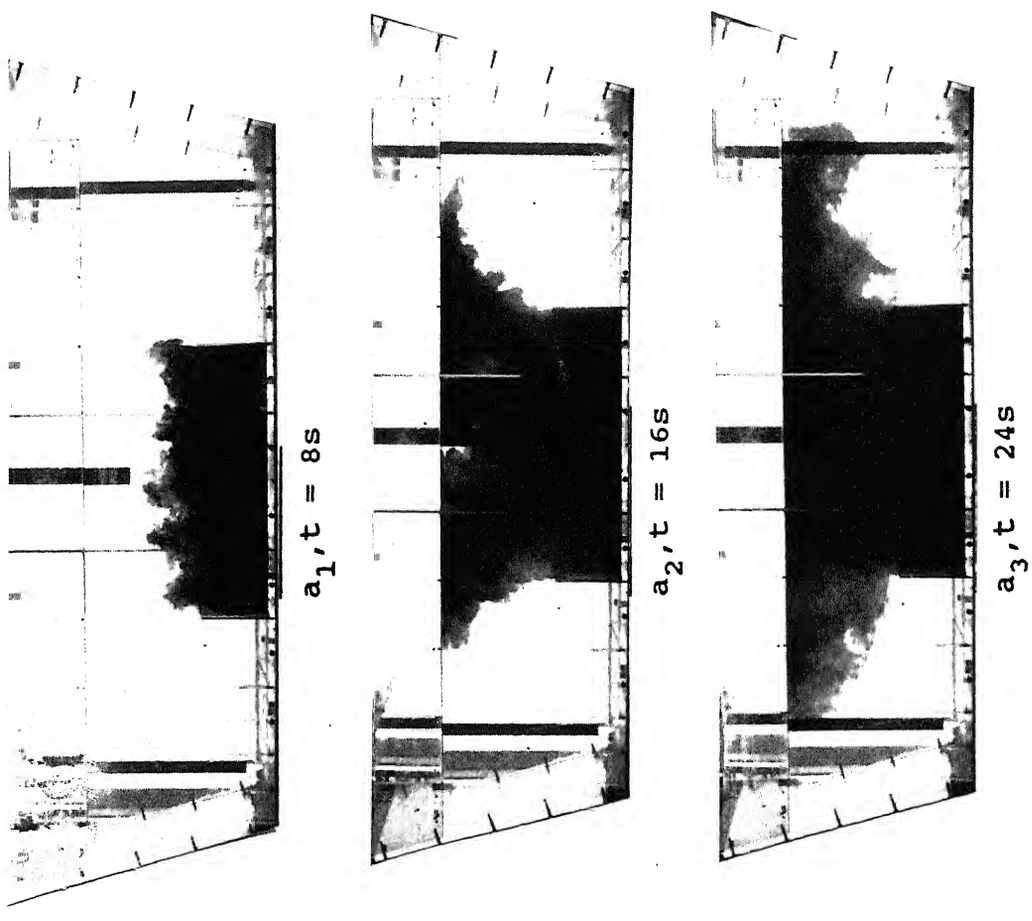

Fig. 5.15 : Tracer dispersion in a ST2-1 tundish for W53D64 weir+dam configuration

iii) The tracer dispersion just near the downstream side of the dam is much greater for weir + dam combination than that of dam alone (compare photographs a_1,b_1 of Fig. 5.14 with those of a_1 and a_2 of Fig. 5.11).

5.1.2 Open Stream Pouring

In these photographic investigations, the inlet stream enters the tundish either through the atmospheric air or through an air chamber.

5.1.2.1 *Without Flow Modifiers*

The visual observations had shown that the inlet stream entrained considerable amount of air into the water bath. The entrained air bubbles, after reaching to about half the bath depth, reversed their direction and moved towards the free surface. In case of the inlet stream falling through the atmospheric air the action of air bubbles was found to spread over to the free surface which has resulted into the wavy nature of the bath surface. Whereas in other case, the action of air bubbles was found to restrict within the air chamber on account of which the bath surface was relatively quiet.

In Fig. 5.16 photographs are displayed to show the tracer dispersion at different intervals of time for OT1-1 and AT1-1 combination when the inlet stream enters through the atmospheric

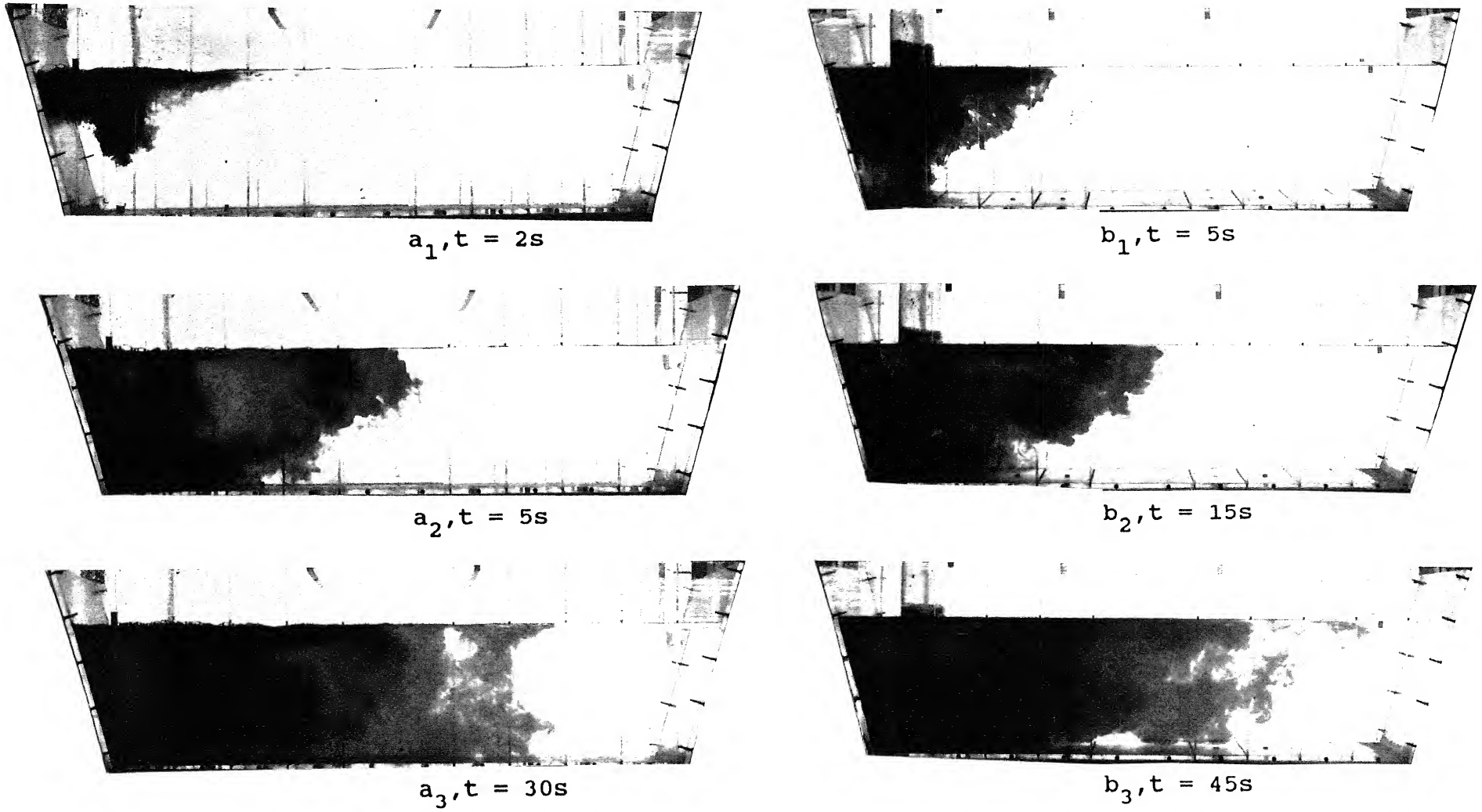

Fig. 5.16 : Tracer dispersion in a tundish for open stream pouring
(A) Inlet stream falls through atmospheric air in OT1-1 tundish
(B) Inlet stream falls through air chamber in AT1-1 tundish

air (5.16A) and through the air chamber (5.16B).

The photographs show that the flow from the inlet towards the exit is initially along the bath surface and then near the middle, it turns down into the bath towards the exit. The rate of tracer dispersion is faster when inlet stream enters through the atmospheric air than when it enters through the air chamber (compare Fig. 5.16A with 5.16B. We note in Fig. 5.16A that in 30s, the tracer could reach the exit whereas in Fig. 5.16B tracer could not reach the exit even after 45s).

It can also be seen that the turbulence of the inlet stream, when it falls through the air chamber, is restricted to the air chamber which results in relatively quiet flow conditions outside the chamber when compared with the open stream falling through the atmospheric air. In the later case the turbulence spreads over the tundish.

5.1.2.2 *With Flow Modifiers*

Fig. 5.17 contains photographs showing the tracer dispersion at 5s, 15s and 30s with W12 (5.17A), D24(5.17B) and W12D24(5.17c). It can be seen in Fig. 5.17A that downstream the weir, air bubbles are not visible. This limits the effect of buoyancy (caused by the rising bubbles) on the fluid flow behaviour within the inlet region. The flow downstream the weir is though surface directed, but not accompanied by surface waves in relation to that of without weir (compare photo of Fig. 5.17A with 5.16A).

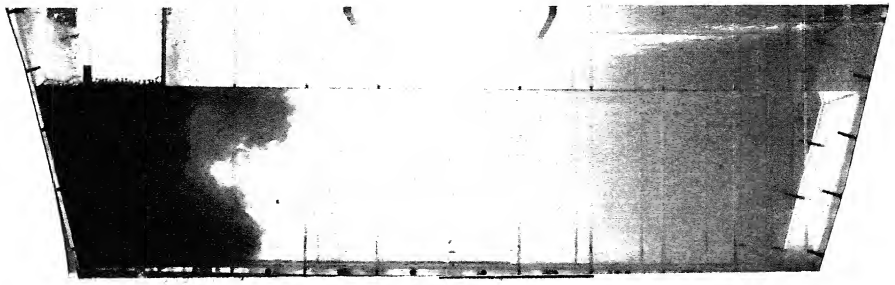

a_1,t = 5s

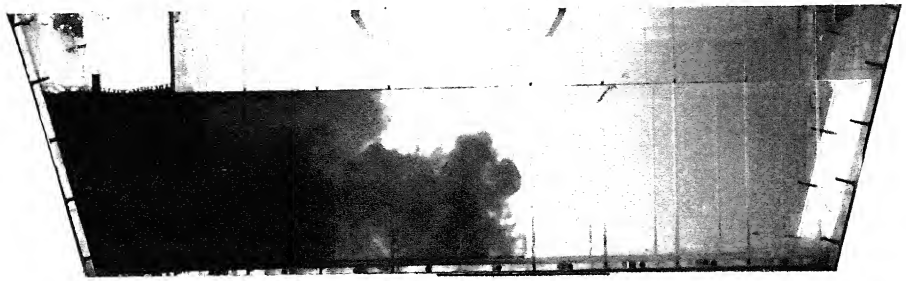

a_2,t = 15s

a_3,t = 30s

Fig. 5.17(A) : Tracer dispersion in OT1-1 tundish (open stream pouring) in presence of weir of W12 configuration

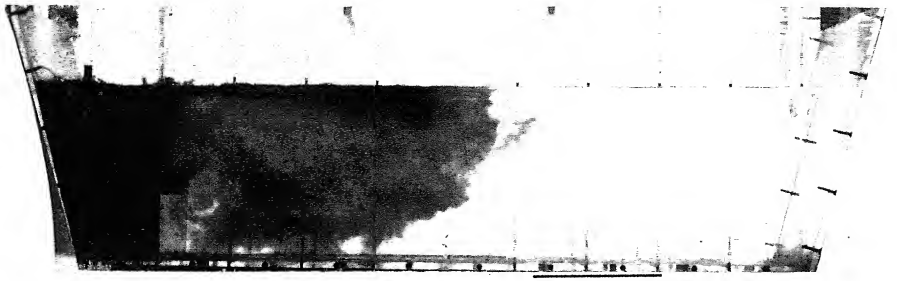

b_1, t = 2s

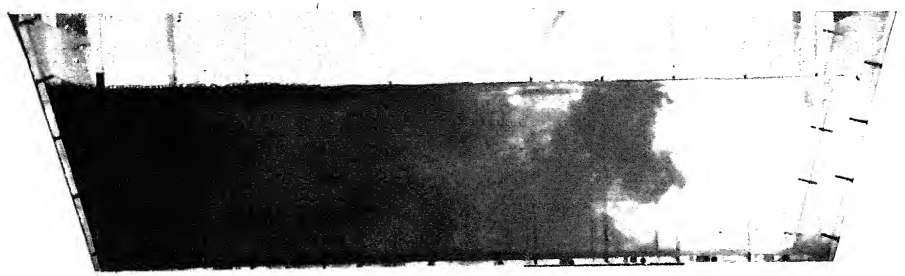

b_2, t = 5s

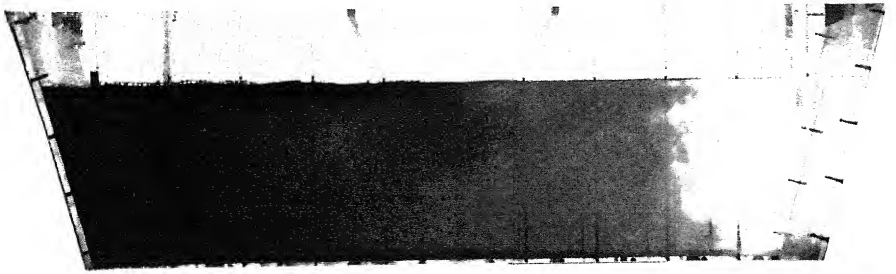

b_3, t = 30s

Fig. 5.17(B) : Tracer dispersion in OT1-1 tundish in presence of dam, D24

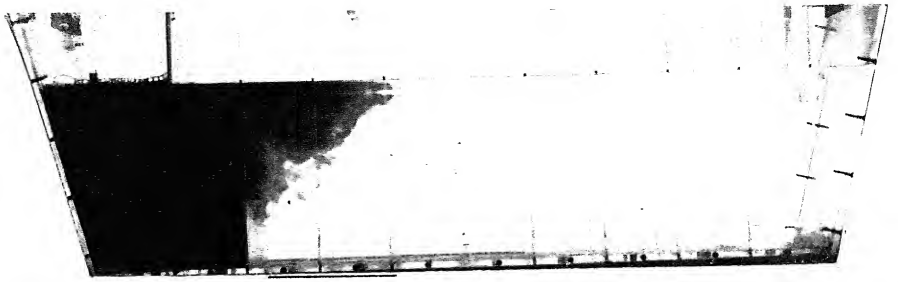

c_1, t = 5s

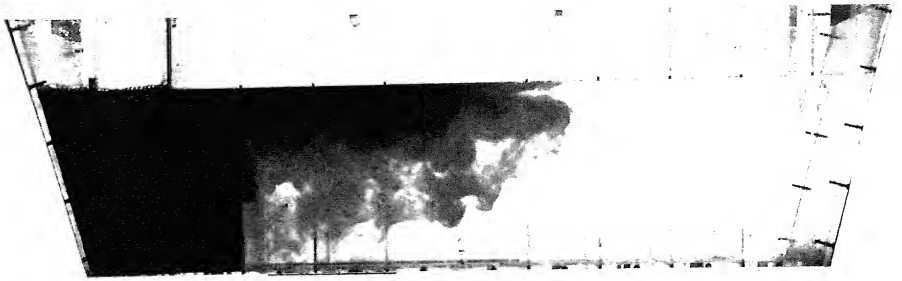

c_2, t = 15s

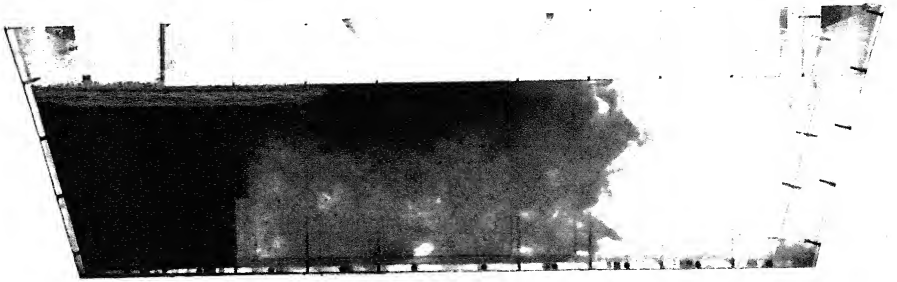

c_3, t = 45s

Fig. 5.17(C) : Tracer dispersion in tundish in presence of dam, W12D24

The effect of dam on the tracer dispersion is somewhat different than that of weir (compare Fig. 5.17B with 5.17A) The dam is unable to limit the entrained air of the inlet stream within the inlet region. The air bubbles can be seen to be present to some distance on the bath surface downstream the dam. The bath surface can be observed to be wavy. Tracer dispersion occurs preferentially along the surface and then down into the bath towards the exit (see photo b_2). At 30s (photo b_3) the tracer has arrived at the exit. Comparison of these photographs with those of without dam (5.16A) shows that the fluid flow behaviour is more or less similar in both cases.

In weir + dam combinations, the tracer dispersion retains the characteristics of both weir and dam. Fig. 5.17C shows tracer dispersion for weir+dam. It can be seen that the effects of the entrained air are restricted within the inlet region (see photo c_1). Downstream weir+dam, neither air bubbles nor wavy nature of surface is visible. Dam directs the liquid to move towards the surface. The tracer front could not reach the exit (see photo c_3) even after 45s. The intensity of colour downstream the dam (see photos c_2 and c_3) shows that fluid velocity in bottom xy-planes is much smaller than those in top planes which suggests that the flow is surface directed.

5.2 VARIATION OF CONCENTRATION

The variation of conductivity of water caused by the differential mixing of the KCl tracer due to differential fluid

velocities in xyz planes was recorded at the exit of the tundish as a function of time for all tundishes of Table 4.1 without and with flow modifiers of different types and configurations as listed in Table 4.2. These conductivity values were converted into concentration and the dimensionless concentration was plotted against dimensionless time as described in section 4.5. Such a plot is commonly called C-curve or residence time distribution curve (hereafter termed RTD). Several experiments were repeated under identical conditions and similar results were obtained. All results were analysed in terms of shape of the curve, residence times and variance and accordingly they are presented below:

5.2.1 Shape

5.2.1.1 *Without Flow Modifiers*

Fig 5.18 shows the effect of width on the shape of the RTD-curves for ST1-1, ST1-12, ST1-14 and ST1-24 and Fig. 5.19 for ST2-1, ST2-3 and ST2-5 tundishes operated with submerged inlet stream. In both figures two different shapes of RTD curve can be seen in the range of widths of the present study; one is characterised by two peak values of concentration (see curves for W/L = 0.215 and 0.310 of fig. 5.18 and W/*l* = 0.62 and 0.3 of Fig. 5.19) and the other by a single peakvalue of concentration (see curves for W/L=0.167 and 0.120 of Fig. 5.18 and W/*l* =0.145 of Fig. 5.19). The reason for the above type of shapes of RTD curves is considered to be due to the following:

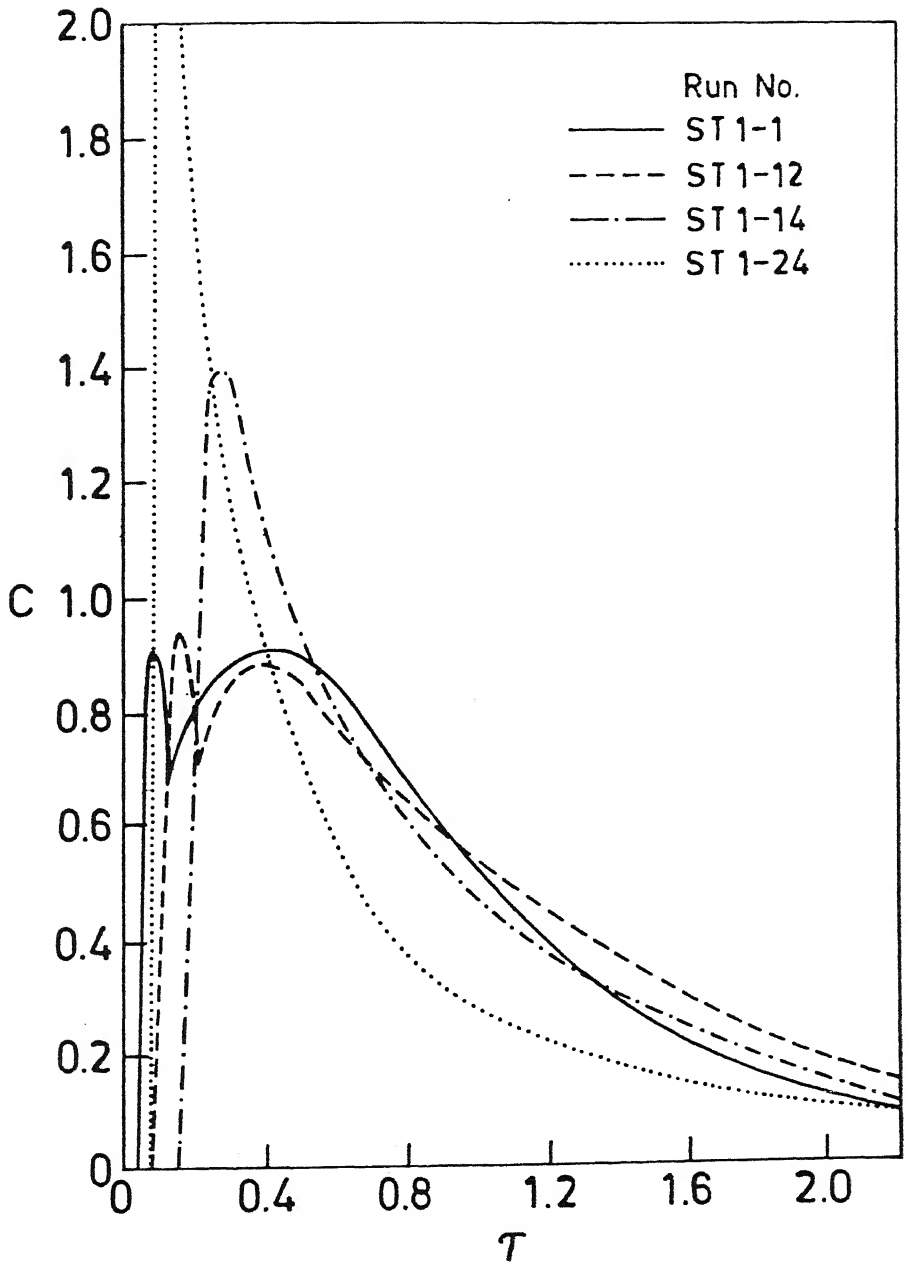

Fig.5.18: RTD curves for various widths of the ST1 type tundishes

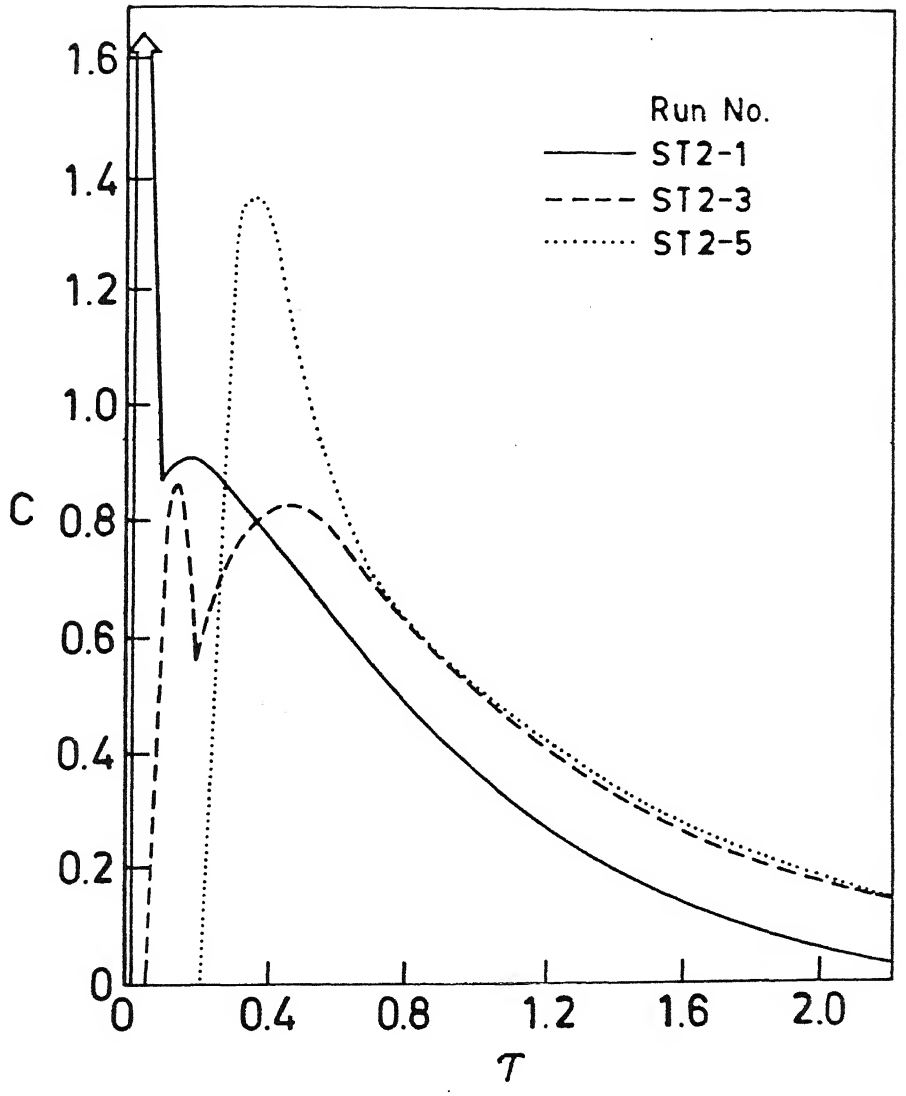

Fig.5.19: RTD curves for various widths of the ST2 type tundishes

The plunging liquid jet goes down to the tundish bottom where it spreads radially near the bottom and then starts ascending near the walls in case of ST1 type of tundish. In case of ST2 type of tundish, the plunging jet, after going down to the tundish bottom spreads on both sides of the inlet stream and starts ascending towards the bath surface. In a wide tundish a portion of the liquid was found to move on the horizontal inlet-exit plane straight towards the exit without being affected by the width-side walls (see Fig. 5.1). Due to this straight movement it reaches earlier at the tundish exit than the rest of the liquid (see Figs. 5.1 and 5.5). Thus the RTD curve (which shows tracer response as a function of time) has to be comprised of two peaks; one due to the straight movement of certain amount of tracer with the portion of the liquid and the other due to the movement of the remaining tracer with the rest of the liquid. By decreasing the tundish width the width-side walls retard the movement of the aforementioned portion of the liquid and at a critical width, the width-side walls force the portion of the liquid towards the middle of the tundish where it mixes with the remaining liquid (see Fig. 5.6). Thus, straight movement of the portion of the liquid and the tracer contained in it are eliminated as a consequence of which RTD curve shows a single peak[50].

It appears from Figs. 5.18 and 5.19 that the ratio W/L determines the shape of the RTD curve. Based on the shape of the RTD curve and the photographic studies, all tundishes with $W/L \geq 0.215$ are termed wider and $W/L < 0.215$ narrower.

The effect of some parameters such as bath height, inlet-exit

distance and diameter of the submerged pipe on the shape of the RTD curve is shown in Figs. 5.20, 5.21 and 5.22. The other parameter like vertical wall tundish (ST1-4), submergence depth of the inlet stream (ST1-1D), flow rate regulating mechanism (ST1-1N), model slag cover (ST1-1S) were found to produce the shape of the RTD curve in accordance with the W/L ratio as shown in Figs. 5.20 to 5.22.

It can be seen in the figures that in all the above cases the RTD curves are characterized by two peak values of concentration for W/L = 0.310 and single peak value for W/L = 0.150. Similarly in ST2 tundishes (see Fig. 5.23) two peak values of concentration are observed for W/l = 0.3 and single peak value for W/l = 0.145.

In case of open stream pouring the shape of the RTD curve was found to show only a single peak value of concentration at all tundish widths. Fig. 5.24 shows the shape of the RTD curves for AT1-1 (W=0.310L), AT1-12 (W=0.215L) and AT1-21 (W=0.120L) when the inlet stream falls through the air chamber and for OT1-1 (W=0.310L) when the inlet stream falls through the atmospheric air. In all the cases the shape of the curve is identical and is characterised by single peak value of concentration.

5.2.1.2 *With Flow Modifiers*

(A) *Influence of Weir*

Fig. 5.25 shows the influence of weir on the shape of the RTD

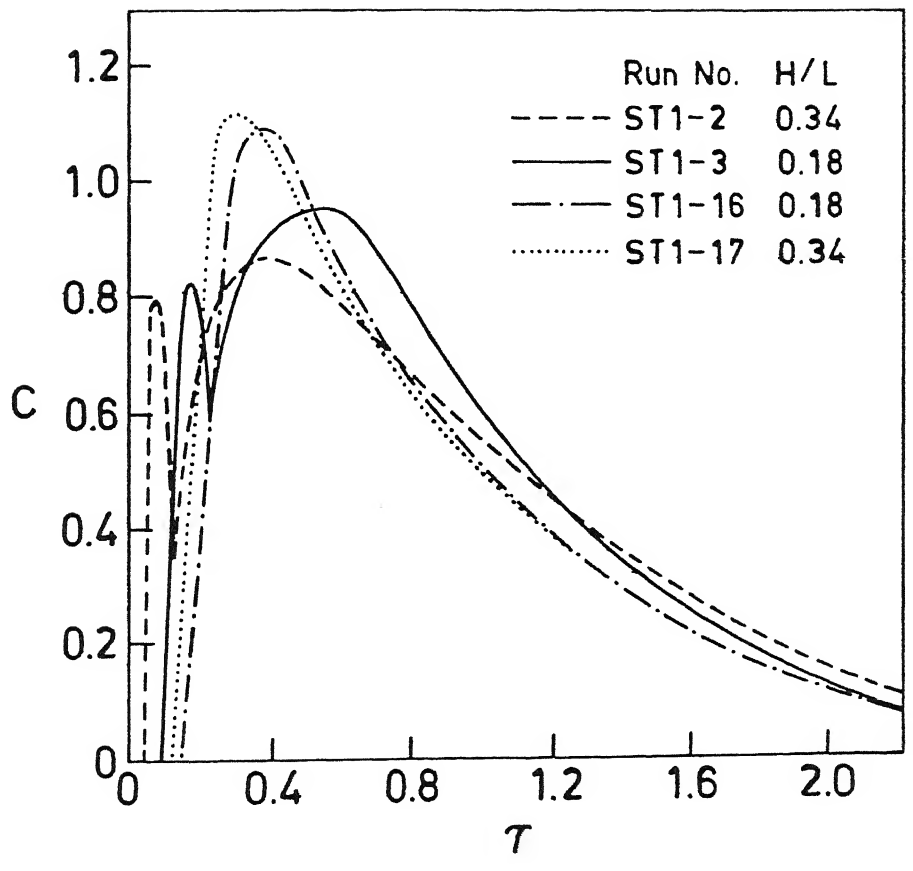

Fig.5.20: RTD curves for different bath heights in wide and narrow tundishes.

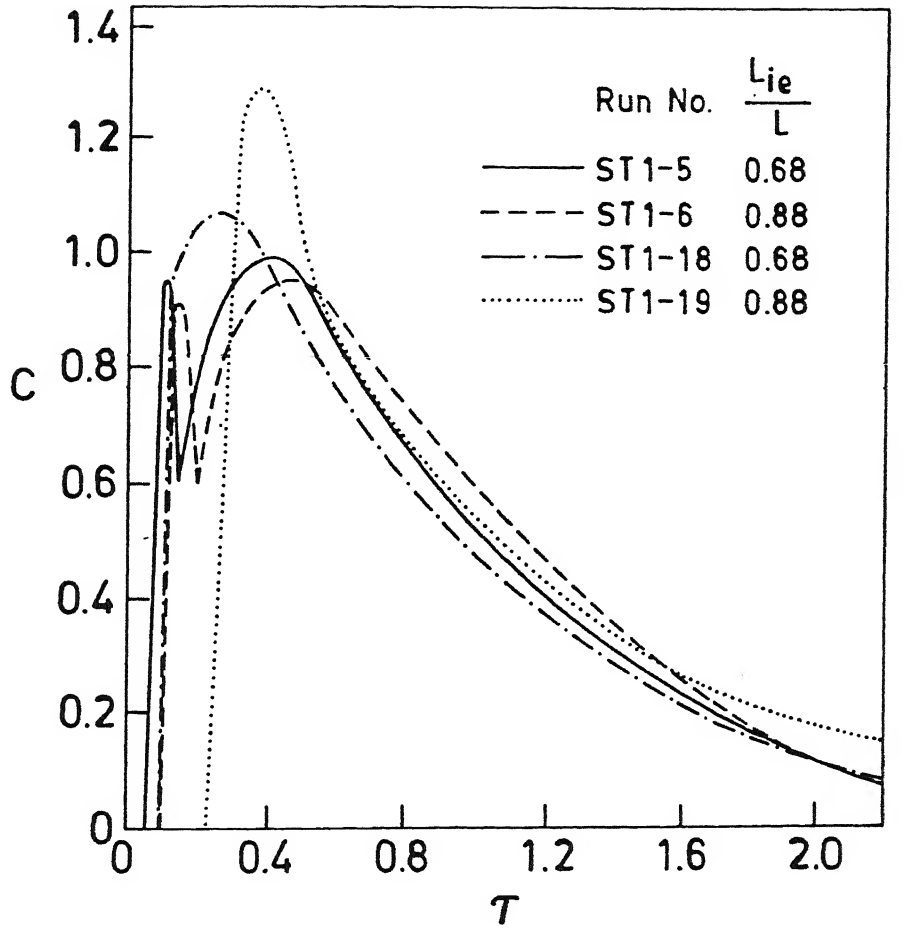

Fig.5.21: RTD curves for different inlet-exit distances in wide and narrow tundishes.

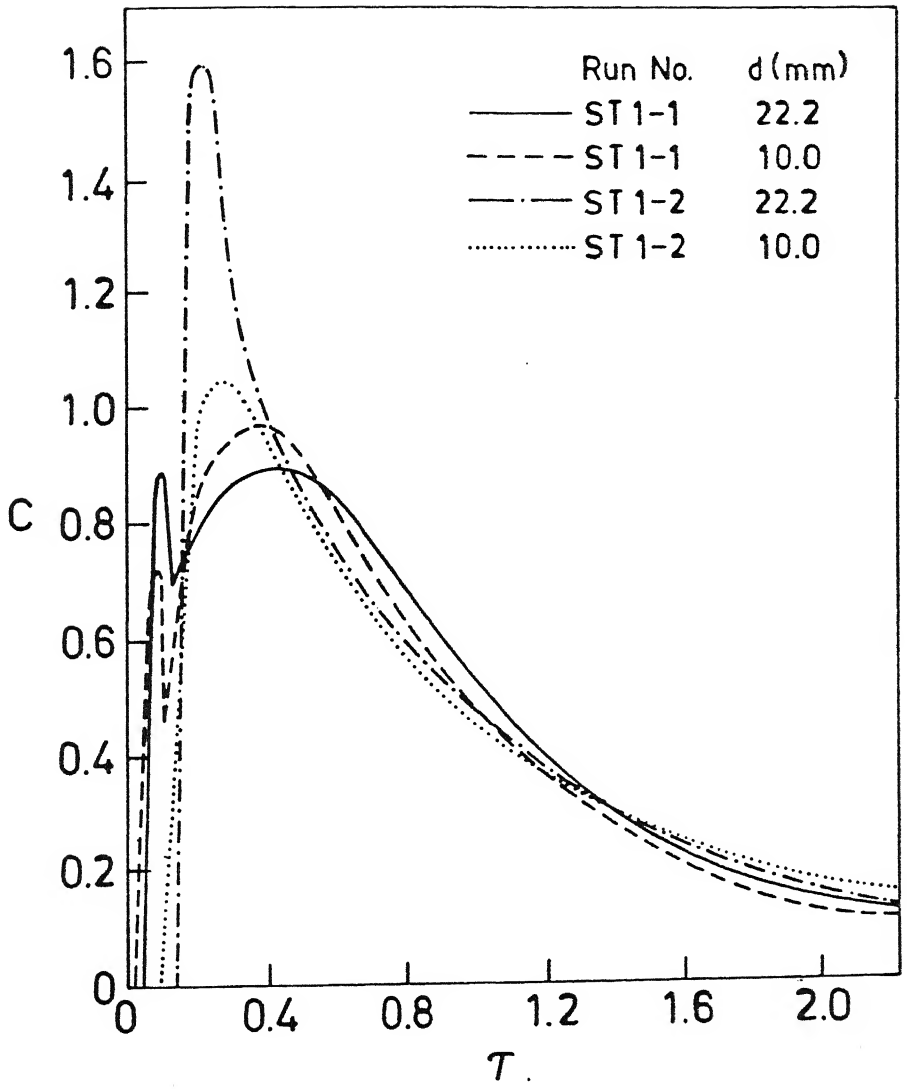

Fig.5.22: RTD curves for different diameters of the submerged pipe in wide and narrow tundishes.

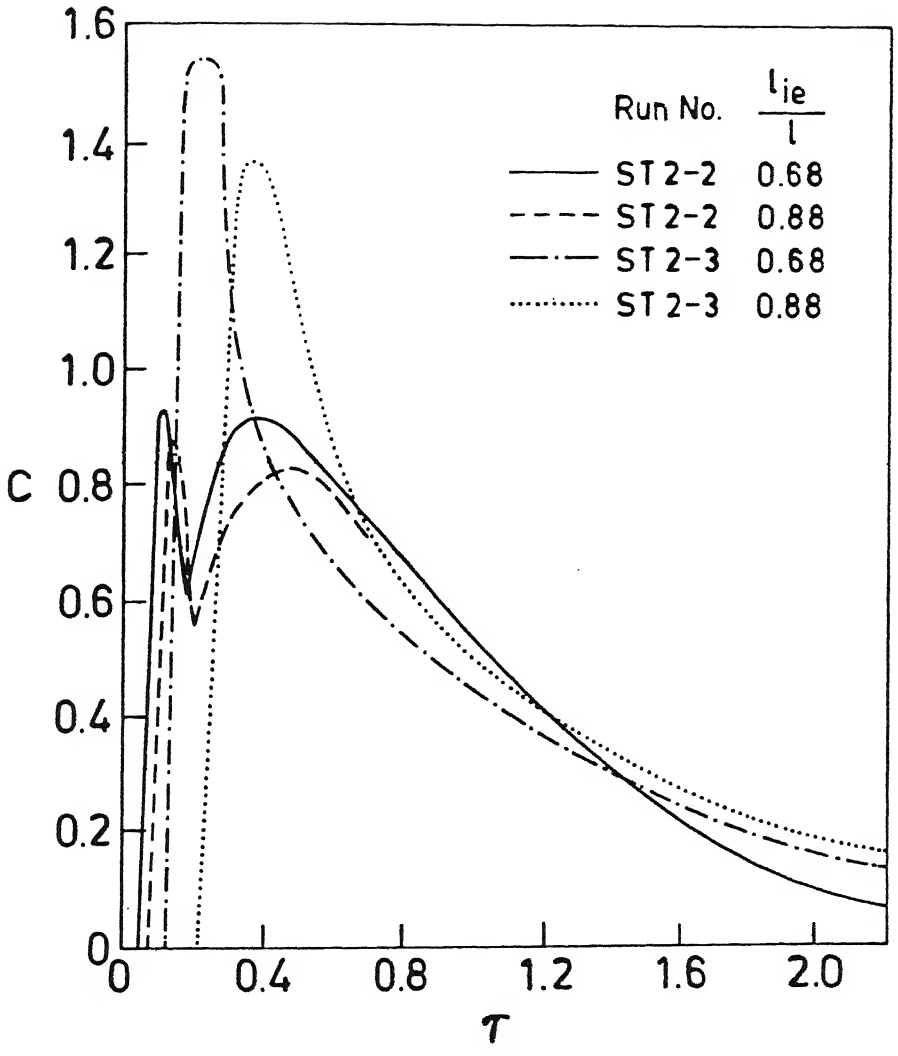

Fig.5.23: RTD curves for different inlet-exit distances in ST2 tundishes.

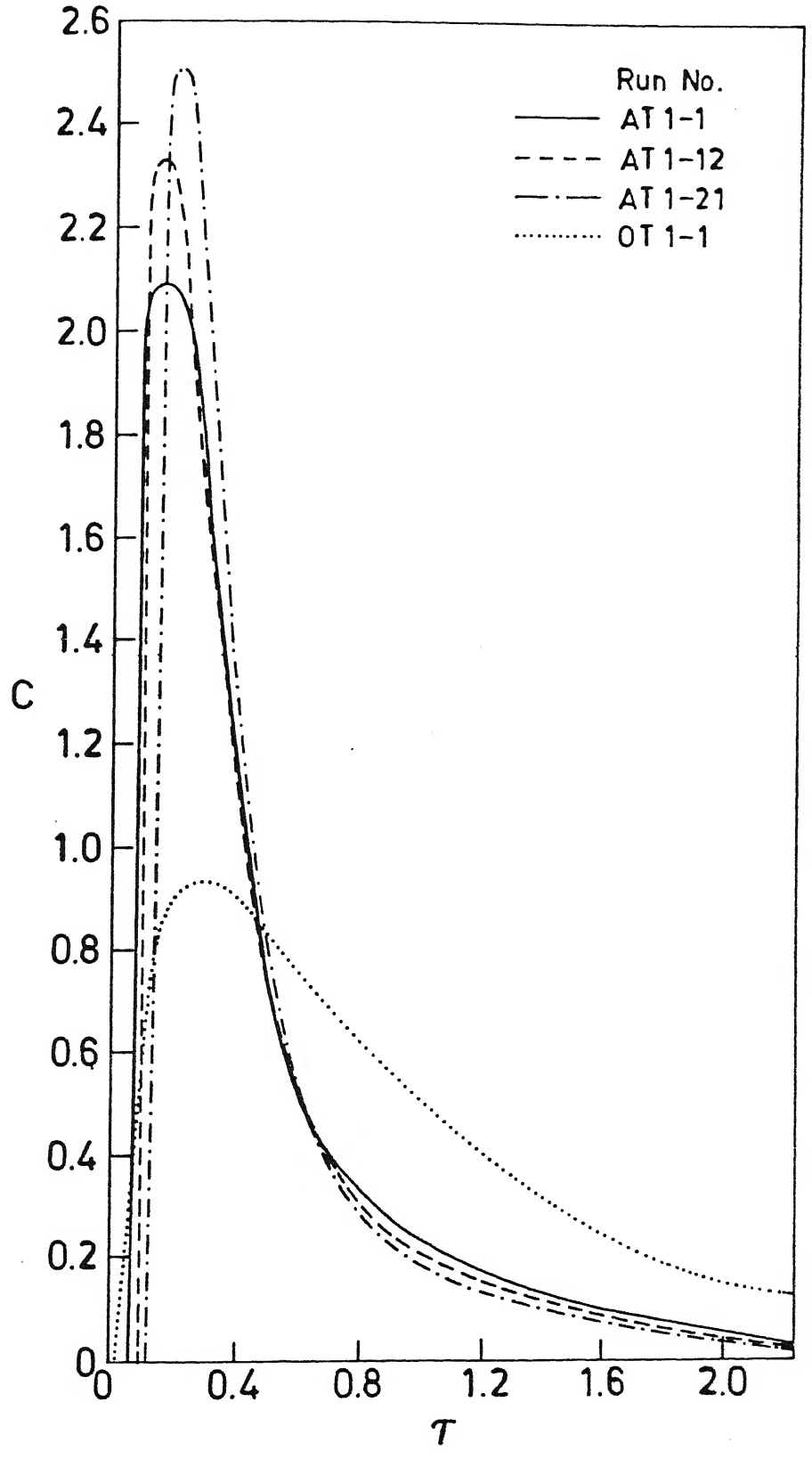

Fig.5.24: RTD curves due to open and air shrouded stream pouring in tundishes of different widths.

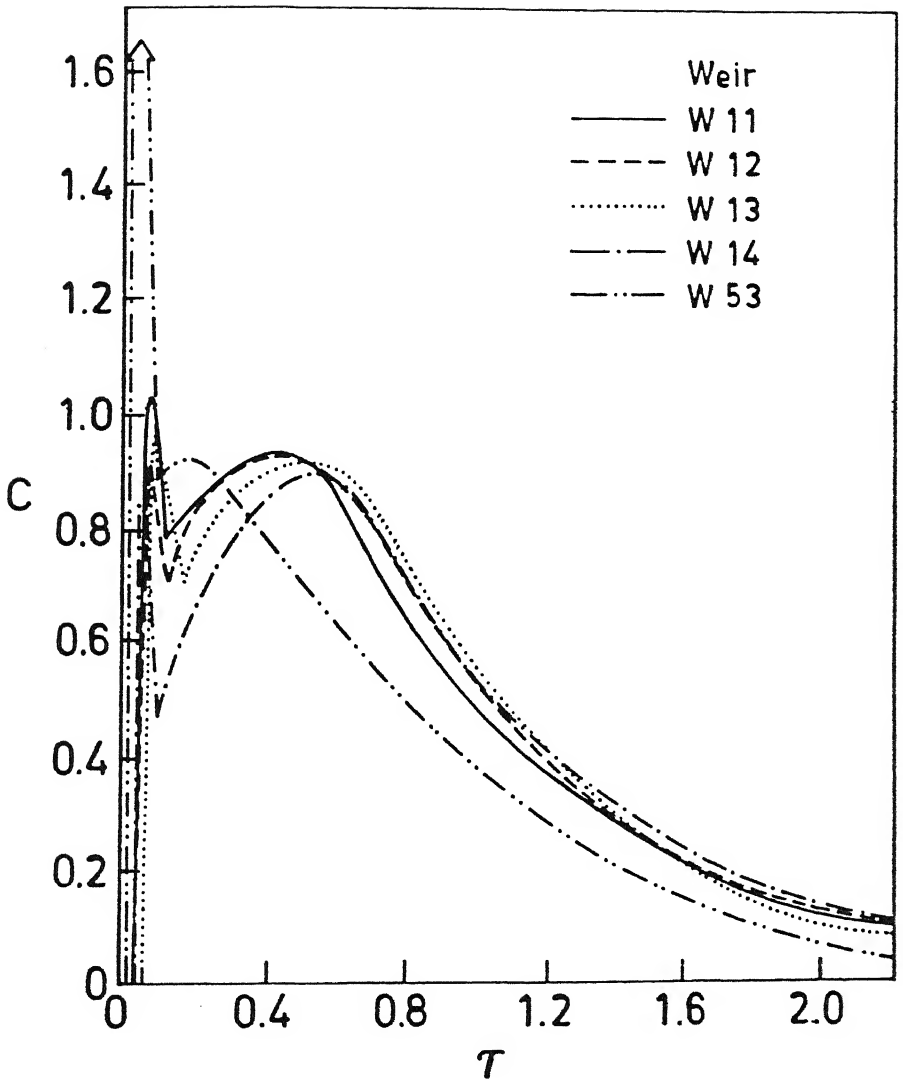

Fig.5.25: RTD curves for different configurations of weir in ST1 and ST2 tundishes.

curve in ST1-1 with W11, W12, W13 and W14 and in ST2-1 with W53 weir configurations for submerged inlet stream. Other weir configurations i.e W22, W32 and W42 have given the same shape. Two peak values of the concentration are discernible on all RTD curves at different intervals of time. This is due to the effect of the short circuiting of the fluid as mentioned in section 5.1.1.2.

(B) *Influence of Dam*

As pointed out in section 5.1.1.2 that dam whether placed alone or in combination with weir eliminates short circuiting in a wide tundish, therefore, one would expect a single peak value of concentration in a RTD curve. All configurations of dam i.e. D11 to D64, weir + dam i.e. W12D21 to W53D64 and slotted dam + dam i.e. SD21D24 and SD31D44 have resulted in a RTD curve with single peak value of concentration in all tundishes of Table 4.1. As an example, few curves are shown in Figs. 5.26 to 5.30.

5.2.2 *Variation of Residence Times*

Each RTD curve is characterised by the minimum, peak and mean residence time and spread; the square of the spread is termed as variance. The time for the first appearance of the tracer at the exit is termed minimum residence time. The time to attain the maximum concentration is called peak residence time. Both these times are determined very carefully from the record of the

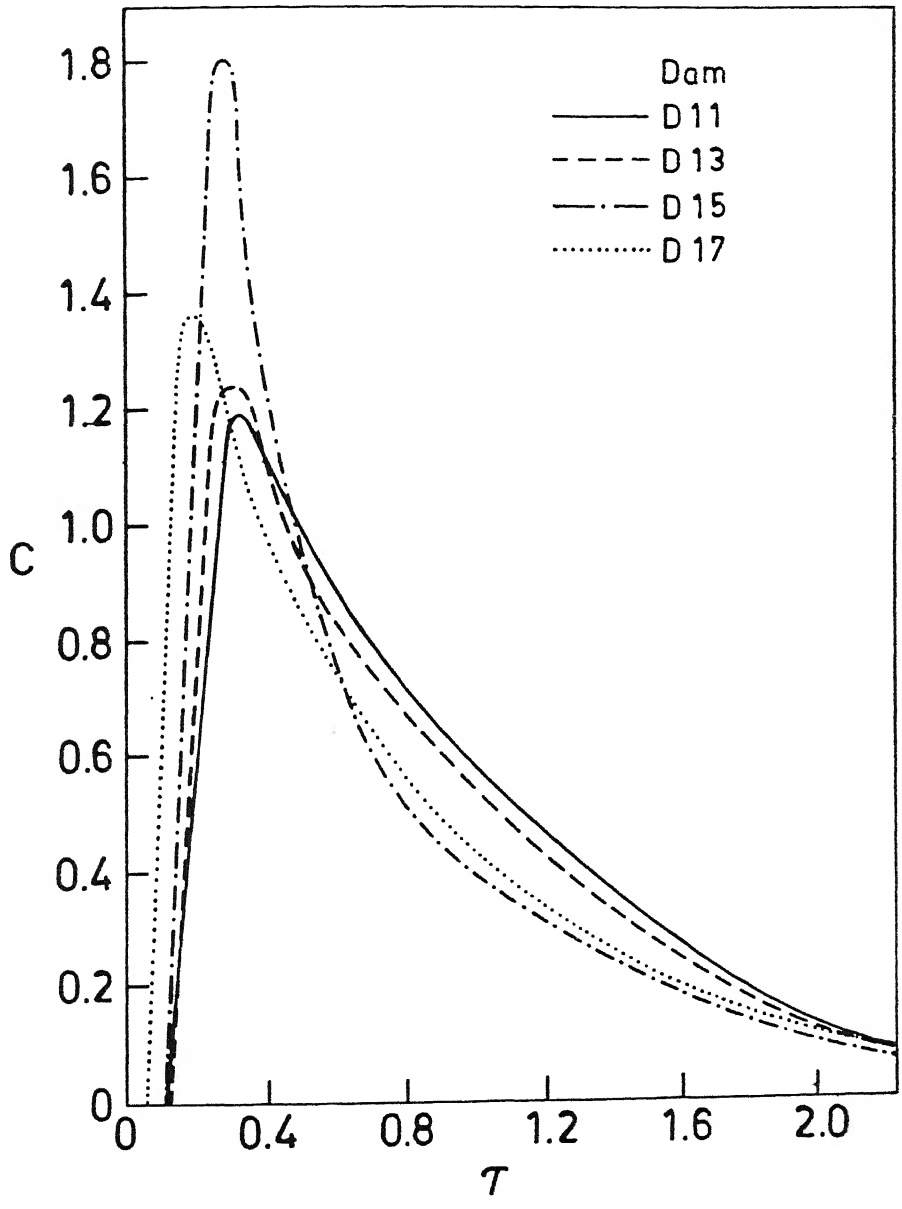

Fig.5.26: RTD curves for different dam heights in ST1-1 tundish.

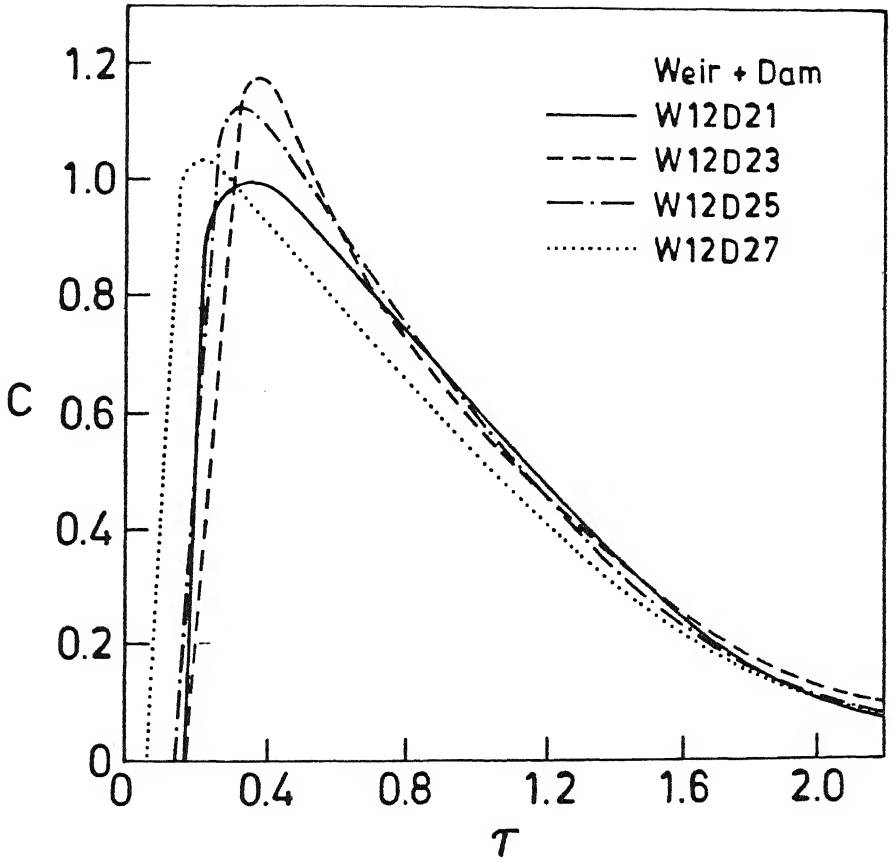

Fig.5.27: RTD curves for different dam heights in weir+dam combination in ST1-1 tundish.

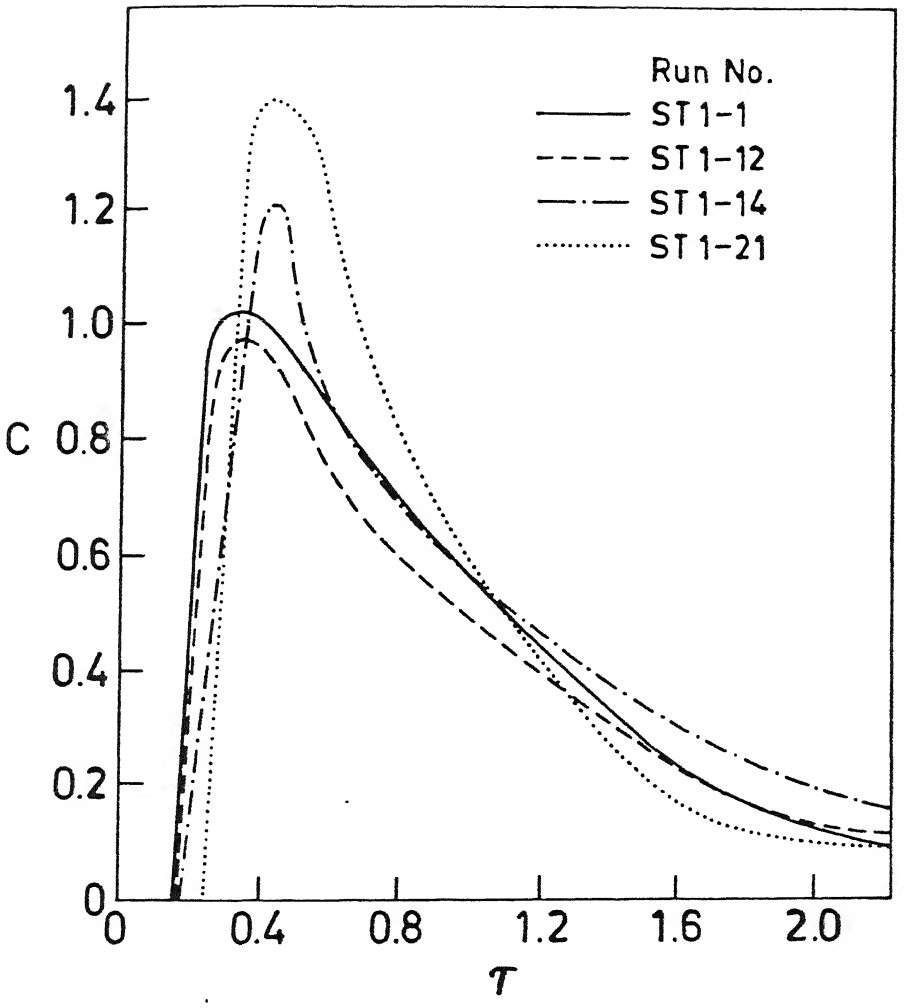

Fig.5.28: RTD curves for different widths of the tundish in presence of dam D24.

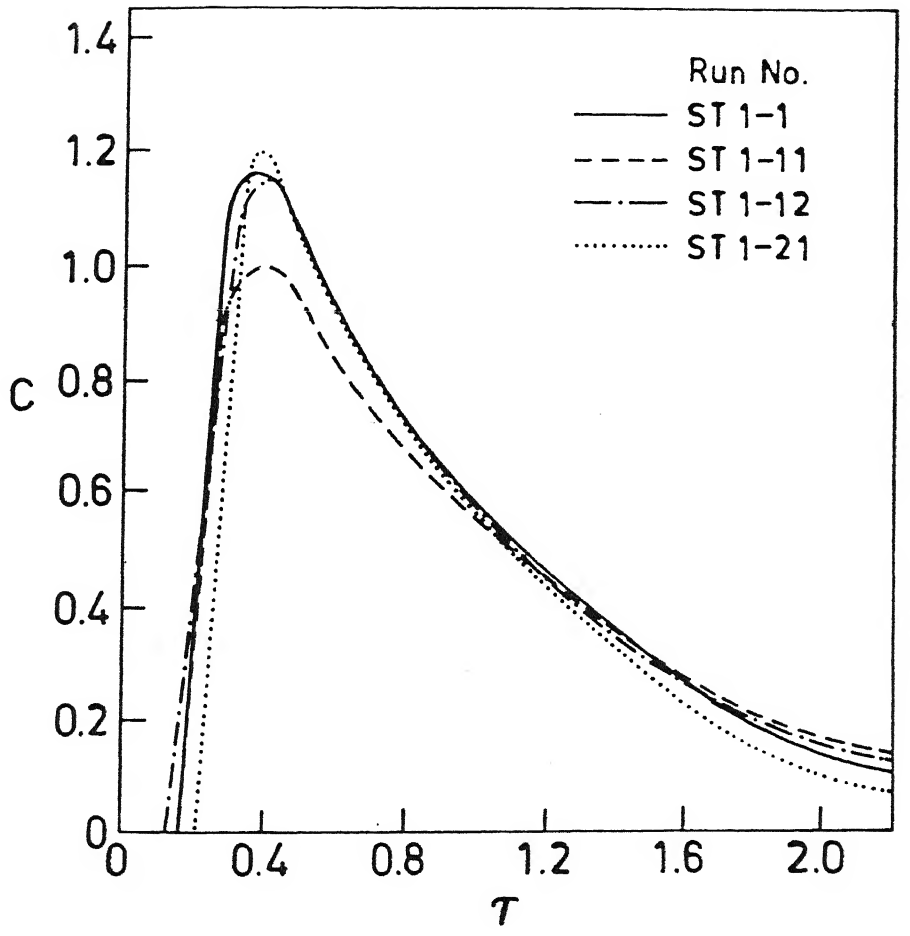

Fig.5.29: RTD curves for different tundish widths in presence of weir+dam combination (W12D24).

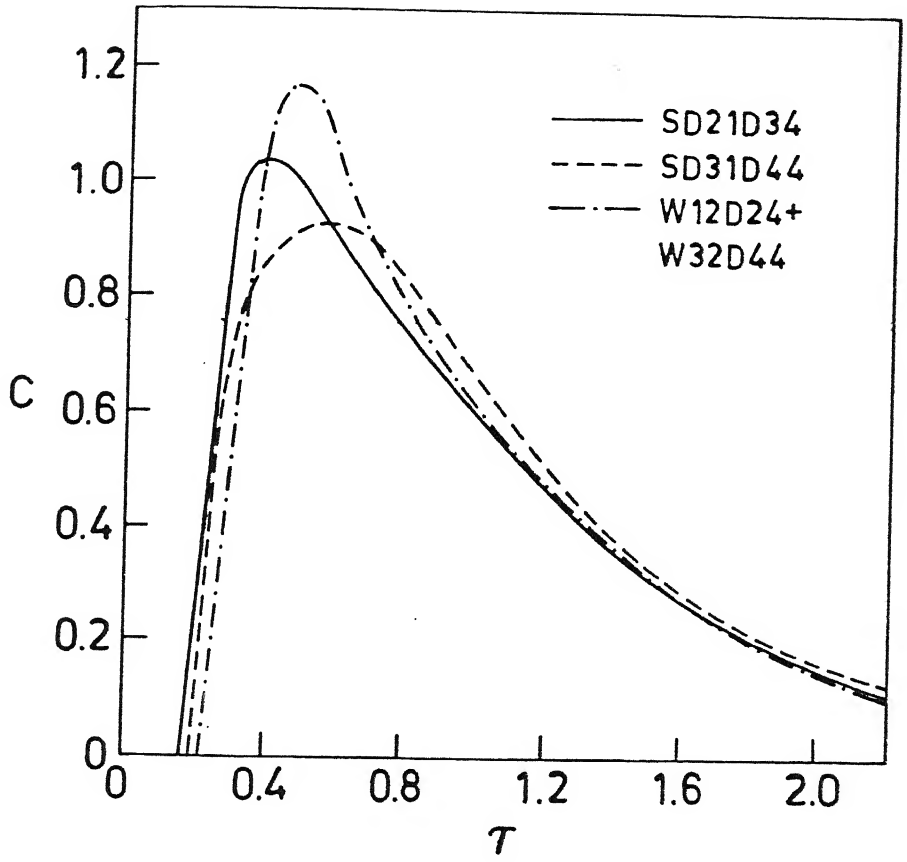

Fig.5.30: RTD curves for different combinations of types of Flow Modifiers.

concentration vs time data. Mean residence time and variance are calculated by the Eqs. 4.7 and 4.8. The values of all residence times are given in Tables 5.1 to 5.3 for submerged and open stream pouring into the tundish without and with FMs.It must be mentioned here that each value in the above tables is an average of two runs.

5.2.2.1 *Submerged Stream Pouring*

(A) *Without Flow Modifiers*

i) *Effect of Width*

Fig. 5.31 shows the variation of residence times and variance as a function of width for T1 tundishes. Fig. 5.31A shows that as the tundish width decreases successively from 310mm to around 150mm, the minimum residence time (t_{min}) increases for all Froude numbers and inlet-exit distances. Further decrease in the width decreases t_{min}.

The other residence times i.e. t_{peak} (see Fig. 5.31B) and t_{mean} (see Fig. 5.31C) decreases continuously with the decrease in the width. An increase in t_{min} and decrease in t_{peak} indicate the decrease in axial or longitudinal dispersion of the tracer, since $t_{min} = t_{peak}$ in the absence of the longitudinal mixing of tracer. Thus, the decrease in width upto 150mm appears to decrease the extent of axial dispersion of the tracer, which indicates that the north-south walls contribute to attain the flow uniformity in the

Table 5.1 : The values of residence time and variance for tundishes of Table 4.1 for submerged stream pouring.

Run	d (mm)	Residence time (s)			Variance	$\tau_{min} = \frac{t_{min}}{\bar{t}}$	τ_{peak}	τ_{mean}	σ^2
		t_{min}	t_{peak}	t_{mean}	($s^2 x 10^{-4}$)				
ST1-1	22.2	31	262	444	7.42	0.056	0.469	0.795	0.240
ST1-1D	22.2	29	249	428	7.73	0.052	0.448	0.769	-
ST1-1N	22.2	30	255	431	7.42	0.054	0.459	0.775	-
ST1-1S	22.2	31	228	428	8.04	0.056	0.410	0.769	-
ST1-1	12.5	27	238	-	-	0.048	0.428	-	-
ST1-1	10.0	23	220	450	7.71	0.041	0.396	0.809	0.249
ST1-2	22.2	35	253	618	13.17	0.047	0.341	0.827	0.239
ST1-3	22.2	32	209	310	3.16	0.082	0.552	0.819	0.222
ST1-4	22.2	35	222	423	7.07	0.067	0.427	0.813	0.261
ST1-5	22.2	23	234	419	7.51	0.041	0.421	0.753	0.243
ST1-6	22.2	43	256	456	7.57	0.077	0.459	0.820	0.245
ST1-7	22.2	23	171	296	3.20	0.067	0.451	0.803	0.234
ST1-8	22.2	14	112	221	1.81	0.052	0.418	0.825	0.252
ST1-9	22.2	16	123	217	1.81	0.060	0.448	0.832	0.242
ST1-10	22.2	21	123	229	1.77	0.078	0.459	0.854	0.246
ST1-11	22.2	28	214	377	5.23	0.060	0.455	0.802	0.237
ST1-11	12.5	25	196	-	-	0.055	0.417	-	-
ST1-11	10.0	21	176	382	5.34	0.045	0.374	0.813	0.242
ST1-12	22.2	38	160	315	3.64	0.098	0.414	0.816	0.244
ST1-12	12.5	31	148	-	-	0.080	0.383	-	-
ST1-12	10.0	25	136	322	3.68	0.065	0.352	0.834	0.246
ST1-13	22.2	43	114	279	2.96	0.128	0.339	0.830	0.262
ST1-14	22.2	43	099	239	2.37	0.143	0.330	0.797	0.263
ST1-14	12.5	34	087	-	-	0.113	0.290	-	-
ST1-14	10.0	30	087	241	2.49	0.100	0.290	0.803	0.277
ST1-15	22.2	44	078	216	1.86	0.163	0.290	0.786	0.257
ST1-15	12.5	33	067	208	1.93	0.123	0.249	0.773	0.267
ST1-15	10.0	28	062	214	2.09	0.104	0.230	0.795	0.289
ST1-16	22.2	44	101	283	3.03	0.117	0.281	0.791	0.235
ST1-17	22.2	36	072	150	0.78	0.191	0.393	0.819	0.233
ST1-18	22.2	27	078	202	1.79	0.100	0.290	0.751	0.247
ST1-19	22.2	62	103	222	1.81	0.230	0.379	0.825	0.250
ST1-20	22.2	36	065	198	1.57	0.149	0.268	0.816	0.268
ST1-21	22.2	30	045	175	1.21	0.139	0.209	0.803	0.262
ST1-21	12.5	25	051	-	-	0.116	0.237	-	-
ST1-21	10.0	23	054	175	1.19	0.107	0.251	0.814	0.257
ST1-22	22.2	25	051	112	0.57	0.164	0.349	0.774	0.267
ST1-23	22.2	21	040	075	0.24	0.219	0.406	0.771	0.260
ST1-24	22.2	12	020	100	0.43	0.085	0.147	0.767	0.258
ST1-24	12.5	07	017	-	-	0.054	0.131	-	-
ST1-24	10.0	06	021	098	0.44	0.046	0.163	0.760	0.264
ST1-25	22.2	08	016	094	0.42	0.054	0.124	0.720	0.252
ST1-26	22.2	24	032	103	0.44	0.176	0.246	0.783	0.264
ST2-1	22.2	10	104	389	7.51	0.018	0.187	0.700	0.242
ST2-2	22.2	06	049	100	0.39	0.046	0.377	0.769	0.231
ST2-3	22.2	09	062	109	0.42	0.069	0.477	0.836	0.248
ST2-4	22.2	07	014	047	0.11	0.113	0.226	0.758	0.260
ST2-5	22.2	13	023	052	0.10	0.210	0.371	0.839	0.260

Table 5.2 : The values of residence time and variance for different tundishes with flow modifiers for the case of submerged stream pouring.

Run	FM	d (mm)	Residence time (s)			Variance				
			t_{min}	t_{peak}	t_{mean}	($s^2 x 10^{-4}$)	ε_{min}	ε_{peak}	ε_{mean}	ε_S
ST1-1	W11	22.2	27	265	441	7.74	0.871	1.011	0.993	1.043
ST1-1	W12	22.2	29	300	430	7.76	0.935	1.145	0.968	1.046
ST1-1	W13	22.2	29	330	439	7.75	0.935	1.259	0.989	1.044
ST1-1	W14	22.2	35	300	431	7.19	1.129	1.145	0.971	0.969
ST1-1	W21	22.2	30	277	442	7.71	0.967	1.057	0.995	1.039
ST1-1	W22	22.2	31	323	436	7.79	1.000	1.233	0.982	1.050
ST1-1	W23	22.2	33	254	426	7.13	1.064	0.969	0.959	0.960
ST1-1	W24	22.2	40	242	443	7.42	1.290	0.923	0.998	1.000
ST1-1	W32	22.2	46	300	426	6.98	1.483	1.145	0.959	0.940
ST1-1	W42	22.2	37	266	438	7.38	1.193	1.015	0.986	0.994
ST1-1	D11	22.2	71	173	481	6.97	2.290	0.660	1.083	0.934
ST1-1	D12	22.2	107	175	462	5.65	3.451	0.668	1.040	0.761
ST1-1	D13	22.2	80	162	458	7.34	2.580	0.618	1.031	0.989
ST1-1	D14	22.2	84	160	445	7.62	2.709	0.610	1.002	1.026
ST1-1	D15	22.2	77	150	403	7.22	2.484	0.572	0.908	0.973
ST1-1	D16	22.2	77	139	395	7.40	2.484	0.531	0.889	0.997
ST1-1	D17	22.2	39	104	403	8.09	1.258	0.397	0.908	1.090
ST1-1	D21	22.2	85	208	485	6.69	2.742	0.793	1.088	0.901
ST1-1	D22	22.2	103	202	483	6.19	3.323	0.770	1.092	0.834
ST1-1	D23	22.2	75	180	466	7.42	2.419	0.687	1.049	1.000
ST1-1	D24	22.2	77	180	472	7.30	2.484	0.689	1.063	0.983
ST1-1	D25	22.2	75	162	466	7.28	2.419	0.618	1.049	0.981
ST1-1	D26	22.2	72	150	459	7.54	2.323	0.572	1.034	1.016
ST1-1	D27	22.2	45	173	456	6.95	1.452	0.660	1.027	0.936
ST1-1	D34	22.2	76	202	477	7.33	2.452	0.771	1.074	0.988
ST1-1	D44	22.2	63	208	465	7.21	2.032	0.794	1.047	0.972
ST1-5	D24	22.2	63	184	468	7.53	2.739	0.786	1.117	1.003
ST1-6	D24	22.2	109	196	490	6.71	2.535	0.766	1.075	0.883
ST1-1	D24	12.5	66	162	438	7.28	2.444	0.680	-	-
ST1-1	D24	10.0	52	156	460	7.37	2.261	0.709	1.022	0.956
ST1-11	D21	22.2	74	175	420	5.08	2.642	0.818	1.114	0.971
ST1-11	D22	22.2	83	172	405	4.99	2.964	0.804	1.074	0.954
ST1-11	D24	22.2	64	156	389	4.85	2.286	0.729	1.031	0.927
ST1-11	D25	22.2	70	152	397	4.99	2.500	0.710	1.053	0.954
ST1-11	D24	12.5	52	146	-	-	2.080	0.745	-	-
ST1-11	D24	10.0	43	127	392	6.02	2.048	0.722	1.026	1.127
ST1-12	D21	22.2	63	131	355	3.67	1.658	0.944	1.127	1.008
ST1-12	D22	22.2	73	143	348	3.68	1.921	0.894	1.105	1.011
ST1-12	D24	22.2	59	135	337	3.60	1.552	0.844	1.070	0.989
ST1-12	D25	22.2	58	132	328	3.62	1.526	0.825	1.041	0.994
ST1-12	D24	12.5	45	123	-	-	1.452	0.831	-	-
ST1-12	D24	10.0	39	112	315	3.63	1.560	0.636	0.978	0.986
ST1-14	D21	22.2	57	131	256	2.23	1.326	1.323	1.071	0.941
ST1-14	D22	22.2	63	127	267	2.31	1.465	1.283	1.117	0.975
ST1-14	D24	22.2	54	127	274	2.30	1.256	1.285	1.146	0.970
ST1-14	D25	22.2	54	121	263	2.18	1.256	1.222	1.100	0.920
ST1-14	D24	12.5	42	118	-	-	0.977	1.192	-	-
ST1-14	D24	10.0	38	109	266	2.31	0.884	1.101	1.113	0.975
ST1-21	D24	22.2	52	094	201	1.09	1.733	2.089	1.149	0.000
ST1-21	D24	12.5	43	098	-	-	1.720	1.921	-	-

Continued

Table 5.2 : The values of residence time and variance for different tundishes with flow modifiers for the case of submerged stream pouring (Continued)

Run	FM	d (mm)	Residence time (s)			Variance				
			t_{min}	t_{peak}	t_{mean}	($s^2 x 10^{-4}$)	ε_{min}	ε_{peak}	ε_{mean}	ε_S
ST1-21	D24	10.0	45	107	200	1.04	1.956	1.981	1.143	0.874
ST1-24	D24	22.2	27	54	121	0.41	2.250	2.700	1.210	0.953
ST1-24	D24	12.5	24	43	118	0.42	3.428	2.529	-	-
ST1-24	D24	10.0	22	46	119	0.41	3.667	2.190	1.214	0.931
ST1-1	SD11	22.2	70	207	457	6.95	2.258	0.790	1.029	0.936
ST1-1	SD21	22.2	72	243	492	6.55	2.323	0.927	1.108	0.883
ST1-1	W12D21	22.2	87	208	473	6.38	2.806	0.794	1.063	0.860
ST1-1	W12D22	22.2	112	202	487	6.24	3.613	0.771	1.097	0.841
ST1-1	W12D23	22.2	96	192	485	6.77	3.097	0.733	1.092	0.912
ST1-1	W12D24	22.2	87	198	476	7.11	2.806	0.756	1.072	0.958
ST1-1	W12D25	22.2	82	181	469	6.86	2.645	0.691	1.056	0.925
ST1-1	W12D26	22.2	74	175	456	5.94	2.387	0.668	1.027	0.935
ST1-1	W12D27	22.2	42	127	433	7.49	1.355	0.485	0.975	1.009
ST1-1	W13D21	22.2	96	254	-	-	3.097	0.969	-	-
ST1-1	W13D22	22.2	120	231	478	5.83	3.871	0.882	1.076	0.786
ST1-1	W13D24	22.2	100	196	466	6.59	3.226	0.741	1.049	0.888
ST1-1	W13D25	22.2	87	197	458	6.60	2.806	0.752	1.031	0.889
ST1-1	W11D24	22.2	75	212	474	7.24	2.419	0.809	1.067	0.976
ST1-1	W14D24	22.2	76	202	448	6.50	2.451	0.771	1.009	0.876
ST1-1	W22D34	22.2	83	289	494	7.38	2.677	1.103	1.112	0.994
ST1-1	W32D44	22.2	78	323	508	6.59	2.516	1.233	1.144	0.888
ST1-1	W12D24	12.0	69	197	474	6.73	2.555	0.829	-	-
ST1-1	W12D24	10.0	57	176	471	6.70	2.476	0.800	1.047	0.869
ST1-5	W12D24	22.2	67	200	472	7.07	2.913	0.855	1.126	0.941
ST1-5	W13D24	22.2	73	200	472	6.97	3.180	0.855	1.126	0.928
ST1-6	W12D24	22.2	120	208	484	6.51	2.790	0.813	1.061	0.860
ST1-6	W13D24	22.2	128	208	475	6.58	2.976	0.813	1.041	0.869
ST1-1	SD21D3	22.2	97	220	502	6.78	3.129	0.839	1.131	0.913
ST1-1	SD31D4	22.2	107	300	507	6.62	3.451	1.145	1.142	0.892
ST1-1	W12D24	-	-	-	-	-	-	-	-	-
	W32D44	22.2	122	254	514	6.57	3.935	0.969	1.156	0.885
ST1-11	W12D24	22.2	69	185	416	5.61	2.464	0.864	1.103	1.072
ST1-11	W12D24	12.5	56	166	-	-	2.240	0.846	-	-
ST1-11	W12D24	10.0	45	146	397	3.70	2.413	0.829	1.039	1.067
ST1-11	W13D24	22.2	84	195	420	3.10	3.000	0.911	1.114	0.975
ST1-12	W12D24	22.2	59	159	343	3.51	1.555	0.994	1.088	0.964
ST1-12	W12D24	12.5	47	135	-	-	1.516	0.912	-	-
ST1-12	W12D24	10.0	35	111	311	3.74	1.400	0.816	0.965	1.016
ST1-12	W13D24	22.2	72	135	349	3.53	1.895	0.844	1.108	0.969
ST1-14	W12D24	22.2	51	112	256	2.16	1.186	1.131	1.071	0.911
ST1-14	W12D24	12.5	43	99	-	-	1.265	1.138	-	-
ST1-14	W12D24	10.0	43	102	264	2.10	1.433	1.172	1.095	0.843
ST1-14	W13D24	22.2	63	106	262	2.09	1.465	1.071	1.096	0.882
ST1-21	W12D24	22.2	47	85	197	1.06	1.567	1.889	1.125	0.876
ST1-21	W12D24	12.5	39	92	-	-	1.560	1.804	-	-
ST1-21	W12D24	10.0	46	94	195	1.12	2.000	1.740	1.114	0.941
ST1-24	W12D24	22.2	25	54	113	0.41	2.083	2.700	1.180	0.953
ST1-24	W12D24	12.5	18	41	108	0.38	2.571	2.412	-	-
ST1-24	W12D24	10.0	17	50	116	0.42	2.835	2.380	1.224	0.954

Continued

Table 5.2 : The values of residence time and variance for different tundishes with flow modifiers for the case of submerged stream pouring (Continued)

Run	FM	d (mm)	Residence time (s)			Variance				
			t_{min}	t_{peak}	t_{mean}	($s^2 x 10^{-4}$)	ε_{min}	ε_{peak}	ε_{mean}	ε_S
ST2-1	W53	22.2	08	104	312	6.370	0.800	0.981	0.802	0.848
ST2-1	D54	22.2	34	070	401	7.470	3.400	0.660	1.031	0.995
ST2-1	D64	22.2	31	116	414	7.740	3.100	1.094	1.064	1.030
ST2-1	W53D64	22.2	47	174	466	8.160	4.700	1.641	1.198	1.086
ST2-3	D52	22.2	22	056	114	0.341	2.444	0.903	1.046	0.812
ST2-3	D62	22.2	17	057	119	0.391	1.889	0.919	1.092	0.931
ST2-3	W11D21	22.2	23	084	122	0.391	2.555	1.355	1.120	0.931
ST2-5	D11	22.2	16	039	058	0.090	1.231	1.696	1.150	0.900

Table 5.3 : The values of residence time and variance for open stream pouring.

Run	FM	Residence time (s)			Variance	τ_{min} or ε_{min}	τ_{peak} or ε_{peak}	τ_{mean} or ε_{mean}	σ^2 or ε_S
		t_{min}	t_{peak}	t_{mean}	($s^2 x 10^{-4}$)				
AT1-1	None	43	93	266	5.51	0.077	0.167	0.478	0.178
AT1-1	D24	86	133	386	6.84	2.000	1.430	1.451	1.241
AT1-11	None	33	74	247	4.08	0.070	0.157	0.525	0.185
AT1-11	D24	86	122	319	4.39	2.606	1.648	1.291	1.076
AT1-12	None	35	64	199	2.92	0.091	0.165	0.515	0.196
AT1-12	D24	80	120	279	2.67	2.286	1.875	1.402	0.914
AT1-14	None	36	59	157	1.88	0.120	0.197	0.523	0.209
AT1-14	D24	67	84	216	1.80	1.861	1.423	1.376	0.957
AT1-21	None	30	52	124	1.06	0.139	0.242	0.576	0.229
AT1-21	D24	55	76	165	1.07	1.830	1.461	1.331	1.007
OT1-1	None	24	168	441	8.26	0.943	0.302	0.793	0.268
OT1-1	W12	50	126	428	8.21	2.083	0.762	0.970	0.991
OT1-1	D24	32	151	446	8.28	1.333	0.899	1.011	1.000
OT1-1	W12D24	69	232	478	7.82	2.875	1.381	1.084	0.944

Explanation : A : Inlet stream through an air chamber
O : Inlet stream through atmospheric air

τ_{min}, τ_{peak}, τ_{mean} and σ^2 values are for tundishes without FM, i.e., = $t/\bar{t}$ or $s^2/\bar{t}^2$

ε_{min} , ε_{peak}, ε_{mean} and ε_S values are for tundishes with FM, i.e., $(t)_{FM}/(t)_{NFM}$ or $(s^2)_{FM}/(s^2)_{NFM}$

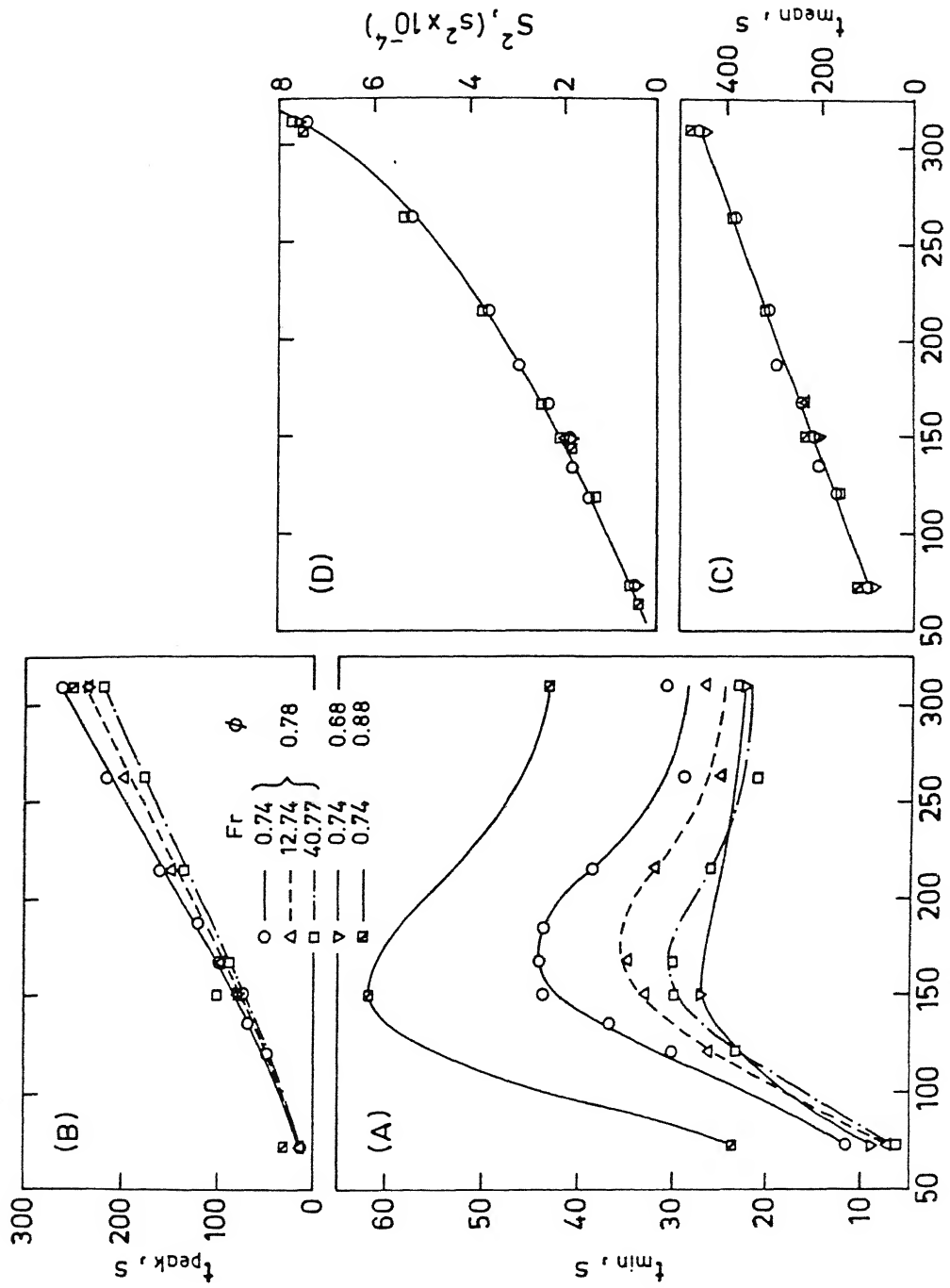

Fig.5.31: Variation of (A) minimum (B) peak and (C) mean residence time and (D) variance with the width of the tundish for different Froude numbers and inlet-exit distances.

tundish flow system. For tundish width lower than 150mm both the times i.e. t_{min} and t_{peak} decrease and hence axial dispersion remains constant.

The mean residence time (Fig. 5.31C) decreases with decrease in tundish width for all inlet Froude numbers and inlet-exit distance. The decrease in mean residence time with decrease in width is due to the decrease in volume available for dispersion of tracer in the tundish. The Froude number and the inlet-exit distance have no influence on the value of t_{mean}.

Fig. 5.31D shows that the variance (S^2) decreases continuously with the decrease in width for all Froude numbers and inlet-exit distances. The higher values of S^2 correspond to gradual increase or decrease in tracer concentration in the RTD curve, and smaller values of S^2 indicate the faster increase or decrease in tracer concentration. The former type of RTD curve with higher values of S^2 indicates larger reversing and recycling of the tracer within the tundish in relation to the later type of curve.

ii) *Effect of Bath Height*

Fig. 5.32 shows the variation of residence times and variance with bath height for different tundish widths. All the residence times i.e. t_{min} (Fig. 5.32A), t_{peak} (Fig. 5.32B) and t_{mean} (Fig. 5.32C) are found to increase continuously with the increase in bath height. The variance increases with increase in bath height

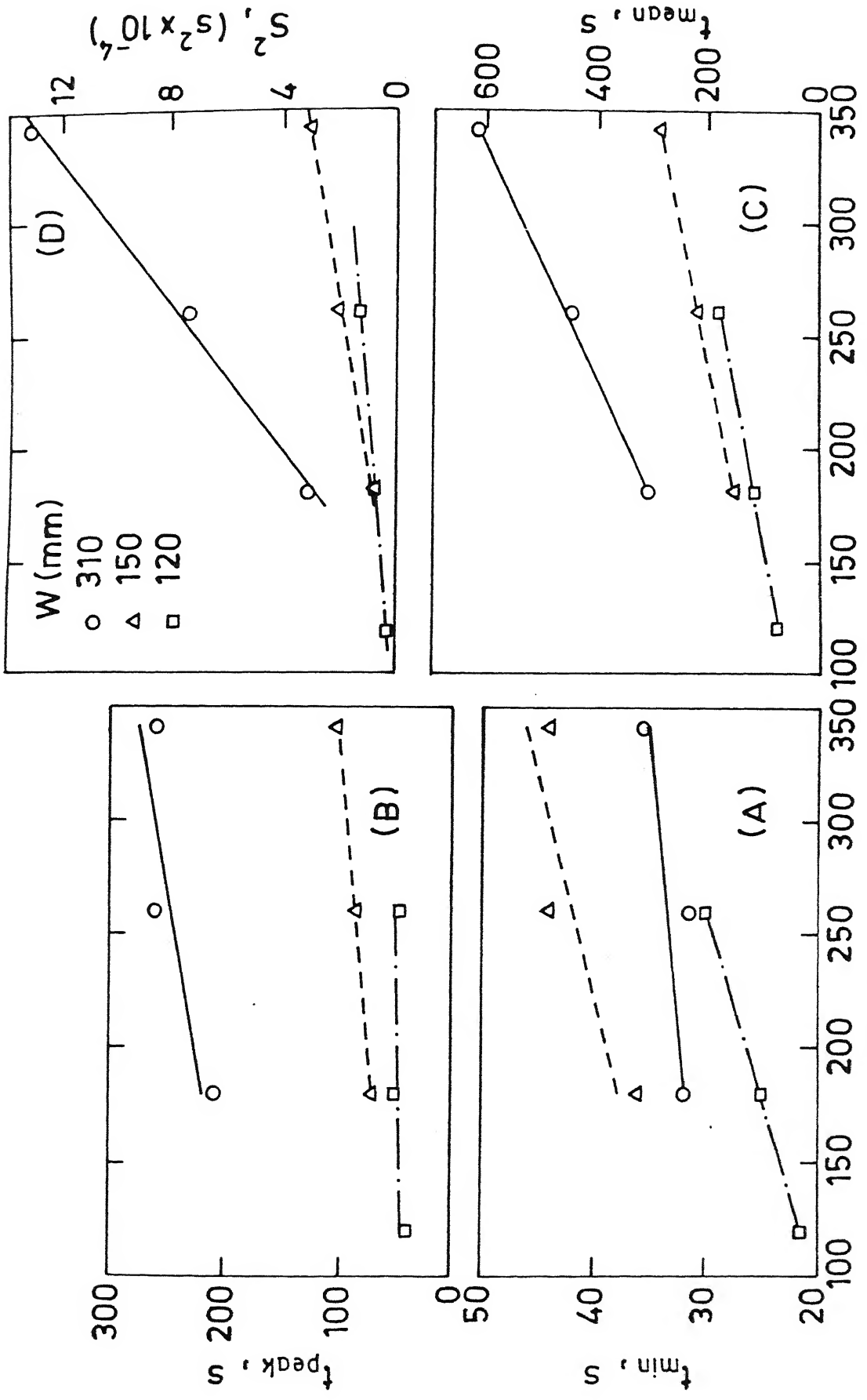

Fig.5.32: Variation of t_{min}, t_{peak}, t_{mean} and S^2 with the tundish bath height.

(see Fig. 5.32D). This is due to the increase in the volume of liquid for tracer dispersion.

iii) *Effect of Inlet-Exit Distance*

Fig. 5.33 shows the variation in residence times and variance as a function of inlet-exit distance for different tundish widths. The values of minimum residence time (see Fig. 5.33A) increase rapidly with increase in inlet-exit distance. This is because the increase in inlet-exit distance increases the spatial flow path of the liquid. The other residence times i.e. t_{peak} (Fig. 5.33B) and t_{mean} (Fig. 5.33C) also show a marginal increase with increase in inlet-exit distance. Fig. 5.33D shows that inlet-exit distance has negligible influence on variance of the RTD curve.

iv) *Effect of Inlet Flow Rate*

Fig.5.34 shows the variation of residence times and variance as a function of inlet flow rate (Q) in a 310mm wide tundish. The figure shows that all the residence times i.e. t_{min} (see Fig. 5.34A), t_{peak} (see Fig. 5.34B) and t_{mean} (see Fig. 5.34C) decreases continuously with increase in inlet flow rate. This is due to the increase in mean flow velocities in the tundish. Fig. 5.34D shows that with increase in inlet flow rate the variance of RTD curve decreases continuously. The increase in mean flow velocity in the tundish due to increase in flow rate causes the tracer concentration to increase and decrease rapidly in the RTD

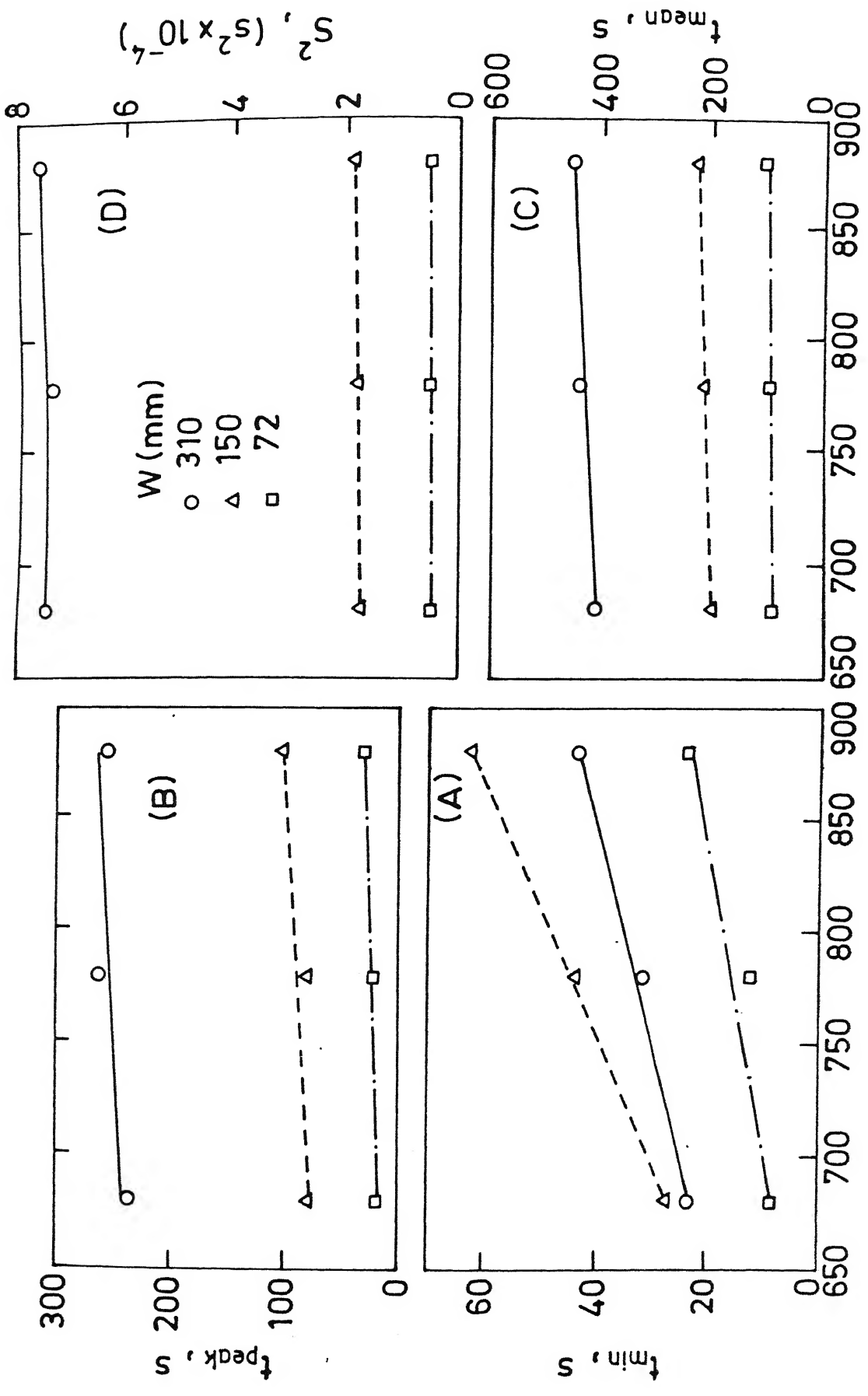

Fig.5.33: Variation of t_{min}, t_{peak}, t_{mean} and S^2 with the inlet-exit distance.

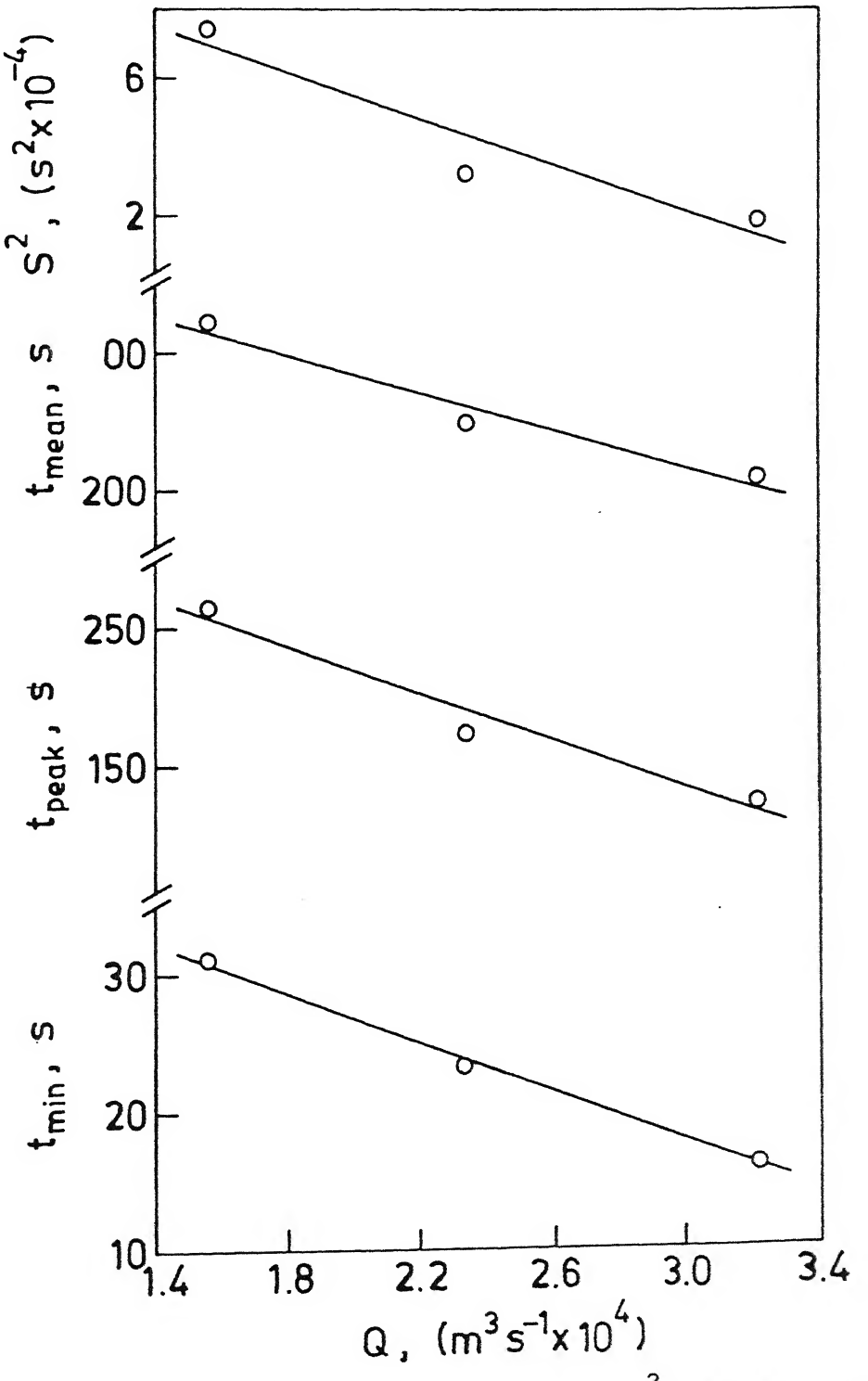

Fig.5.34: Variation of t_{min}, t_{peak}, t_{mean} and S^2 with the inlet flow rate.

curve.

(B) With Flow Modifier

i) *Effect of Height of FM*

Fig. 5.35 (A-D) shows the variation of residence times and variance with height of the FM (FM is either dam or weir) in ST1-1, ST1-11, ST1-12 and ST1-14 tundishes of different widths. The dotted line refer to the variation of weir height for W1 and W2 and the solid line to that of dam height for D1 and D2 configurations. The dashed and dotted-dashed lines refer to the specific combination of weir + dam of configurations W12D2, W13D2 and W1D24. In W12D2 and W13D2 height of the weir is kept constant and dam height is varied while in W1D24 dam height is constant and weir height is varied. In case of singularly placed FM, the residence time at FM height = 0 refers to the value without FM. While in case of weir + dam combination, the residence time at FM height = 0 refers to the value without weir or without dam.

It can be seen in Fig. 5.35A that increase in weir height in a 310mm wide tundish increases t_{min} marginally (see dotted line). This is true for both W1 and W2 configurations of weir. Following this observation no further experiments were conducted in tundishes of other widths with weir.

On the other hand dam leads to increase in t_{min} (see solid lines) for all the tundish widths. The increase, however, depends

FM	W	w_h	d_h	
	(mm)			
——— Dam	310			○
	262			△
	215			□
	167			▽
····· Weir	310			▼
- - - - - Weir + Dam	310	104		●
		156		▲
—·—·— Weir + Dam	310		91	■

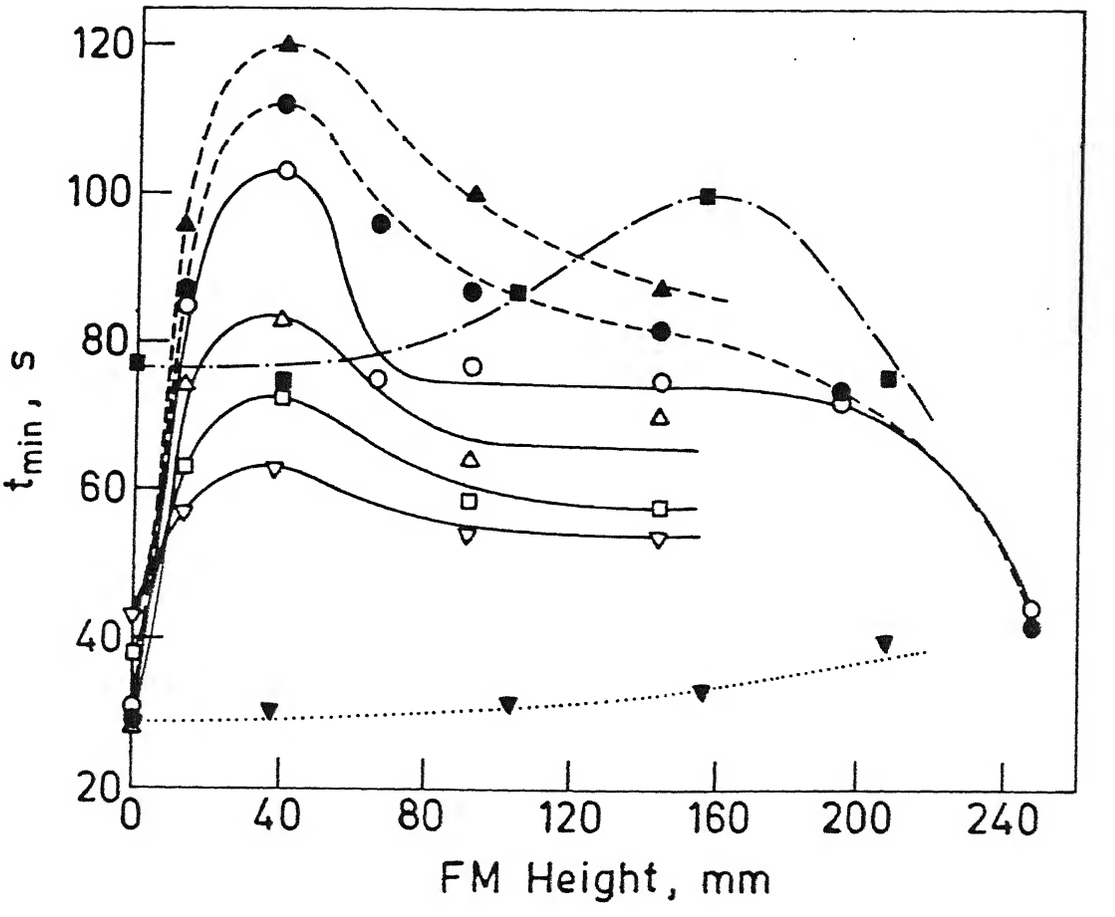

Fig.5.35(A): Variation of t_{min} with the FMs height for different types of FMs in different widths of the tundish

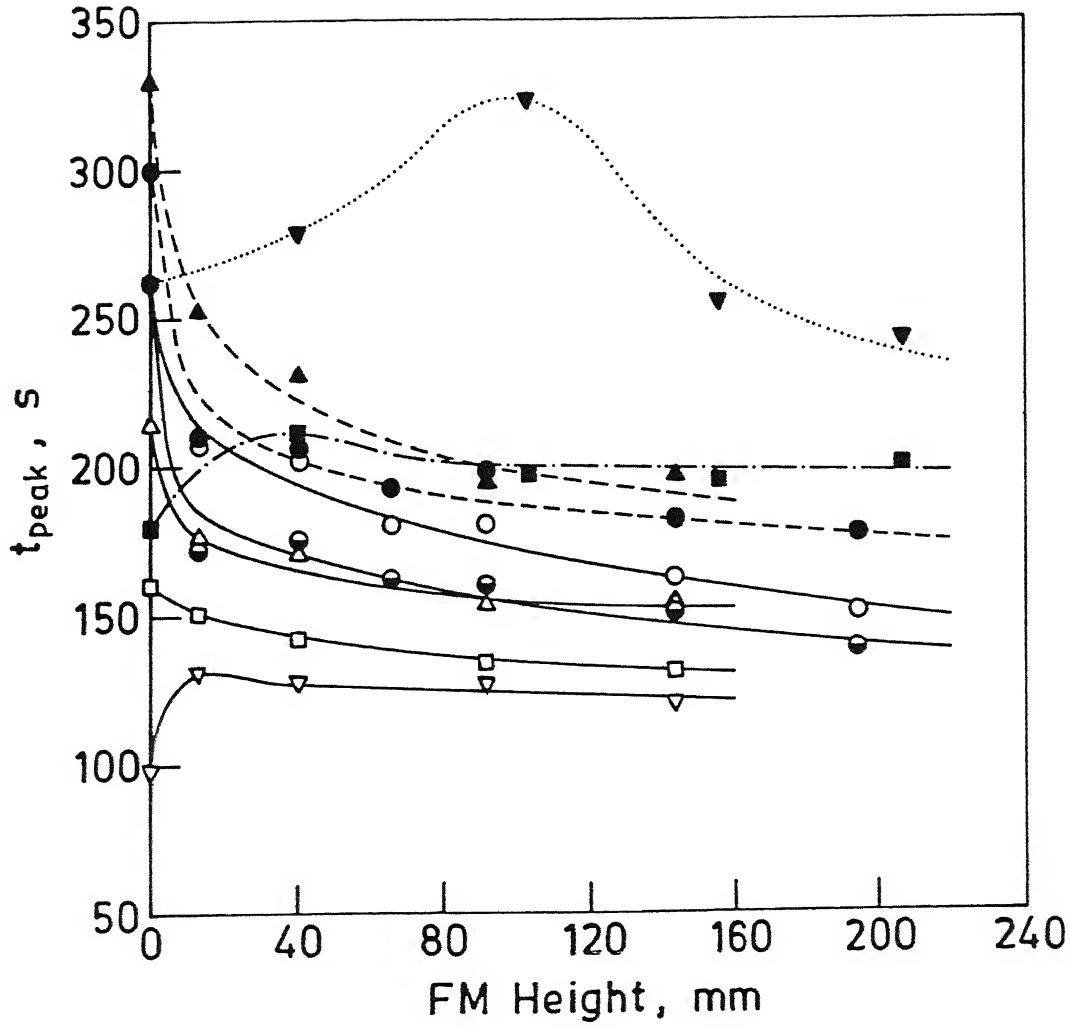

Fig.5.35(B): Variation of t_{peak} with FMs height for different types of FMs in different widths of the tundish (for the symbols see Fig. 5.35A).

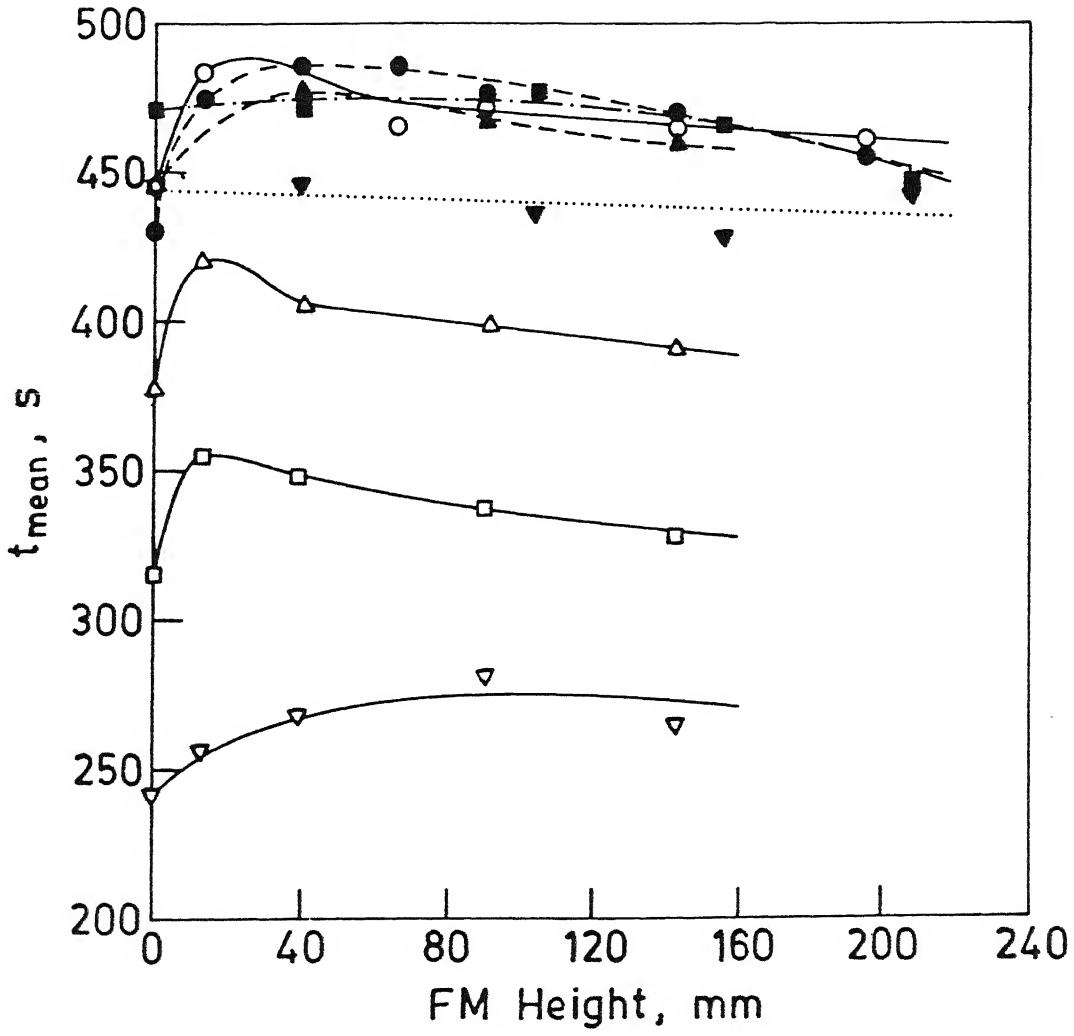

Fig.5.35(C): Variation of t_{mean} with FMs height for different types of FMs in different widths ofthe tundish (for the symbols see Fig. 5.35A)

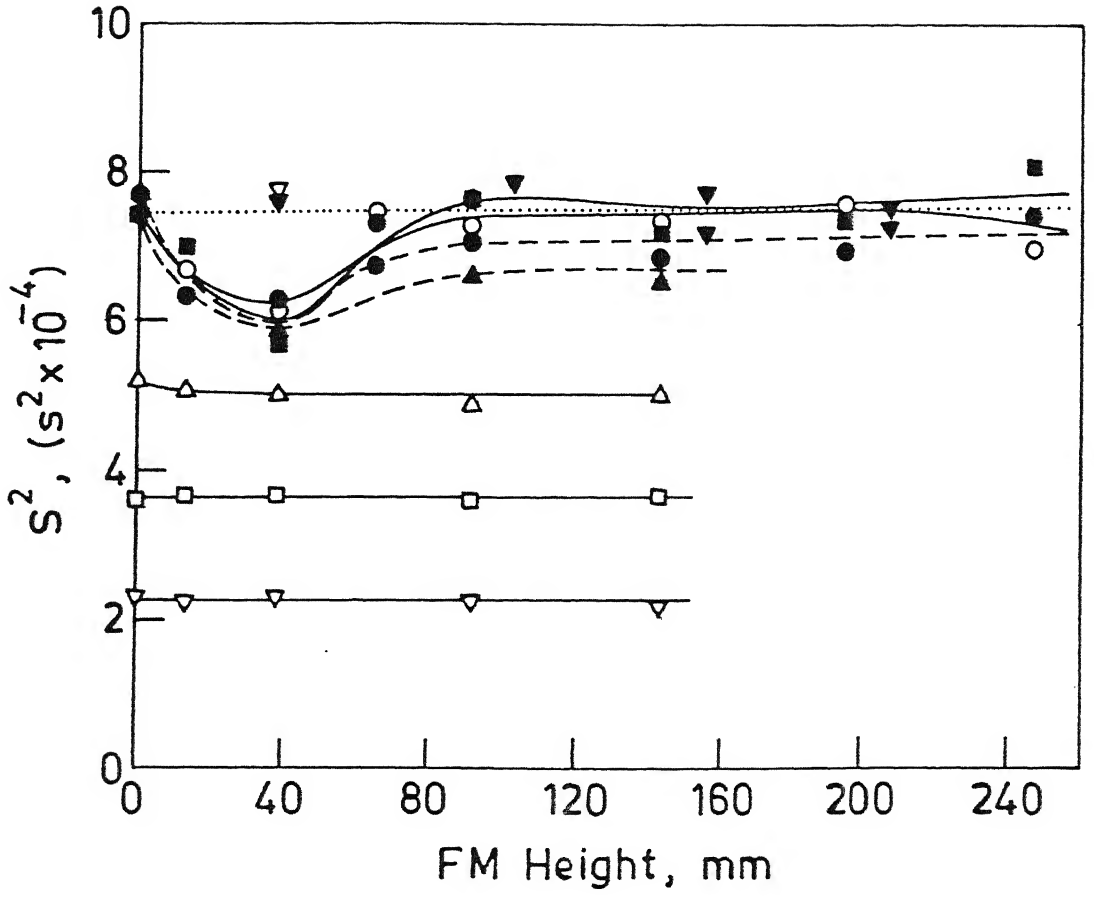

Fig.5.35(d): Variation of variance (S^2) with FMs height for different types of FMs in different widths of the tundish(for symbols see Fig. 5.35A).

on the dam height and tundish width as shown in the figure. The dam of height 38mm (0.15H) in D1 or D2 configuration gives maximum t_{min} for all the tundish widths which is possibly due to the cumulative effect of the elimination of short circuiting, deceleration of the inlet stream velocity, the restriction of the turbulence within the inlet region and forcing the liquid to flow towards the surface before it flows into the rest of the tundish. Further increase in dam height in between 38mm to 65mm decreases t_{min}. But when dam height is increased further from 65mm to 190mm, it is interesting to note that t_{min} does not change significantly.

In weir+dam combination, weir height and dam height can be varied independently. For a constant weir height, the variation of dam height (see dashed lines) results in the behaviour similar to that of dam except within the range of d_h = 38mm to 190mm. Beyond 38mm dam height the value of t_{min} is greater than that for dam alone. When dam height is kept constant, the variation of weir height (see dotted - dashed line) changes the behaviour, and t_{min} is found to attain the maximum value at weir height 156mm.

In Fig. 5.35B, t_{peak} initially increases with increase in weir height and after attaining a maximum value at a weir height of 104mm, starts decreasing. Dam placed alone in the tundish decreases t_{peak} in tundishes of all widths except in 167mm wide tundish. In 167mm wide tundish t_{peak}, after an initial increase for smaller dam heights (<38mm), does not change with further increase in dam height.

Weir alone in the tundish influences t_{mean} (see Fig. 5.35C) to a very small extent. The increase in weir height has a negligible effect on t_{mean}. The use of dam alone or in combination with weir influences significantly the values of t_{mean}. The increase in dam height initially increases t_{mean} and then tends to level-off with the further increase in dam height for all the tundish widths.

The increase in dam height in weir + dam combination also shows the same trend. The use of dam or weir+dam of any configuration increases the value of t_{mean} with respect to NFM, except when dam alone is placed very close to the inlet i.e. at 50mm from the inlet. It can be seen that for a constant dam height (dotted-dashed line), the increase in weir height shows a marginal decrease in the value of t_{mean} .

In Fig. 5.35D, it can be seen that the weir height has no influence on the variance. The dam alone or in combination with weir in a 310mm wide tundish decreases the value of variance upto dam height 38mm. Further increase in dam height to 65mm shows an increase in variance. The increase in dam height beyond 65mm shows a negligible change in variance. In all other widths, the increase in dam height shows no effect on variance.

ii) *Effect of Tundish Width*

In the section 5.2.2.1 the effect of width on the residence times is described in tundishes without flow modifiers.

Fig. 5.36(A-D) shows the variation of t_{min}, t_{peak} and t_{mean} as a function of tundish width for D24 dam (solid lines) and W12D24 weir+dam (dashed lines) and W13D24 weir+dam (dotted dashed lines) configurations at different Froude numbers. It can be seen that t_{min} is maximum for 310mm wide tundish at all Froude numbers and for both dam and weir + dam combinations. t_{min}, then decreases with the decrease in width. However, the decrease in t_{min} with the decrease in width from 310mm to 215mm is somewhat greater than decrease in width from 215mm to 120mm. In the later range of widths, it appears that $t_{min,}$ after attaining the minimum value, has a tendency to increase.

As seen in Fig. 5.36B, t_{peak} decreases with the decrease in the tundish width for dam and weir+dam at all Froude numbers. Since t_{min} and t_{peak} both decrease, their ratio i.e. t_{min}/t_{peak} (this ratio determines axial dispersion) is not influenced significantly as a consequence of which the axial dispersion may not be influenced significantly by the decrease in width.

The mean residence time as shown in Fig. 5.36C decreases with the decrease in the tundish width for all types and combinations of flow modifiers (see solid line); the vertical bar represents the variation in t_{mean} due to different heights and positions of dam and weir+dam at different inlet Froude numbers.

The variation of variance with width is shown in Fig. 5.36D for all types and combination of flow modifiers; the vertical bar is the limit of values obtained due to different heights and configurations of FM. Variance decreases with the decrease in the

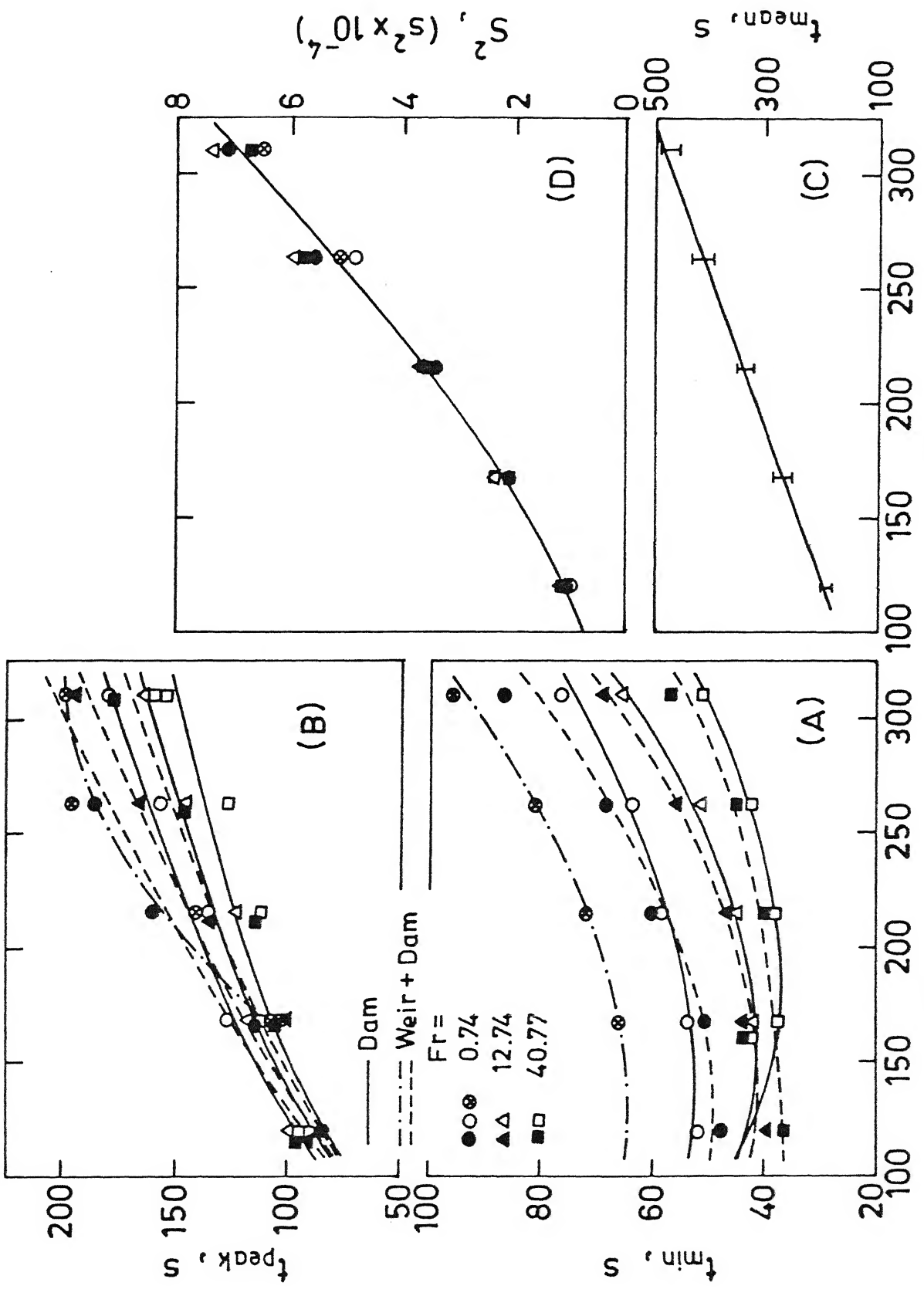

Fig.5.36: Variation of (A) t_{min} (B) t_{peak} (C) t_{mean} and (D) S^2 with the tundish width at different Froude numbers for dam and weir+dam combination.

width.

iii) *Effect of Position of FM*

The effect of position of the FM (dam, weir or weir+dam) on residence times and variance is shown in Fig. 5.37, for a 310mm wide tundish with inlet shroud diameter 22.2mm. For weir+dam combination the position refers to the distance between the inlet stream and the dam, and position of weir is always 100mm from the dam on it's upstream side.

The increase in position of the weir increases t_{min} slightly but decreases t_{peak}, which shows a decrease in axial dispersion in the bath. t_{mean} is independent of weir position. The increase in position of dam in single or in combination wwith weir decreases t_{min}, but increases t_{peak}, resulting in increase in axial dispersion. t_{mean} is found to increase slightly with increase in dam position. The values of variance are found to decrease with increase in position of FM (i.e. weir, dam alone or in weir+dam).

iv) *Effect of Inlet-Exit Distance*

Fig. 5.38(A-D) shows the effect of inlet-exit distance on the variation of residence times and variance for dam alone (solid line) and weir+dam combination (dashed and dotted - dashed line). Dam alone or in combination with weir is placed at 0.15L and is of height 0.35H in both the cases. Weir is placed at 0.05L and is of height 0.40H (dashed line) or 0.60H (dotted-dashed line) in

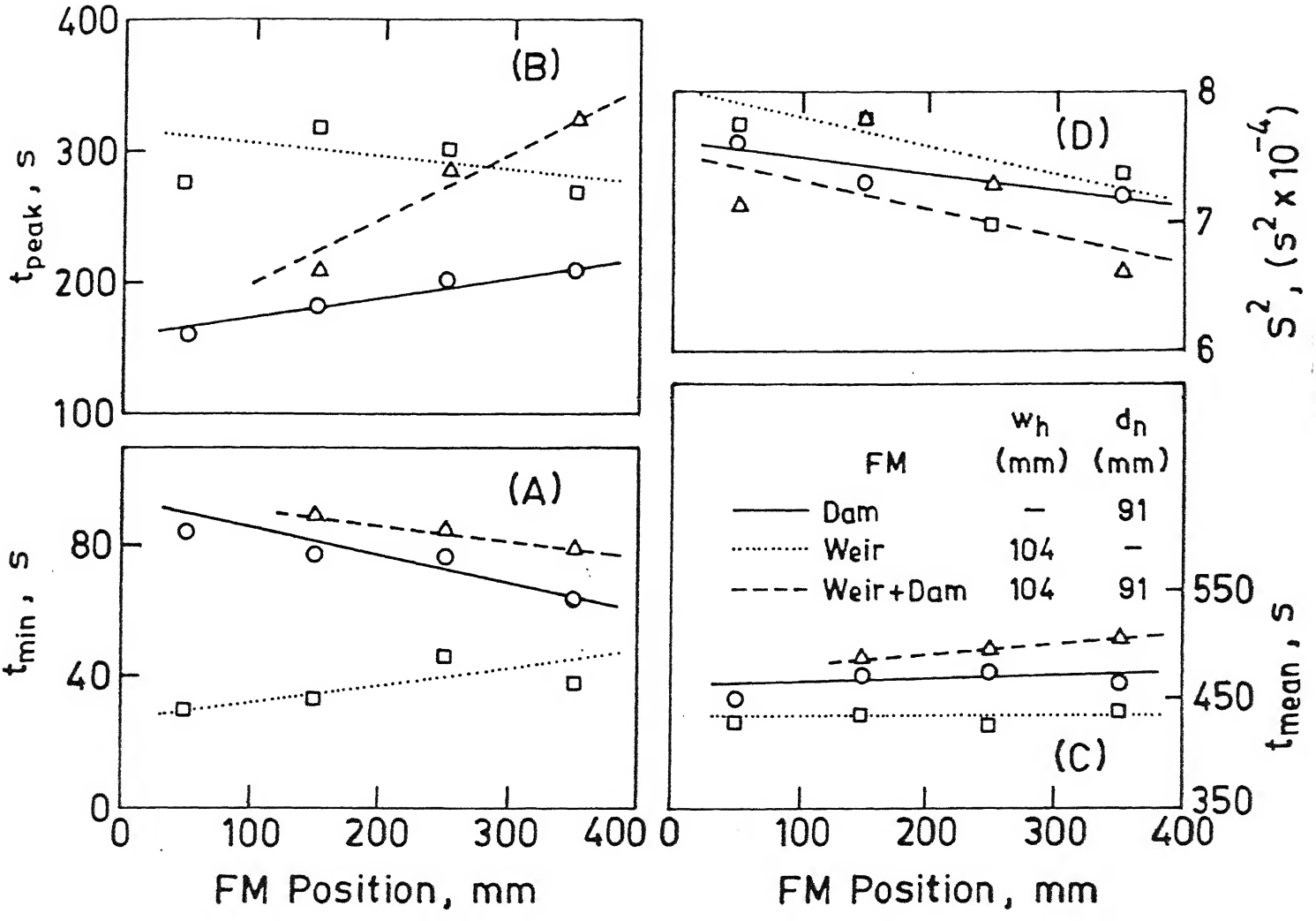

Fig.5.37: Variation of (A) t_{min} (B) t_{peak} (C) t_{mean} and (D) S^2 with the position of different types of FM.

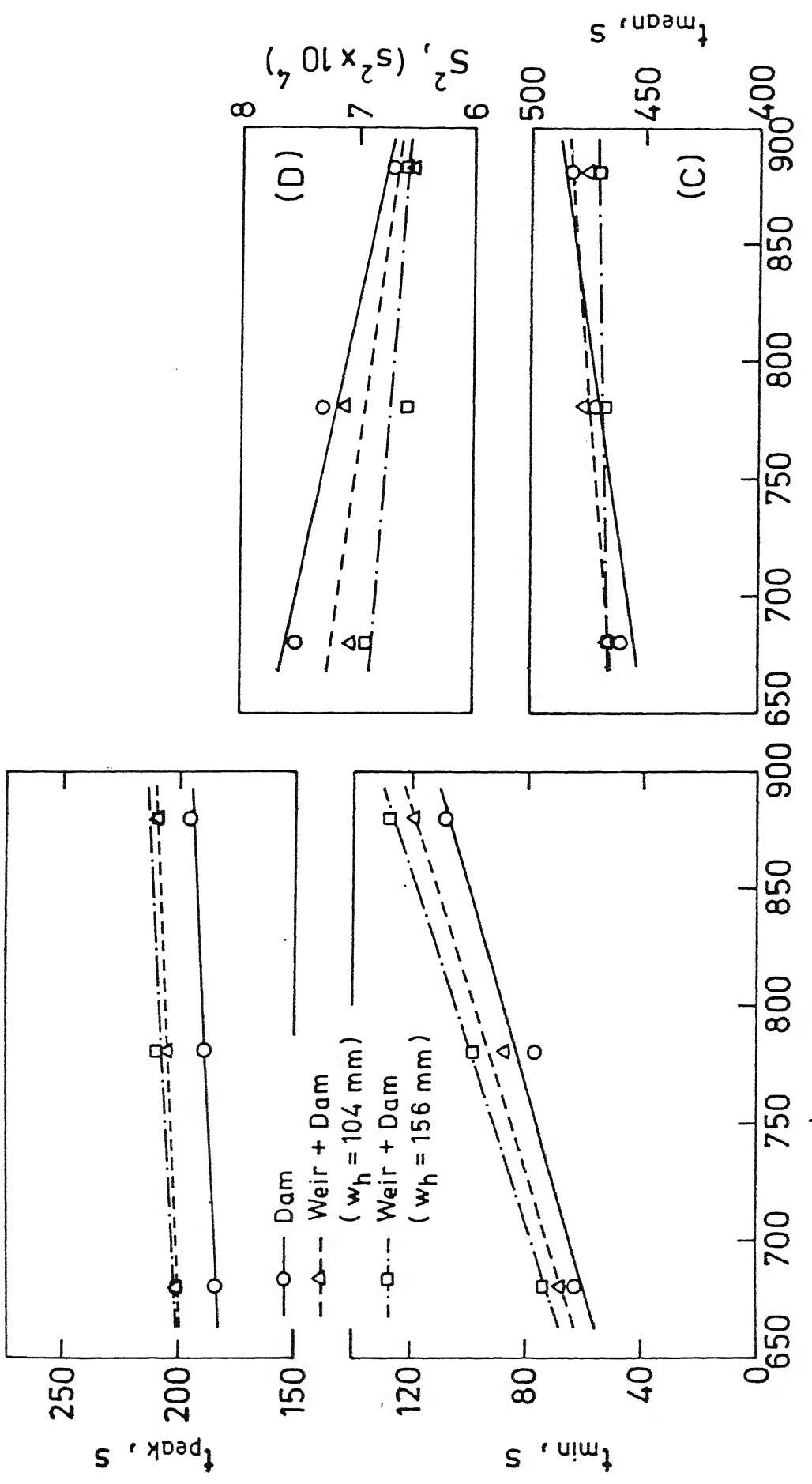

Fig.5.38: Variation of (A) t_{min} (B) t_{peak} (C) t_{mean} and (D) S^2 with the inlet-exit distance for dam and weir+dam combination.

weir+dam combination.

As seen in the Fig. 5.37A, t_{min} increases with increase in inlet exit distance and for all distances t_{min} for weir+dam combination is greater then that for dam. Deeper weir in weir+dam combination produces higher values of t_{min} than shallow weir. t_{peak} and t_{mean} are marginally influenced by inlet-exit distance. t_{peak} is greater for weir+dam combinations than for dam alone at all inlet exit distances. The increase in inlet-exit distance increases the overall flow path of water, which results in increase in all the residence times. Variance in Fig. 5.38D is found to decrease with increase in inlet-exit distance, for all types of flow modifier. It is probably due to the decrease in reversing and recirculation of liquid in the bath, with increase in inlet-exit distance.

5.2.2.2 *Open Stream Pouring*

Fig. 5.39(A-D) shows the variation of residence (Dashed line) times and variance with the width of the tundish without FMs (dashed lines) and in presence of dam (solid line) for the open stream pouring through air chamber. As seen in Fig. 5.39A, the minimum residence time decreases continuously with the decrease in the tundish width for both the cases. It may be noted that this type of variation of t_{min} with W is quite different than that observed for submerged inlet stream pouring in tundishes without FM (see Fig. 5.31A and section 5.2.2.1). This may be due to the difference in the tundish fluid flow behaviour caused by submerged and open stream pouring. In submerged inlet stream, there is no

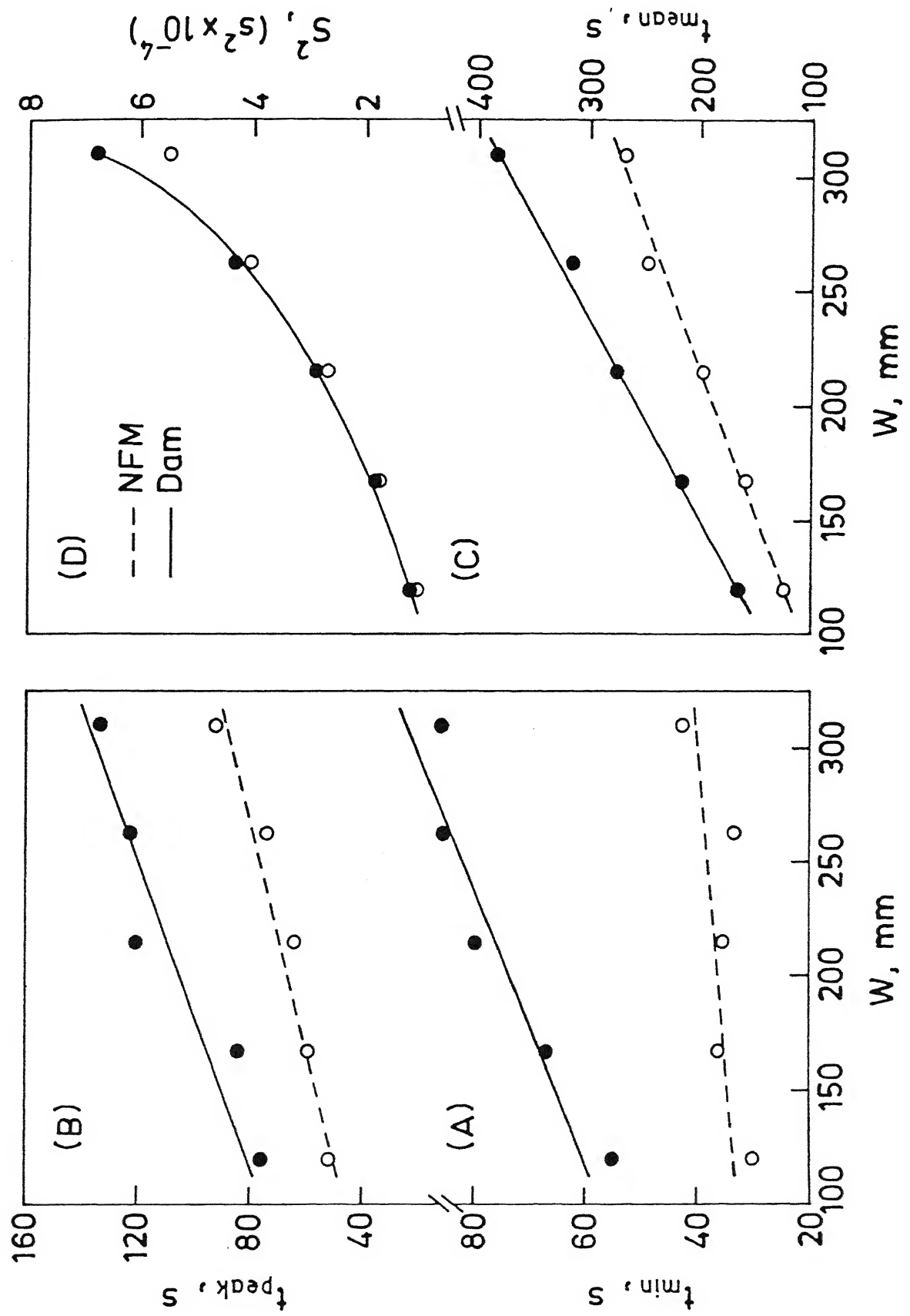

Fig.5.39: Variation of (A) t_{min} (B) t_{peak} (C) t_{mean} and (D) S^2 with the tundish width for air shrouded stream pouring.

entrainment of air, but a strong flow is generated along the tundish bottom which leads to short circuiting of the fluid. The presence of short circuiting and its retardation and increase in overall average velocity of the fluid with the decrease in width were responsible for the duel variation of t_{min} with the decrease in W. However, in case of open stream pouring, considerable amount of air is entrained into the inlet stream. This entrained air creates surface directed flow and helps preventing short circuiting. Thus, decrease in width increases the overall velocity of the fluid which leads to early appearance of the tracer at the exit and hence decrease in t_{min}.

Similarly t_{peak} and t_{mean} decrease continuously with the decrease in width and the values of t_{peak} and t_{mean} are greater for dam than that for without dam. The variance of the RTD curve decreases with the decrease in the width. Here the effect of dam is not observed on the values of the variance.

When the stream falls through the atmospheric air (i.e. without air chamber) into the tundish, the minimum residence time for 310mm wide tundish without FM is very much smaller than that when the stream falls through the air chamber (see Table 5.3). In the same tundish, weir is found to increase t_{min} more than that of dam. However, weir+ dam combination increases t_{min} very much when compared with NFM (see Table 5.3).

The peak and mean residence time, i.e., $t_{peak}$and t_{mean} are much greater for open stream pouring as compared with open stream with air chamber.

CHAPTER - 6

DISCUSSIONS

In the tundish fluid flow investigations, flow pattern and residence time of the fluid are the two important aspects. From the results on mechanism of tracer dispersion and the variation of tracer concentration with time, i.e. RTD curve, the information on the pattern of fluid flowing in the tundish is obtained. The residence time data are used to develop the empirical correlations. In this section the results of Chapter - 5 are discussed in relation to flow pattern and residence times.

6.1 FLOW PATTERN

6.1.1 Concepts

There are two idealized patterns for the fluid flowing in a vessel: plug and mixed flow. In the plug flow pattern, the flow of the fluid through the reactor is orderly with no element of fluid overtaking or mixing with any other ahead or behind. The necessary and sufficient condition for plug flow is for the residence time in the reactor to be the same for all elements of fluid. In the mixed flow pattern the contents of the vessel are well mixed and uniform throughout.

The real reactor never fully follows these flow patterns. This deviation can be caused by channeling of the fluid, by

recycling of fluid or by creation of stagnant regions in the vessel or by short circuiting of the fluid. From the shape of the RTD curve,the flow pattern can be derived easily by multiparameter model[47]. In multiparameter model, a real reactor is considered to consist of different regions (plug, dispersed plug, mixed, dead water) interconnected in various ways (bypass, recycle, short circuiting etc.)[47]. Depending on the type of flow and interconnection of these regions, different shapes of RTD curves are obtained[47]. Fig. 6.1 shows some simple flow models and their tracer response curves in terms of C vs. τ plot[47].

As seen in the figure, the flow models in a real reactor are characterized by the dead region (the term dean region accounts for the portion of fluid which is relatively slow moving, and which, as an idealization, sometimes is taken to be completely stagnant[47]). In i) tracer response curve is shown for plug flow exchanging with dead region. The tracer exits the vessel in time less than theoretical residence time. Whereas in ii) a mixed model flow reactor alongwith dead region is shown alongwith its tracer response curve; in which at $\tau = 0$, $C > 1$. In flow model iii) a real reactor is considered to consist of plug and mixed flow. The tracer response curve in case of short circuiting is shown in iv). It is characterized by two peaks.

6.1.2 Derivation

The flow pattern in the present study is derived from the shape of the RTD - curves.

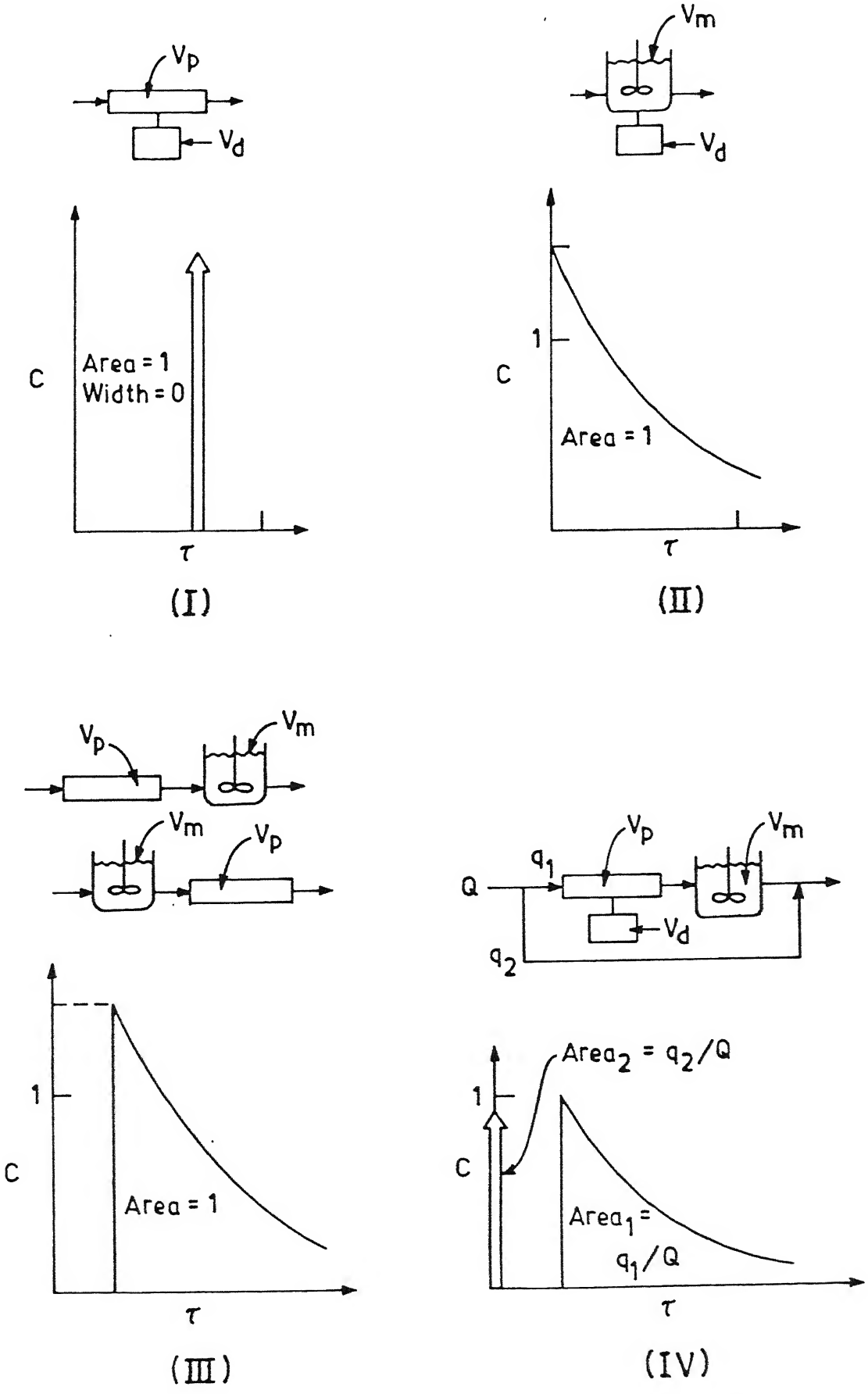

Fig.6.1: Some idealized models for flow of fluid in a vessel alongwith their tracer response curves.

In the present study two different shapes of RTD curves are obtained (see section 5.2.1) for submerged and open stream pouring into tundishes with and without FMs for a wide range of tundish design and operating parameters. One shape of the curve is characterised by two peak values of concentration and the other characterized by single peak value of concentration. In Fig. 6.2(A) an experimental RTD curve (d) with two peak values of concentration is compared with the ideal RTD - curves (a,b,c). Whereas, in Fig. 6.2(b), an experimental RTD curve with single peak value of concentration (curve c) is compared with the ideal RTD - curve (a and b). The experimental curves shown in Fig. 6.2 are typically observed in the present study for a wide range of variables (see Tables 4.1 and 4.2). The fluid flow pattern in case of Fig. 6.2(a) consists of dispersed plug flow (since in ideal plug flow $t_{min} = t_{peak}$), mixed flow and short circuited flow. Whereas in Fig. 6.2(b) the flow pattern consists of mixed, and plug flow which are followed by dead volume. Both the flow patterns are sketched in Fig. 6.2(c) and (d). The flow pattern 6.2(C) is valid for a wide tundish, i.e., W/L>0.210, and for without FM in case of submerged stream pouring. Whereas in all other cases of the present study, the flow pattern of Fig. 6.2(d) is valid. This includes submerged stream with FM, open stream without and with FM and narrow tundishes.

In some full and fractional scaled water model studies, the flow pattern was found to consist of dispersed plug and mixed flow alongwith dead water region for submerged and open stream pouring[6,35-41]. Very few investigators have reported short circuiting in the tundish fluid flow system[5,22]. In some studies

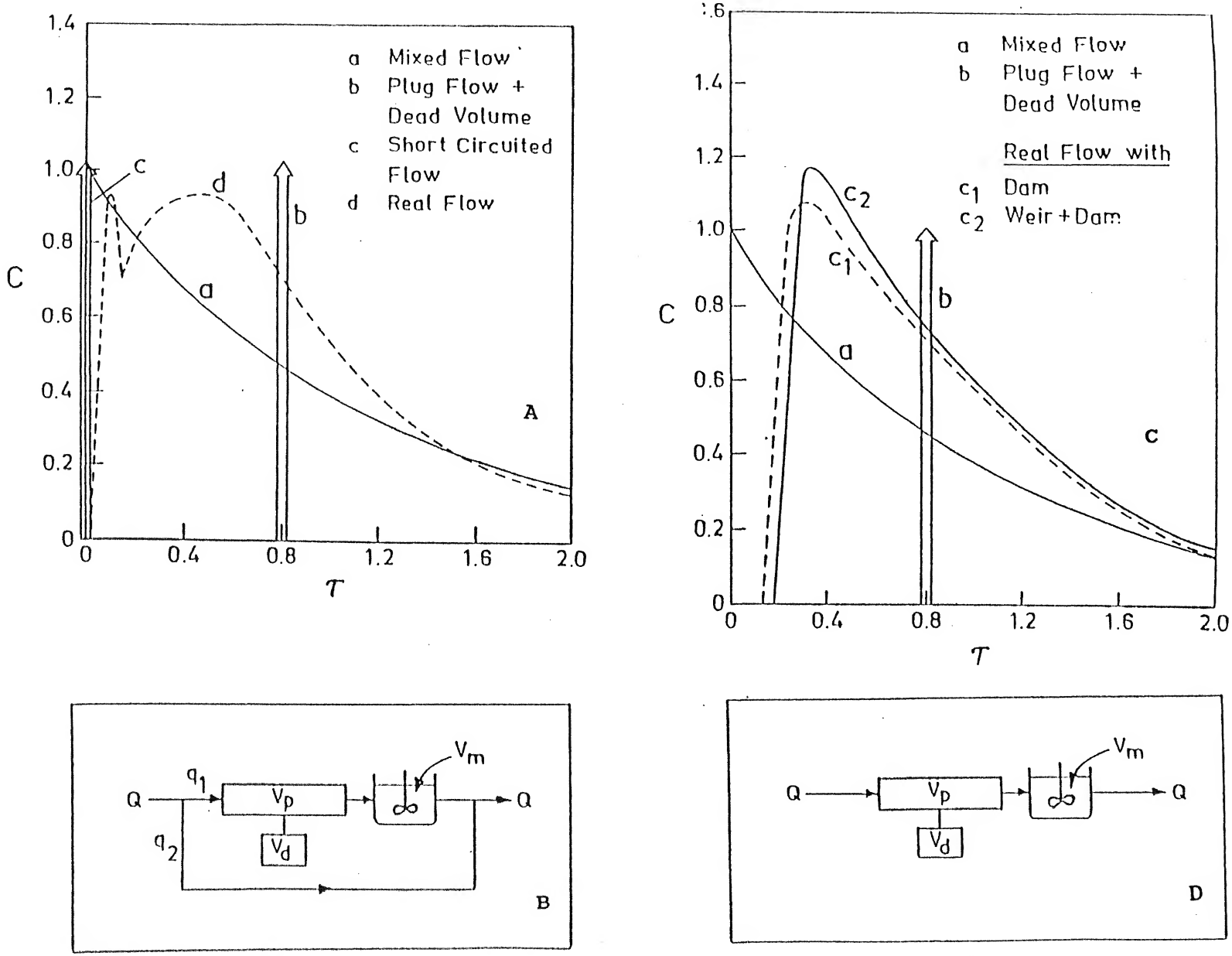

Fig.6.2: Derivation of flow pattern from the shape of the RTD curves (A) RTD curve with two peak values of concentration, (B) flow pattern associated with A, (C) RTD curve with single peak value of concentration and (D) flow pattern.

it has been reported that the velocity component of the fluid flowing on the inlet-exit plane is greater than rest of the planes[5,22]. For the flow of molten steel, the RTD curve was found to be identical to that of water flow.[37]

Considering the finding of the flow pattern of the present study and those of other investigators, it appears that the flow patterns sketched in Figs. 6.2(C) and (D) are a characteristic feature of water flowing in fractional or full scale water model and molten steel flowing in the actual tundish. This indicates that the dissimilarity in the magnitude of the Reynolds number between the present study (see Table 3.2) and caused by fractional scaled water model with the industrial tundishes does not seem to influence the flow pattern of the fluid flowing in the tundish.

6.1.3 Explanation

In the following, an attempt has been made to explain the observation of the similarity of flow pattern for flow of water in model tundishes and molten steel in real tundishes using some simple features of turbulent flow.

In the turbulent flow, the transport of momentum to the neighbouring fluid layers occurs via eddies[48]. The largest eddies are of size comparable with the pipe diameter and the fluctuating velocities are of the order of maximum velocity at the centre of the pipe. These are low frequency eddies and contain perhaps as much as 20% of the total kinetic energy of the

isotropic turbulence. Then, there are medium size eddies which are called energy containing eddies and make the main contribution to the kinetic energy. Small eddies in which dissipation by viscous effects increase, are formed during continuous degradation of large eddies. The smallest size eddies have very large frequency and viscous forces are as important as inertial forces. Most of the turbulence energy resides in the large and medium size eddies and very little in the smallest size eddies which are at the bottom of the eddy spectrum.

In pipe flow turbulence the various lengths of eddies and the associated velocities are given by the following equations[48].

$$l'_e = 0.05d\ (Re)^{-1/8} \text{ and } \bar{u}'_e = 0.2\ (Re)^{7/8}(\nu/d) \qquad (6.1)$$

$$l'_d = 0.20d\ (Re)^{-0.78} \text{ and } \bar{u}'_d = 0.442\ \ u_m\ (Re)^{-0.22} \qquad (6.2)$$

$$l'_k = 4d\ (Re)^{-0.78} \quad \text{and } \bar{u}'_k = 0.26\ \ u_m\ (Re)^{-0.22} \qquad (6.3)$$

In the tundish, fluid (water in model or steel in prototype) enters via the submerged shroud. The Reynolds number at the exit of the shroud is normally within the range 10^4 to 10^5 (see Table 3.2) and hence the flow is highly turbulent. Therefore, the momentum from the plunging jet must be transferred in the tundish via eddies which leads to the generation of the flow pattern and the residence time distribution of fluid flowing in the tundish. Using Eqs. 6.1 to 6.3, the lengths and corresponding velocities of different eddies are calculated for water flowing in the model tundish and molten steel flowing in the prototype.

In Fig. 6.3 the energy/unit mass ratio i.e. $(\bar{u}'/u_m)^2$ (where $\bar{u}' = \bar{u}'_e$ or $\bar{u}'_d$ or $\bar{u}'_k$) is plotted against dimensionless eddy length i.e. d/l' (where $l' = l'_e$ or l'_d or l'_k)[49]. In this plot the scale factor for the model tundish varies from 1/6 to 1 and Reynolds number from 10^4 to 10^5.

According to Davies the length of the largest eddy is of the order of pipe radius[48]; hence d/l' for these eddies is 2. Further the largest eddies contain only about 20% of the total turbulence energy, the energy per unit mass ratio corresponding to largest eddy length ratio for different tundishes is a singular value which is shown by a star in the Figure 6.3. The calculated values of the present study are also shown in the Figure 6.3.

It can be seen that the different lengths of the eddies produced at the exit of the submerged shroud for water and steel, irrespective of the scale of the model and type of fluid, distribute uniformly along the line drawn in the figure. This plot indicates that the mechanism of momentum transfer as governed by the eddies at different Reynolds numbers from the submerged shroud (the momentum of the plunging jet is infact the source of production of fluid flow pattern in the tundish and a flow modifier can be considered as a device which redistributes the momentum of the plunging jet in favour of one type of fluid flow pattern or the other) to the rest of the tundish is nearly identical in steel and in different scaled water model tundishes including the present study. Therefore, it is plausible to expect the similar flow pattern irrespective of the type of fluid and difference in the Reynolds number within the turbulent regime.

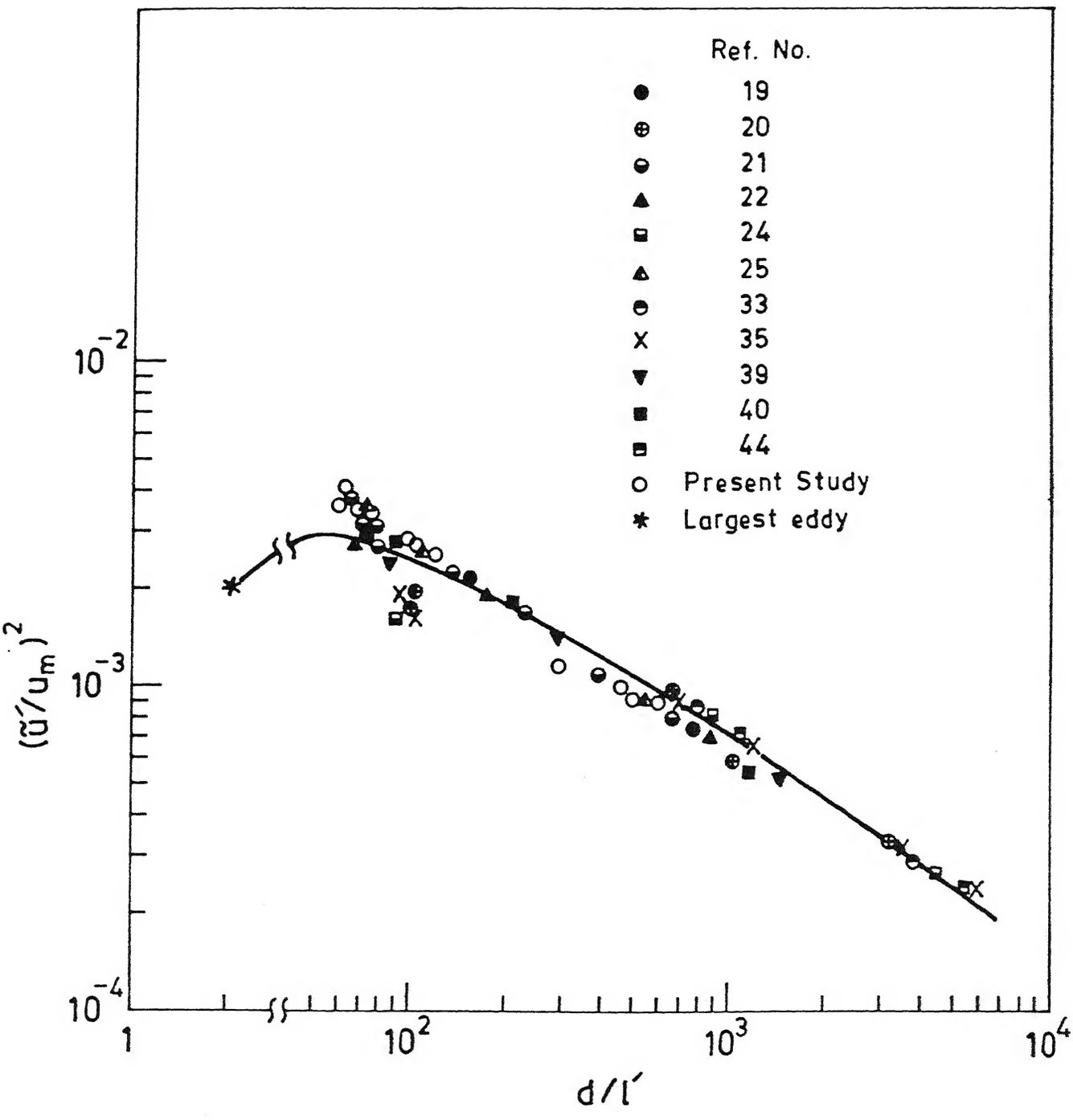

Fig.6.3: Turbulence eddy spectrum in steel and water model tundishes (* denotes largest eddy).

6.2 DEVELOPMENT OF CORRELATIONS

The residence times of the fluid flowing in the tundish is found to depend on several factors as mentioned in Chapter - 5. From the data bank, correlations are developed to calculate residence times. It is to be mentioned that the nature of the variation of the residence times in tundishes without flow modifier is different than those with flow modifiers; hence separate correlations are required to be developed. Further, correlations for residence times are obtained for submerged inlet stream. The residence time data for open stream are discussed with reference to that of submerged inlet stream.

6.2.1 Residence Times

6.2.1.1. *Without Flow Modifiers*

(A) *Selection of Parameters*

The results have shown that all the residence times increase with the increase in the bath height and the inlet-exit distances. The effect of Froude number is found to be small in comparison to the other parameters. Further, it is observed that the minimum residence time first increases with the decrease in width and then decreases with the further decrease in the width (see Fig. 5.31). This duel effect of width on t_{min} appears to be due to the simultaneous effect of the north-south walls of the tundish and the mean velocity of the fluid and is explained as follows:

Many investigators have computed the velocity of the fluid flowing in the tundish and diagrams of the spatial velocity field are given in terms of arrows[5,14,16-28]. From these diagrams, the maximum velocity of the fluid on the horizontal xy-plane at z=0 (the velocity of the fluid on this plane governs the minimum residence time of that fluid) is determined in the present study from the available literature[16-19,22]. It may be noted that very few authors specified complete experimental conditions. The dimensionless velocity i.e. u_{max}/u_{ag} (where $u_{ag} = Q/WH$) is plotted in Fig. 6.4 as a function of tundish width. The line is drawn to show the trend of results. The said dimensionless velocity is maximum for the widest tundish and decreases with the decrease in width.

The above observations (derived from Fig. 6.4) helps to explain the cause of duel effect of width on the t_{min}[50]. With the decrease in width, the north-south walls tends to retard the movement of the fluid on the horizontal plane which results in increase in t_{min}. But decrease in width results simultaneously in increase in the mean flow velocity. After attaining a peak value of t_{min} (at W = 0.15L) it appears that the effect of increase in mean flow velocity on t_{min} becomes more predominant and t_{min} starts decreasing[50].

(B) *Mathematical Function*

Based on the above trend, the following functions are used to correlate the minimum, peak and mean residence times[50]:

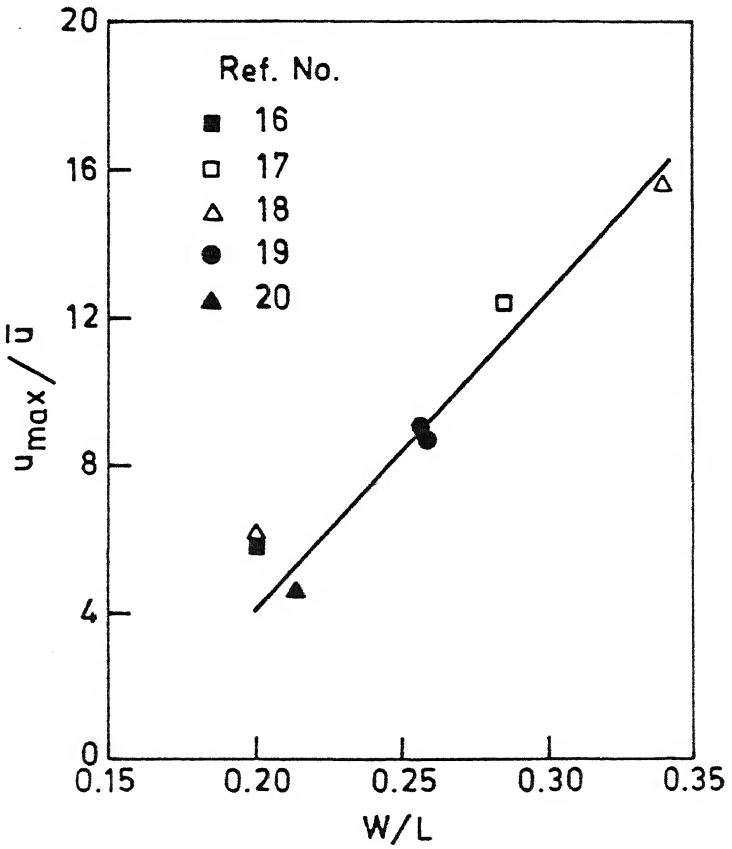

Fig.6.4: The dimensionless plot of the x-component velocity of the fluid near the bottom plane as a function of tundish width.

$$\tau_{min} = (a_0 + a_1\alpha + a_2\alpha^2 + a_3\alpha^3)\beta^m\phi^n Fr^k \quad (6.4)$$

$$\tau_{peak} = A\sigma^c\beta^m\phi^n Fr^k \quad (6.5)$$

$$\tau_{mean} = B\alpha^c\phi^m \quad (6.6)$$

Function 6.4 describes the maximum or minimum value of τ_{min} with respect to α and is in accordance with the experimental observations. The maxima or minima would depend on the sign and the magnitude of the constants a_0, a_1, a_2 and a_3. The influence of other parameters, i.e., β, ϕ and Fr is described by exponential variation, although experimental data could be described by a linear function. The peak and mean residence time, i.e., τ_{peak} and τ_{mean} are also described by an exponential function. The values of all constants and exponents appearing in functions 6.4 to 6.6 are determined by the multiple regression analysis[51,52]. The following results are obtained:

$$\tau_{min} = (-0.383 + 8.638\alpha - 44.14\alpha^2 + 67.180\alpha^3) \times \beta^{-0.607}\phi^{3.044}Fr^{-0.082} \quad (6.7)$$

$$\tau_{peak} = 0.546\ \alpha^{0.676}\ \beta^{-0.684}\ \phi^{1.121}Fr^{-0.029} \quad (6.8)$$

$$\tau_{mean} = 0.93\alpha^{0.042}\phi^{0.30} \quad (6.9)$$

The F-test is performed and the calculated F-values are 136, 75 and 41 for τ_{min}, τ_{peak} and τ_{mean} correlation respectively. These values are much greater than the theoretical F-values ($F_{0.05} \approx 2.7$

- 3.3[51)] which confirm the reliability of prediction.

The Eqs. 6.7 and 6.8 show that the dimensionless times are inversely proportional to the bath height which is due to the rapid increase in $\bar{t}$, in relation to t_{min} or t_{peak} (see Fig. 5.32A to C). However, in terms of dimensional values t_{min} or t_{peak} still increase with increase in H (t_{min} and t_{peak} can be derived easily to be proportional to $H^{0.39}$ and $H^{0.32}$ respectively from Eqs. 6.7 and 6.8) which is consistent with the trend shown in Figs. 5.32A and B. Further, the dimensionless minimum and peak residence times increase rapidly with the increase in inlet-exit distance. The increase in inlet-exit distance increases the spatial flow path of the liquid which causes the entire RTD curve to shift to right and hence to increase in residence times. Similarly, τ_{min} and τ_{peak} decreases with the increase in the submergence depth of the inlet stream. With the increase in β, the velocity component facing towards the tundish bottom increases which generates faster fluid flow conditions and hence decrease in τ_{min} and τ_{peak}. Since the exponent value of β in Eq.6.7 and 6.8 is very small (which means that the decrease in t_{min} or t_{peak} due to β is almost similar), the axial dispersion may not be influenced by β. The effect of Fr on τ_{mean} and τ_{peak} is negligibly small as expected. The effect of α on τ_{mean} is negligibly small than that of ϕ.

6.2.1.2 *With Flow Modifiers*

(A) *Selection of Parameters*

The main objectives of employing FM in a tundish are to eliminate short circuiting, to create surface directed flow, to increase the minimum residence time, to decrease the peak residence time and to obtain flow uniformity.

The results of submerged inlet stream show that weir alone is not a suitable flow modifier since it produces short circuiting of the fluid flowing in the tundish. Hence no correlation is developed for weir. In contrast, dam alone or in combination with weir alters the flow behaviour both in terms of residence time and the flow pattern.

The minimum residence time is found to increase with the increase in the dam height in tundishes of different widths of the present study; the increase, however, depends on the dam height (see section 5.2.2.1) and the tundish width. The smaller dam height, though gives maximum t_{min} but is considered too small to create surface directed flow. Between 38 and 190mm dam heights, t_{min}, after an initial rapid decrease has a tendency to decrease very slowly. This differential variation in t_{min} is thought to be due to the differential variation in the path and the velocity of fluid flowing into the rest of the tundish towards exit. By increasing the dam height the average velocity of the fluid increases into the rest of the tundish (average velocity in presence of dam = flow rate/$W(H-d_h)$, where d_h is height of the

dam). So if the path of the fluid remains same, t_{min} has to decrease and this is possibly happening for dam heights 38 to 65mm. Beyond 65mm dam height, though the average velocity is increasing but the path of the fluid is also increasing which may result in very slow decrease in t_{min} as observed in the present study. It is expected that within the region of dam heights 38mm to 190mm, the surface directed component of the liquid must also be sufficiently larger. For the development of correlations, dam height is varied within the range 38mm to 190mm.

It is interesting to note the effect of the tundish width on the residence times in presence of dam or weir+dam in relation to without FM. For this purpose the ratio $\varepsilon = (t)_{FM}/(t)_{NFM}$ is evaluated from the data and this ratio is plotted in Fig. 6.5A to C as a function of dimensionless widths for dam (solid line) and weir+dam (dashed line). In this representation ε values for two strand tundishes (ST2) are also shown. As can be seen in Fig. 6.5(A) that the ratio ε_{min} decreases with the decrease in width and then it increases with the further decrease in width for dam and weir+dam combination. Further, ε_{min} for weir+dam is somewhat greater than that of dam for W/L>0.20, whereas for W/L in between 0.072 and 0.20, ε_{min} for dam is somewhat greater than that of weir+dam. This modified fluid flow behaviour due to dam or weir+dam is considered to be due to the combined effects of the elimination of short circuiting, north-south walls of the tundish (as discussed in section 6.2.1.1), the mean flow velocity and that of weir in case of weir+dam[53]. For 310mm wide tundish (widest in this study), the maximum ε_{min} is due to the elimination of short circuiting. The decrease in ε_{min} with the decrease in width is

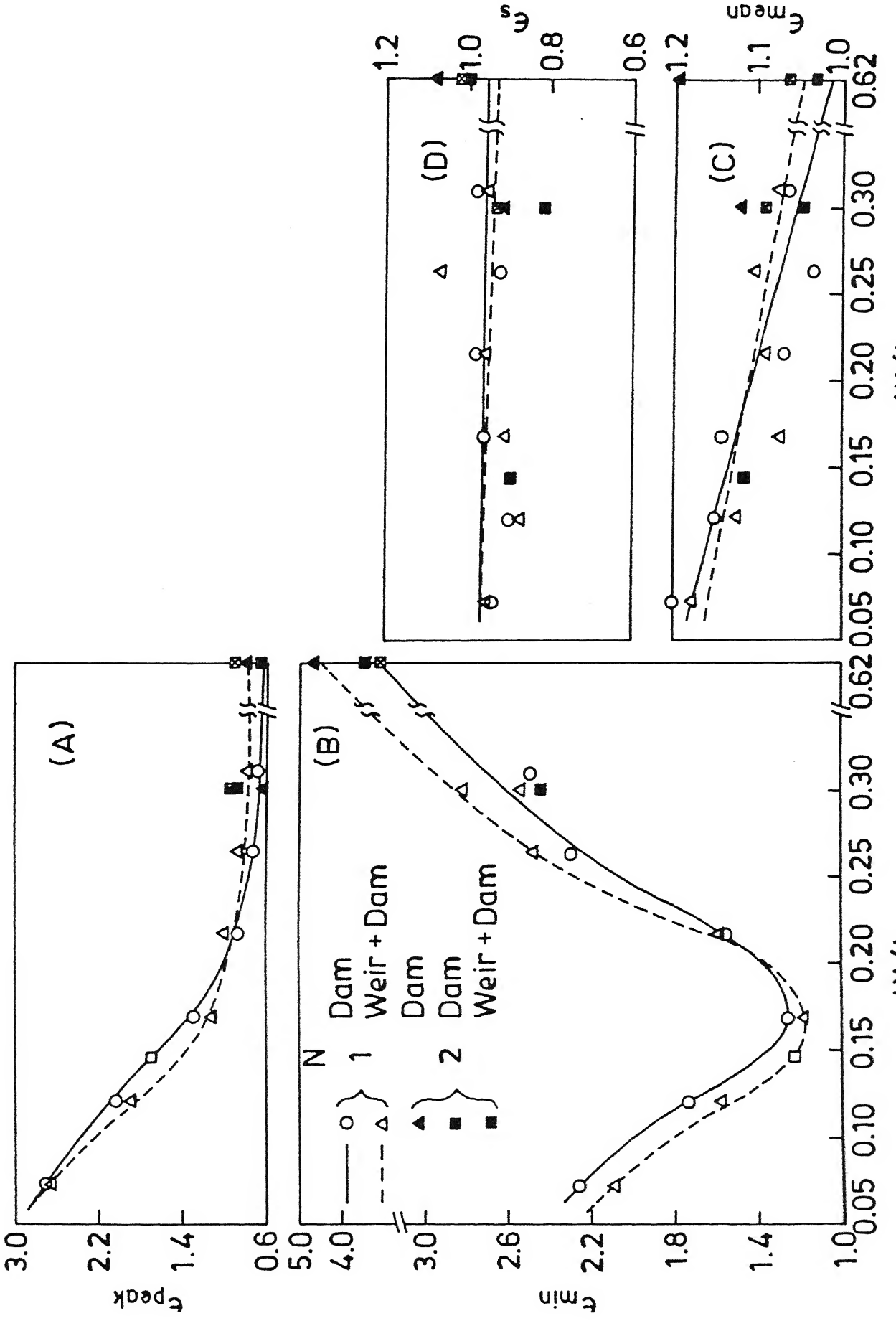

Fig.6.5: The ratio of residence time with FM/without FM as a function of dimensionless width (W/L) for single (ST1) and two strand (ST2) casting tundishes.

due to the increase in the mean flow velocity. With further decrease in width, the interaction between north-south walls of the tundish and the mean flow velocity causes further increase in ε_{min}.

Similarly ε_{peak} (6.5B), after a very slow increase with the decrease in tundish width, increases with the further decrease in width below W/L = 0.2. It appears that the experimental data do not show a very sharp minimum value of τ_{peak} with W/L as that in ε_{min} vs. W/L variations. However, it is considered that ε_{peak} does posses a minimum value at some value of W/L.

(B) *Mathematical Function*

The functions 6.4 to 6.6 are slightly modified to take into account the effect of additional parameters on the residence times introduced by FMs[53].

$$\left.\begin{matrix}\varepsilon_{min} \\ \text{or} \\ \varepsilon_{peak}\end{matrix}\right\} = (a_0 + a_1\alpha + a_2\alpha^2 + a_3\sigma^3)\ \phi^k Fr^i x_p^m x_h^n \eta_h^p, \qquad (6.10)$$

$$\varepsilon_{mean} = A'\alpha^j \phi^k x_p^m x_h^n \qquad (6.11)$$

It may be noted that τ in Eqs. 6.4 to 6.6 is different than ε in Eqs. 6.10 and 6.11. ε values are made dimensionless by the corresponding values for NFM, whereas τ values refer to $t/\bar{t}$.

The coefficients and exponents of functions 6.10 and 6.11 are

determined by the multiple regression analysis using all the experimental values listed in Table 5.2 for ST1 and ST2 tundishes. The values of these coefficients and exponents are listed in table 6.1. The F-test is also performed for each correlation and the calculated F-values are also listed in the Table 6.1. The calculated F-values are found to be several times greater than that of theoretical $F_{0.05}$ value which confirm the reliability of predictions[53].

For dam and weir+dam combination, the influence of Fr and x_p on ε_{min} is negligibly small (the exponent values are very small). However, in weir+dam combinations, the dam and weir height appear to have an opposing effect on ε_{min}. Increase in the dam height decreases ε_{min} (since exponent value is negative) but increase in weir height increases ε_{min} (since the exponent value is positive). Similarly ε_{peak} is marginally influenced by the Fr for dam and weir+dam combination. Position of the dam is an important parameter in weir+dam combination than that of dam alone (the exponent value of x_p for weir+dam is around 4 times greater than that of dam). The mean residence time is largely influenced by ϕ in comparison to α, x_p and x_h (exponent values of α, x_p and x_h are negligibly small in comparison to ϕ).

The function 6.10 predicts the minimum value of ε_{min}, $(\varepsilon_{min})_{min}$ at α=0.17 for dam and weir+dam combination. For dam the value of $(\varepsilon_{min})_{min}$ is 1.328 according to Eq. 6.10 for ϕ = 0.78, Fr = 0.74 and x_p = 0.05. The effect of ϕ, x_p and Fr on $(\varepsilon_{min})_{min}$ is very small. For weir+dam, putting α=0.17, ϕ=0.78, x_p = 0.15 and Fr = 0.74 in Eq. 6.10 and using appropriate value of the

Table 6.1 : Values of constants and exponents of Equations 6.10 and 6.11

Constants	Residence Times				
	ε_{min}		ε_{peak}		ε_{mean}
	Dam	Weir+Dam	Dam	Weir+Dam	Dam or Weir+Dam
A	-	-	-	-	1.047
a_o	10.410	7.630	6.640	16.310	-
a_1	137.530	-100.790	-55.050	-169.880	-
a_2	638.890	473.250	170.570	670.190	-
a_3	912.990	-667.310	-174.760	-882.800	-
j	-	-	-	-	-0.034
k	0.382	-0.191	-0.174	-0.180	-0.185
i	0.012	-0.034	-0.011	-0.010	-
m	0.060	-0.015	0.149	0.545	0.068
n	0.000	-0.228	-0.165	-0.165	-0.053
p	-	0.224	-	-0.030	-
R^2	0.940	0.970	0.990	0.980	0.500
F	95.400	133.000	564.400	176.600	11.200
$F_{0.05}$	2.780	2.530	2.640	2.530	2.640

constants, the $(\varepsilon_{min})_{min}$ is

$$(\varepsilon_{min})_{min} = 0.975\ \eta_h^{0.224} x_h^{-0.228} \tag{6.12}$$

Ignoring the very small difference between the exponents of η_h and x_h, we get

$$(\varepsilon_{min})_{min} = 0.975 \left(\frac{\eta_h}{x_h}\right)^{0.224} \tag{6.13}$$

For the ratio η_h/x_h = 1.5 and 3.2, the value of $(\varepsilon_{min})_{min}$ is 1.068 and 1.265 according to Eq. 6.13.In both types of FMs, we note that $(\varepsilon_{min})_{min}$ is greater than unity which indicates that dam alone or with weir enhances ε_{min}.

6.2.2 Variance

The variance (S^2) of the curve represents the square of the spread of the distribution around t_{mean}. For a constant amount of tracer input, the gradual increase and decrease of tracer concentration at the tundish exit should lead to larger S^2 in comparison to the faster increase or decrease of tracer concentration which corresponds to smaller spread. The former type of tracer response curve is due to greater reversal and recycling of the tracer than the later type of the curve. In Fig. 6.6 the experimental results of the variance of the RTD-curves without FM are plotted according to the regression function.

$$S^2 = 0.37 t_{mean}^2 \tag{6.14}$$

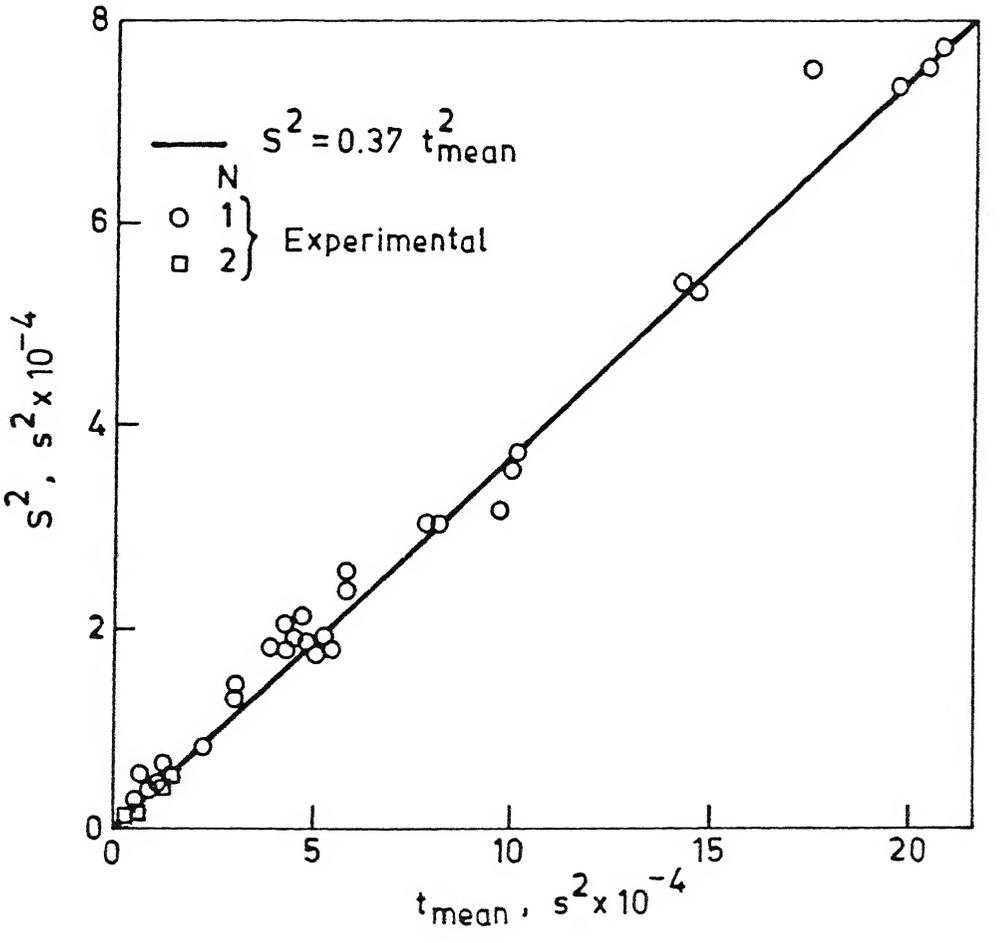

Fig.6.6: Variation of variance (S^2) with the square of the mean residence time for tundishes without Flow Modifiers

We note that the variance is independent of all the tundish design and operating parameters; it depends only on the mean residence time.

In Fig. 6.7 the variance of all RTD-curves obtained with FM is plotted according to the following regression function:

$$(S^2)_{FM} = 0.234\ (t^2_{mean})_{FM}\phi^{-0.482}x_p^{-0.172}\ x_h^{0.131} \qquad (6.15)$$

Where ϕ, x_p and x_h are dimensionless values of inlet-exit distance, dam position and dam height respectively. The value of the exponent of x_h determines the extent of the surface directed flow caused by the dam. For x_h the positive value of the exponent would mean increasing contribution of the dam in creating the surface directed flow. The exponent value of ϕ and x_p would determine the extent of dissipation of the turbulence of the inlet stream. The sign of the exponent values of both ϕ and x_p is negative and the magnitude of the exponent value of ϕ is less than that of x_p which indicates the pronounced effect of ϕ to dampen the turbulence of the inlet stream in comparison to that of x_p for their fractional values.

The ratio (t^2_{mean}/S^2) indicates the number of ideal reactors required to describe the flow pattern of the fluid in the real reactor[54,55] e.g. tundish in the present study. This ratio is 2.70 according to Eq. 6.14 and 3 according to Eq. 6.15 for ϕ = 0.78, x_p = 0.1 and x_h = 0.25. The three reactors i.e. plug flow, mixed flow and dead region are used in section 6.1 to derive the flow pattern which is in accordance with the value of the ratio

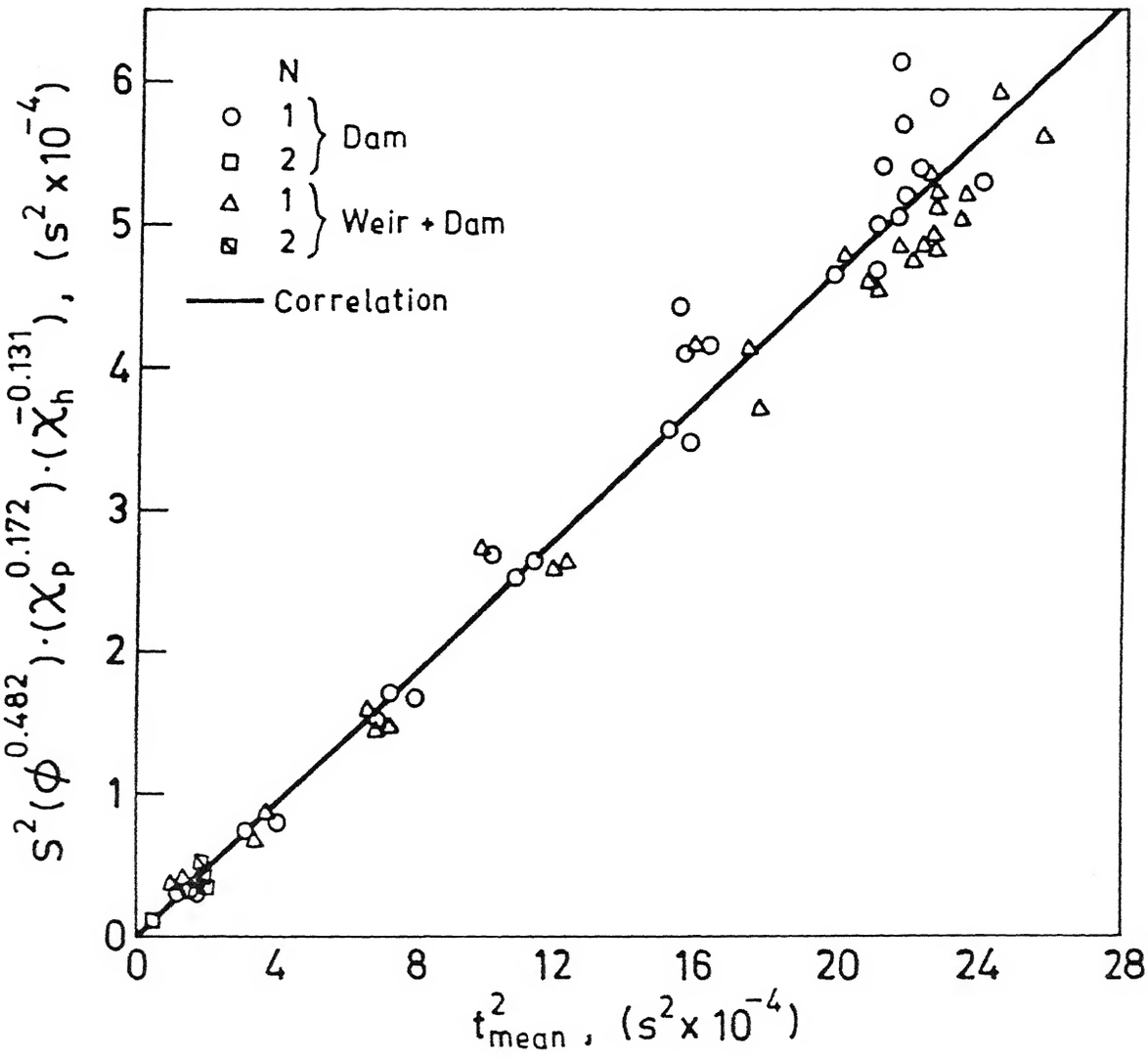

Fig.6.7: Comparison of measured values of variance with those calculated by Eq.6.10 for tundishes with FMs.

t^2_{mean}/S^2 as calculated above.

Experimental points for dam and weir+dam combination are distributed satisfactorily along the regression line represented by Eq. 6.15. The influence of inlet-exit distance on the decrease in the spread is much more pronounced than the dam position and height. Increase in the inlet-exit distance increases the overall flow path of the fluid, whereas increase in the dam position leads to larger dissipation of the turbulence of the inlet stream within the region bounded by the dam and the inlet stream. The effect of both these parameters i.e., the inlet-exit distance and dam position is to decrease the reversal and recycling of the tracer on account of which the flow becomes uniform. On the other hand increase in dam height increases the spread which is possibly due to the increase in the dead region behind the dam.

The ratio

$$\varepsilon_s = \frac{(S^2)_{FM}}{(S^2)_{NFM}} \qquad (6.16)$$

signifies the extent of decrease of reversal and recycling of the fluid flowing in the tundish caused by the dam, whether placed singularly or in combination with any other flow modifier like weir, slotted dam etc. The decrease in reversal and recycling (both these mechanisms are characteristic features of the turbulent flow) leads to the creation of laminar flow conditions in the tundish. By Eqs. 6.14, 6.15 and 6.16 the following equation is obtained.

$$\varepsilon_s = 0.68\alpha^{-0.068}\phi^{-0.846}x_p^{-0.036}x_h^{0.025} \qquad (6.17)$$

The value of ε_s can be influenced significantly by ϕ in comparison to x_p and x. For ϕ = 0.78, α = 0.3, x_p = 0.1 and x_h = 0.4, the value of ε_s is 0.967 which decreases to 0.857. when ϕ is increased to 0.9.

6.3 TESTING OF CORRELATIONS

In the literature no such correlations are available and hence a direct comparison of the coefficients and exponents of Eqs. 6.7 to 6.11 cannot be made. However, various investigators have studied the behaviour of fluid flowing in a tundish without and with FMs by a physical model or in actual trials as given in Table 2.1. Very few investigators have given the complete details of the experimental conditions as required to calculate the residence times by the Equations 6.7 to 6.11. In references[10,20,22-25,27,33,35,39,40,42] complete details could be found about tundish design and operating parameters and those of FMs. The details of tundish design and operating parameter are given in Table 2.1, whereas the details on size and configuration of FMs are given in Table 6.2. It must also be mentioned that most of the authors gave the values of t_{min}, and very few gave the values of t_{peak} and t_{mean}, and none gave the value of the variance.

In Figs. 6.8 to 6.10, the experimental data of the present study on residence times (see Table 5.1) are plotted for tundishes

Table 6.2 : Details of FMs employed by different investigators

Ref. No / Year	N	Type	Position and height (w_p, w_h) + (d_p, d_h)
35 (1981)	2 or 1	Weir+dam	(0.18L-0.224L), (0.20H-0.70H) + (0.27L-0.40L, 0.17H-0.40H)
		Weir+dam	(0.15L, 0.50H OR 0.70H) + (0.22L, 0.17H-0.30H)
33 (1986)	2	Weir+dam	(0.19L, 0.70H) + (0.30L, 0.30H)
39 (1986)	2	Weir+dam	(0.14L-0.31L, 0.45H) + (0.32L-0.49L, 0.45H)
40 (1988)	6 or	Weir+dam	(0.07L, 0.34H) + (0.14L, 0.35H-0.60H)
		dam	0.14L, 0.35H
10 (1990)	1	dam	0.09L-0.58L, 0.30H
22 (1990)	1	Weir+dam	(0.20L, 0.75H) + (0.30L, 0.32H)
27 (1991)	2	Weir+dam	(0.11L, 0.61H) + (0.22L, 0.52H)
25 (1992)	1	Weir+dam	(0.20L, 0.70H) + (0.27L or (0.36L, 0.16H or 0.24H)
24 (1992)	2	Weir+dam	(0.25L, 0.83H) + (0.50L, 0.28H)
	1	dam	
Present	or	Weir+dam	See Table 4.2
Study	2	SD & SD+dam	

For other details of tundish design and operating parametrs see Table 4.1

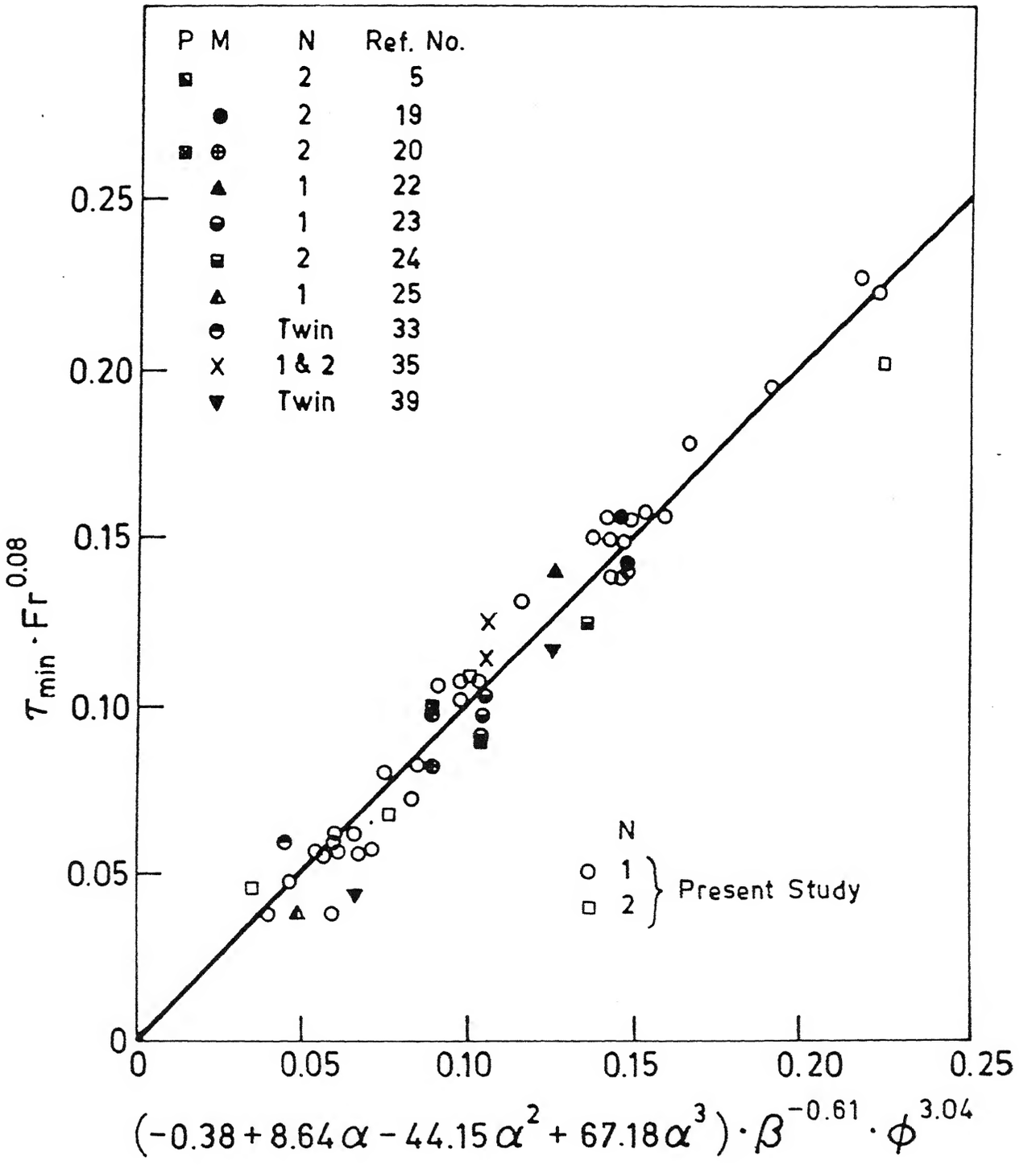

Fig.6.8: Comparison of the measured dimensionless minimum residence time of the present study and other investigators with those calculated by Eq.6.7.

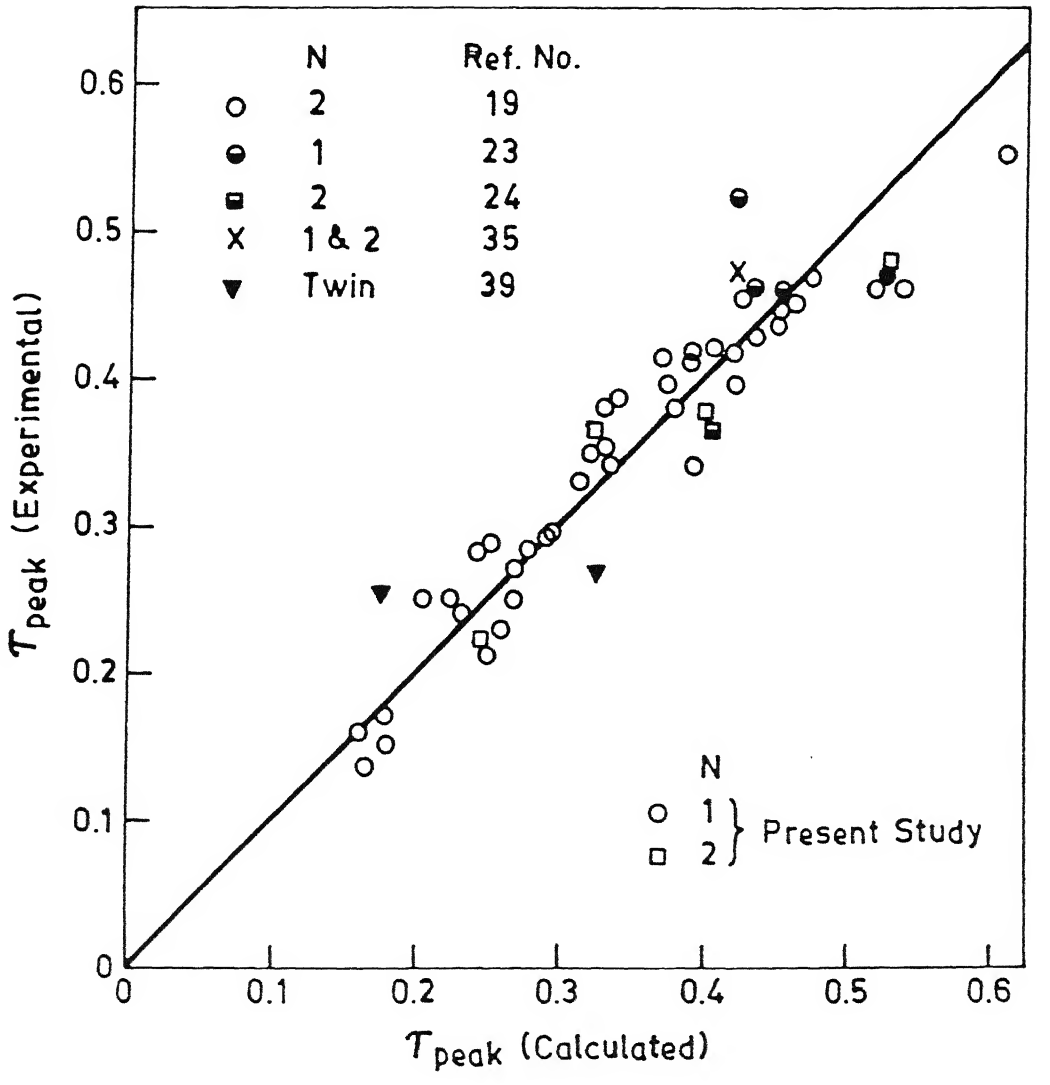

Fig.6.9: Comparison of the measured dimensionless time for peak concentration, i.e., τ_{peak} of the present study and other investigators with those calculated by Eq. 8.

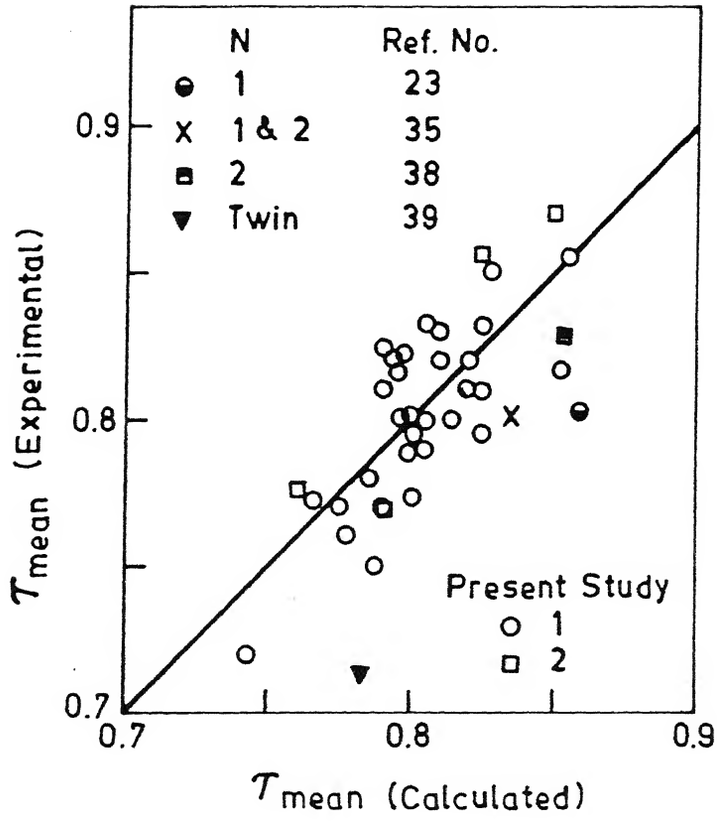

Fig.6.10: Comparison of the dimensionless mean residence time, i.e., τ_{mean} of the present study and other investigators with those calculated by Eq.6.9.

without FMs according to Eqs. 6.7 to 6.9. The available experimental values of τ_{min}, τ_{peak} and $\bar{\tau}$ and those of tundish parameters of different investigators have also been included in the plots of all these figures. For multi-strand casting tundishes and symmetrically placed ladle shroud with reference to the tundish nozzle the fluid flow behaviour in the half of the tundish is found to be similar to the other half. Therefore, only half tundish length is considered to determine α, β and ϕ for calculation of τ_{min}, τ_{peak} and $\bar{\tau}$ values by Equations 6.4 to 6.6. In the Fig. 6.8 the available values of τ_{min} are also shown for steel melt.

Similarly ε_{min}, ε_{peak} and ε_{mean} are calculated by the correlations 6.10 and 6.11 for the operating conditions of the tundishes of all investigators listed in Table 6.2 including the present one. In Figs. 6.11 to 6.13 the above calculated values are compared with those derived experimentally by different investigators.

It may also be noted that the different investigators have performed experiments on different scales. It can be seen in Figures 6.8 to 6.13 that the values of the residence times predicted by the correlations of this study compare fairly well with the experimentally derived values particularly when one considers the variation in tundish design, scale of operation and range of operating variables from one investigator to the other. Since the residence times depend on the type of flow pattern and it is already shown in Fig.6.1 that the flow pattern is identical in fractional or full scale water models and actual tundish.

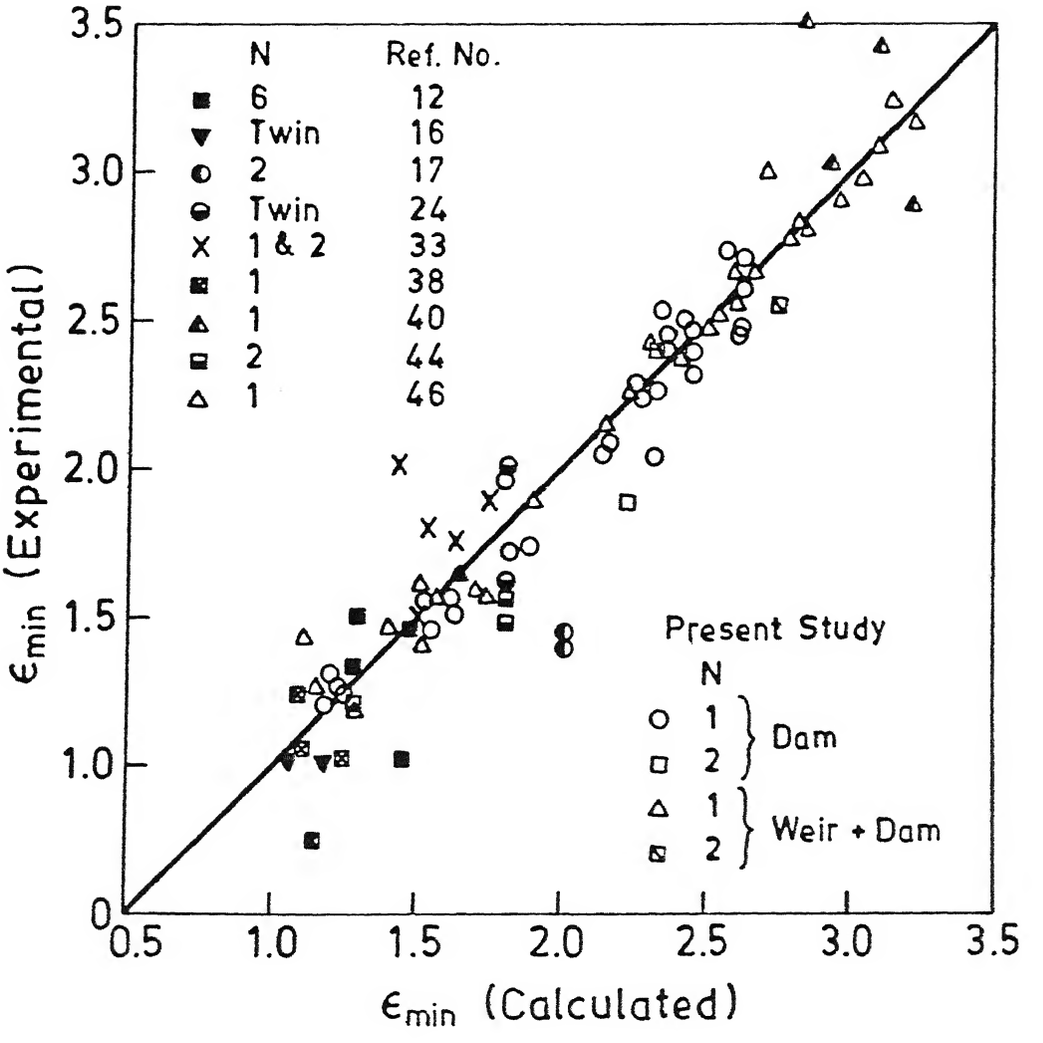

Fig.6.11: Comparison of the measured $\varepsilon_{min} = (t_{min})_{FM}/(t_{min})_{NFM}$ of the present study and other investigators with those calculated by Eq.6.10.

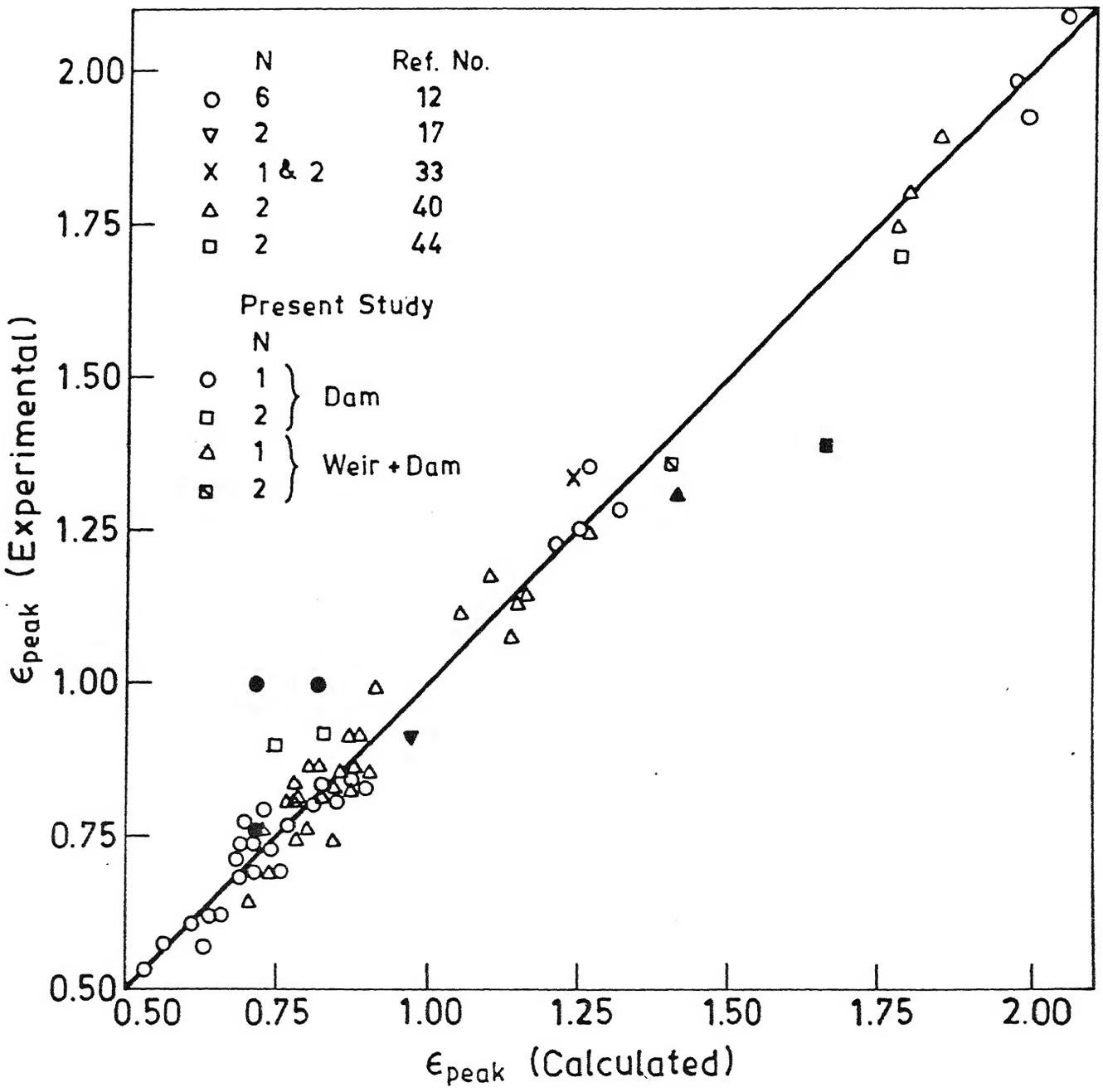

Fig.6.12: Comparison of the measured $\varepsilon_{peak} = (t_{peak})_{FM}/(t_{peak})_{NFM}$ of the present study and other investigators with those calculated by Eq.6.10.

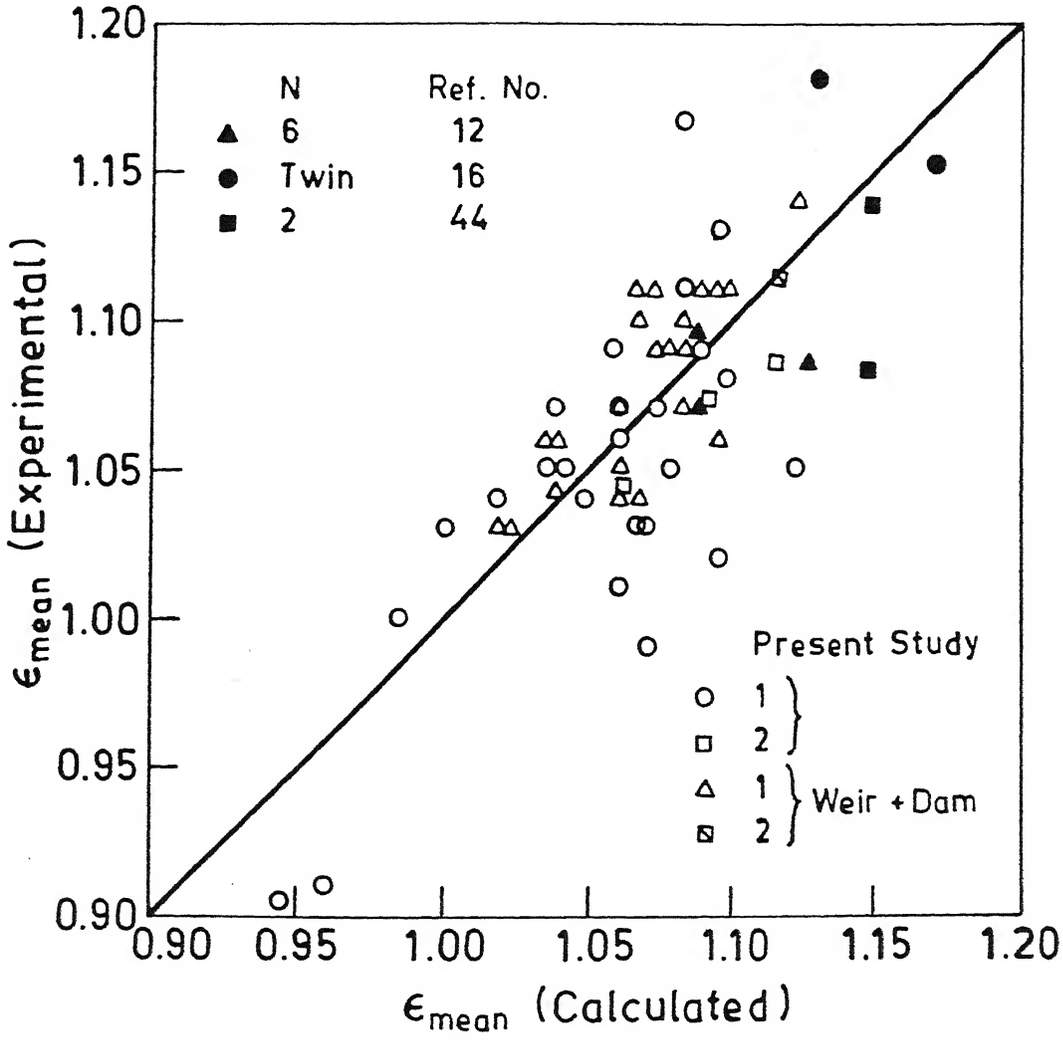

Fig.6.13: Comparison of the measured $\varepsilon_{mean}=(t_{mean})_{FM}/(t_{mean})_{NFM}$ of the present study and other investigators with those calculated by Eq.6.11.

Therefore, it is reasonable to expect the different absolute values of residence times as found by different investigators but when these values are made dimensionless as is done in correlations 6.7 to 6.11, the dimensionless values must show a coherent trend as presented in Figs. 6.8 to 6.13.

6.4 EFFECT OF MISCELLANEOUS PARAMETERS

6.4.1 Submerged Stream

The correlations 6.7 to 6.9 are obtained for the inclined wall tundishes for shroud submergence depth 0.15H, when operated without slag cover and water flow rate is controlled by the stopper rod. The effects of other parameters on the residence times and spread are presented on the bar chart. The ordinate value is defined by

$$\tau_R \text{ or } \psi \text{ or } \varphi = \frac{t \text{ or } S^2}{t \text{ or } S^2 \text{ for ST1-1}} \qquad (6.18)$$

Height of the bar indicates the magnitude of the effect of the parameter under consideration. In Fig. 6.14 the effect of vertical wall tundish, nozzle flow, model slag cover and deeper shroud on the residence times and spread is presented in a tundish when operated without flow modifiers but with submerged stream. The value of the denominator corresponds to the operating conditions of ST1-1 tundish. A vertical wall tundish increases t_{min} by a factor of 1.17 and decreases t_{peak} by a factor of 0.9 but has a very small effect on t_{mean}. Similarly, the slag cover

had almost negligible influence on t_{min} but t_{peak} is decreased by a factor of 0.87. The cumulative effect is that the vertical wall and the slag cover decreases independently the axial dispersion in the tundish fluid flow system.

The presence of model slag cover decreases t_{mean} by a factor of 0.94. The model slag retards the motion of the fluid in its close proximity which probably results in increase in dead volume and hence decrease in mean residence time. The increase in submergence depth of the inlet shroud decreases t_{min} by a factor of 0.92, t_{peak} by 0.96 and t_{mean} by 0.94. This is probably due to the effect produced on the fluid flow by decrease in distance between the shroud exit and the bottom of the tundish.

The variance of the distribution curve is marginally influenced by the parameters mentioned in Fig. 6.14.

In Fig. 6.15 the effect of different types and combinations of FM on the residence time is shown on the bar chart. In this case the ordinate is

$$\psi = \frac{(\varepsilon)_{\text{new type}}}{(\varepsilon)_{\text{dam}}} \quad \text{or} \quad \psi_c = \frac{(\varepsilon)_{\text{new combination}}}{(\varepsilon)_{\text{weir+dam}}} \tag{6.19}$$

In the ratio formulation, ε is either ε_{min}, ε_{peak}, ε_{mean} or ε_S. It can be seen that the ratio $(\psi)_{min}$ decreases and $(\psi)_{peak}$ increases for weir, which indicates that the minimum residence time decreases and axial dispersion increases by the use of weir as compared to dam. Slotted dam (SD) increases $(\psi)_{peak}$ but $(\psi_S)_{min}$ remains close to unity. The cumulative effect is to

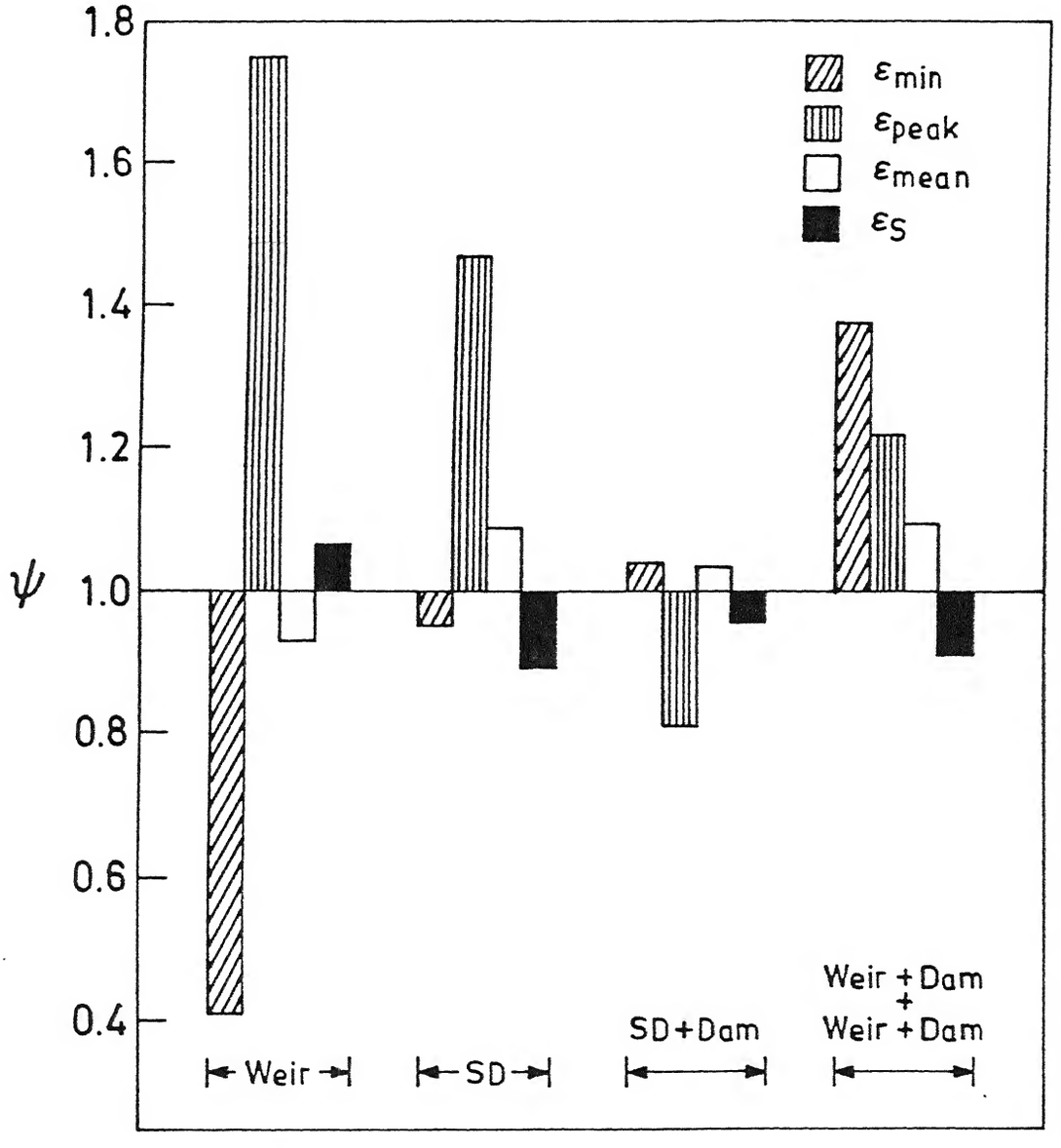

Fig.6.15: Bar chart showing the effect of different types of FMs and their combinations on residence times and variance

increase the axial dispersion, which is due to the presence of holes in the SD and the acceleration of water flowing through these holes. The use of SD+dam increases $(\psi_c)_{min}$ but decreases $(\psi_c)_{peak}$ which indicates the decrease in axial dispersion and therefore uniformity of fluid flow caused by this combination as compared to weir+dam. The use of weir+dam+weir+dam increases $(\psi_c)_{min}$, $(\psi_c)_{peak}$ and $(\psi_c)_{mean}$. This effect is due to the increase in the number of flow obstacles. There is a slight decrease in the spread for all types and combinations except that for weir, in which case the variance increases.

6.4.2 Open Stream

Very few investigators have studied tundish fluid flow behaviour with open stream[14,29,35,38,40]. According to them strong upward flow is created by rising gas bubbles. In the absence of flow modifiers, considerable surface turbulence was reported[14,29,35,38,40]. Use of weir or weir+dam was found to restrict the action of the rising gas bubbles within the inlet region[14,29,35,36,40]. The results of the present study (see section 5.1.2.2) are in agreement with the results reported above of other investigators. It may be mentioned that the value of residence times is given by very few investigators. Using the results of the present study and those of other investigators, the values of ε_{min} for weir are plotted in Fig. 6.16 against the position of the weir, w_p/L. Though, there is a wide scatter in the values, but it appears that ε_{min} has a tendency to decrease with the increase in w_p/L. Thus, position of the weir must be

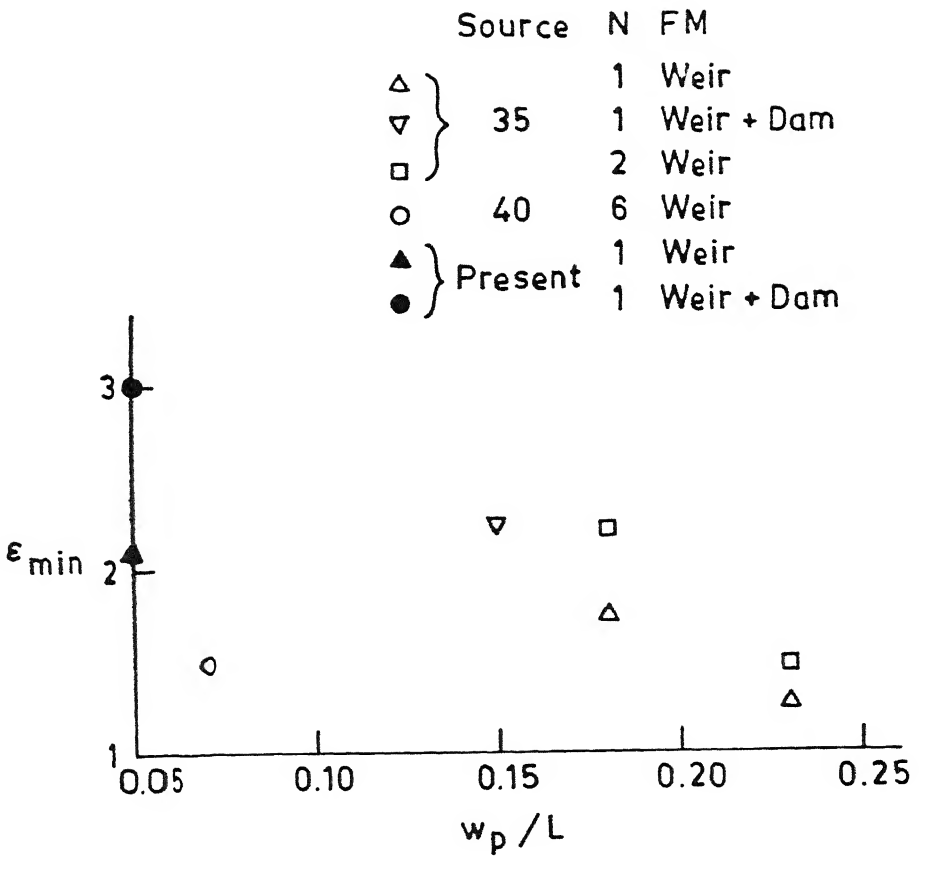

Fig.6.16: The variation of ε_{min} with w_p/L for air shrouded stream pouring.

optimized.

It is interesting to compare the different modes of pouring of water stream into tundish on the residence times and spread without and with FM. It is done in Fig. 6.17 in which the ordinate is

$$\varphi = \frac{(t)_{O \text{ or } A}}{(t)_s} \tag{6.20}$$

As shown in the Figure, φ_{min} is 0.84 and φ_{peak} is 0.64 for open stream pouring into tundish without FM. Decrease of both minimum and peak residence times will make their ratio almost similar to that of submerged stream. Thus, axial dispersion is not significantly influenced. φ_{mean} is almost equal to that of submerged stream. But, the variance φ_s is 0.9. In contrast, when the water stream falls through the air chamber into tundish, φ_{min} increases by a factor of 1.4 and φ_{peak} decreases by 0.35. Increase in t_{min} and decrease in t_{peak} will decrease the axial dispersion in the tundish fluid flow system. φ_{mean} is decreased by 0.6 which indicates that the dead zone region in the tundish increases in comparison to that of submerged stream. The variance φ_s also decreases by a factor 0.74.

Weir increases significantly φ_{min} and decreases φ_{peak} for open stream. The increase in t_{min} is due to the effect of weir in restricting the action of the entrained air within the inlet region (see Fig. 5.17A). φ_{mean} is almost equal to that of submerged stream. φ_s increases marginally. Dam decreases φ_{min}

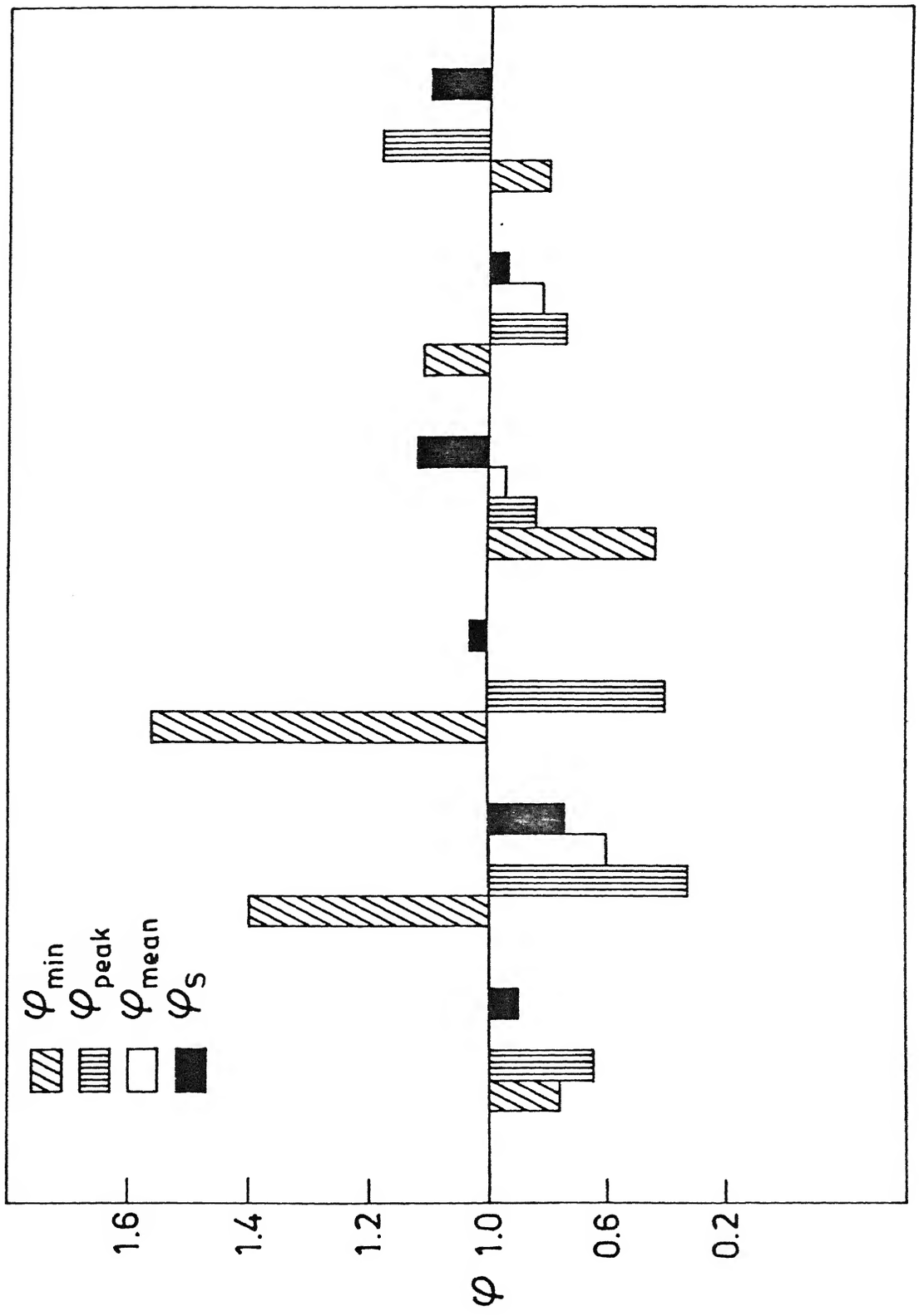

Fig.6.17: Bar chart showing the effect of open stream pouring on the residence times and variance.

φ_{peak} and φ_{mean} but slightly increases φ_s for open stream pouring. But, when water falls through the air chamber, dam increases φ_{min} and decreases φ_{peak}, φ_{mean} and φ_s. Similarly weir+dam combination decreases φ_{min} and increases φ_{peak} and φ_s but φ_{mean} is not influenced for open stream.

CHAPTER - 7

APPLICATIONS

Ever since the realization of the potential use of tundish in performing some metallurgical treatments during the process of continuous casting, most of the continuous casting plants have undertaken water or mathematical study of the behaviour of the molten steel flowing in the tundish for their specific design, operating and steelmaking conditions (see Table 2.1). The main objectives in each of the studies are:

i) To know the type of flow pattern and the residence time distribution and

ii) Once the knowledge in (i) is gained, the introduction of methods to optimize the flow pattern and residence time distribution to make the tundish suitable for metallurgical treatment(s) without much alterations in design and operating conditions.

Since the tundish and its design evolved from the basic needs of the continuous casting, therefore, individual model study of fluid flow dynamics in the tundish is almost necessary (as can be seen in the body of the literature compiled in Table 2.1) and will continue in the near future also. In this connection, mathematical modeling study and physical modeling study leading to a logical conclusion e.g. development of empirical correlations

for fluid flow behaviour may serve useful guidelines to study the fluid flow dynamics in other tundishes.

In the present study, correlations are obtained to determine residence times and variance for submerged stream pouring in single and two strand casting tundishes. It may be mentioned here that submerged stream pouring is the most widely used method of pouring of liquid steel in continuous casting. Though, the effect of buoyancy induced due to temperature variation during flow of molten steel in the tundish on the residence times is not taken into account in the present study, but the correlations still contain the influence of the various tundish design and operating parameters. Thus, correlations of the present study may be used to study the distribution of residence times in other tundishes. From the residence times, the different fluid volumes in the tundish can be calculated easily (method of calculation is given in Appendix - 3).

As an illustration of the use of the correlations, consider a single strand continuous casting machine casting routinely 1500mmx200mm slab at the casting speed 1.2 m min^{-1} . Molten steel is supplied to the 4 m x 1 m x 1 m tundish of rectangular in shape with inclined walls via a 70 mm dia. ladle shroud submerged to the depth of 0.3 x bath height. The distance between inlet and exit is 0.8 times tundish length. Since this tundish has α = W/L = 0.25, so according to the results of the present study, fluid flow in the tundish is accompanied by short circuiting. The t_{min}, t_{peak} and t_{mean} are calculated by the Eqs. 6.7 to 6.9 they are 47s, 276s and 548s, respectively. The theoretical residence time

is 667s according to Eq. 1.1. Since, t_{min} is not equal to t_{peak}, there is axial dispersion in the fluid flow system.

From these times the fractional dispersed plug, dead and mixed volumes are calculated by Eqs. A-3, A-4, A-5 and A-7 of Appendix 3; these are: 0.24, 0.18 and 0.51 respectively. These calculations provide a first hand information about the flow behaviour of steel melt in the aforementioned selected tundish on the basis of which the plans for tundish design modifications may be undertaken depending on the metallurgical objective and other local plant constraints.

In the above tundish design, short circuiting must be eliminated since this volume has a very short stay and enters straight into the mold without mixing into the tundish fluid volume. Without altering any design and operating parameters, installation of dam is one of the way to eliminate the short circuiting according to results of the present study. The dam may be used alone or in combination with weir.

For the installation of the dam alone, size and position are the two important parameters. According to the results of the present study (see Eq. 6.10 and 6.11 and Table 6.1) the dam height in between 0.25H and 0.75H has no influence on the modifying factor for the minimum residence time. The modifying factor for the peak residence time i.e. ε_{peak} is influenced by dam height and position. The modifying factor for the mean residence time is negligibly influenced by size and position of the dam. Substituting $\alpha = 0.25$, $Fr = 3.5$, $\phi = 0.8$ in Eqs. 6.10 and 6.11 and

using the value of the constants from Table 6.1, we get

$$\varepsilon_{min} = 1.816\ x_p^{-0.06} \tag{7.1}$$

$$\varepsilon_{peak} = 0.828\ \frac{x_p^{0.149}}{x_h^{0.165}} \quad \text{and} \tag{7.2}$$

$$\varepsilon_{mean} = 1.144\ \frac{x_p^{0.068}}{x_h^{0.053}} \tag{7.3}$$

For $x_p = 0.05$ and 0.15 we get $\varepsilon_{min} = 2.17$ and 2.03 by Eq. 7.1 i.e. the dam increases t_{min} by a factor of 2.17. Similarly for $x_h = 0.4$ and $x_p = 0.15$, $\varepsilon_{peak} = 0.726$ according to Eq. 7.2 i.e. dam decreases the peak residence time. Since dam increases t_{min} but decreases t_{peak}, the cumulative effect is decrease in the axial dispersion. The modifying factor for mean residence time is slightly influenced by x_p or x_h according to Eq. 7.3. For $x_p = 0.15$ and $x_h = 0.4$, ε_{mean} is 1.055 i.e. dam sightly influences the mean residence time.

For weir+dam combination, size and position of the dam and weir are the important considerations. Using Eqs. 6.10 and 6.11 and substituting the values of ϕ, Fr and α as given above, we get the following equation for the modifying factors:

$$\varepsilon_{min} = 1.584 \left(\frac{\eta_h^{0.224}}{x_h^{0.228}} \right) \approx 1.584 \left(\frac{\eta_h}{x_h} \right)^{0.224} \tag{7.4}$$

$$\varepsilon_{peak} = 1.909 \frac{x_p^{0.545}}{x_h^{0.165}} \eta_h^{-0.03} \qquad (7.5)$$

The equation for ε_{mean} for weir+dam is same as that of dam i.e. Eq. 7.3.

The modifying factor (ε_{min}) depends on the ratio of the height of the weir and dam. For the value of the ratio $\eta_h/x_h = 1$, ε_{min} is 1.584 which increases to 2.16 when the said ratio is increased to 4. Thus in weir+dam combination, heights of both, i.e., weir and dam should be optimized. The modifying factor for peak residence time depends on position and height of the dam and to the small extent on the weir height. For $x_p = 0.15$, $x_h = 0.4$ and $\eta_h = 0.6$, the value of ε_{peak} is 0.835. Similarly, the value of ε_{mean} is 1.055 for the above configuration.

The above calculations show the use of the correlations in predicting residence times for unknown tundishes.

It must be mentioned here that the above example considers the modification of residence times as the criterion of selection of size and configuration of FMs. However, there could be different objectives for installations of FMs in different conditions. From the available informations, a function - objective correlated flow sheet is prepared for the use of FMs[1,4-6,11,18,26,27,34-40,56,57]. This flow sheet is shown in Fig. 7.1. As can be seen in the figure that the objectives could be different and accordingly must also be considered while using correlations of the present study.

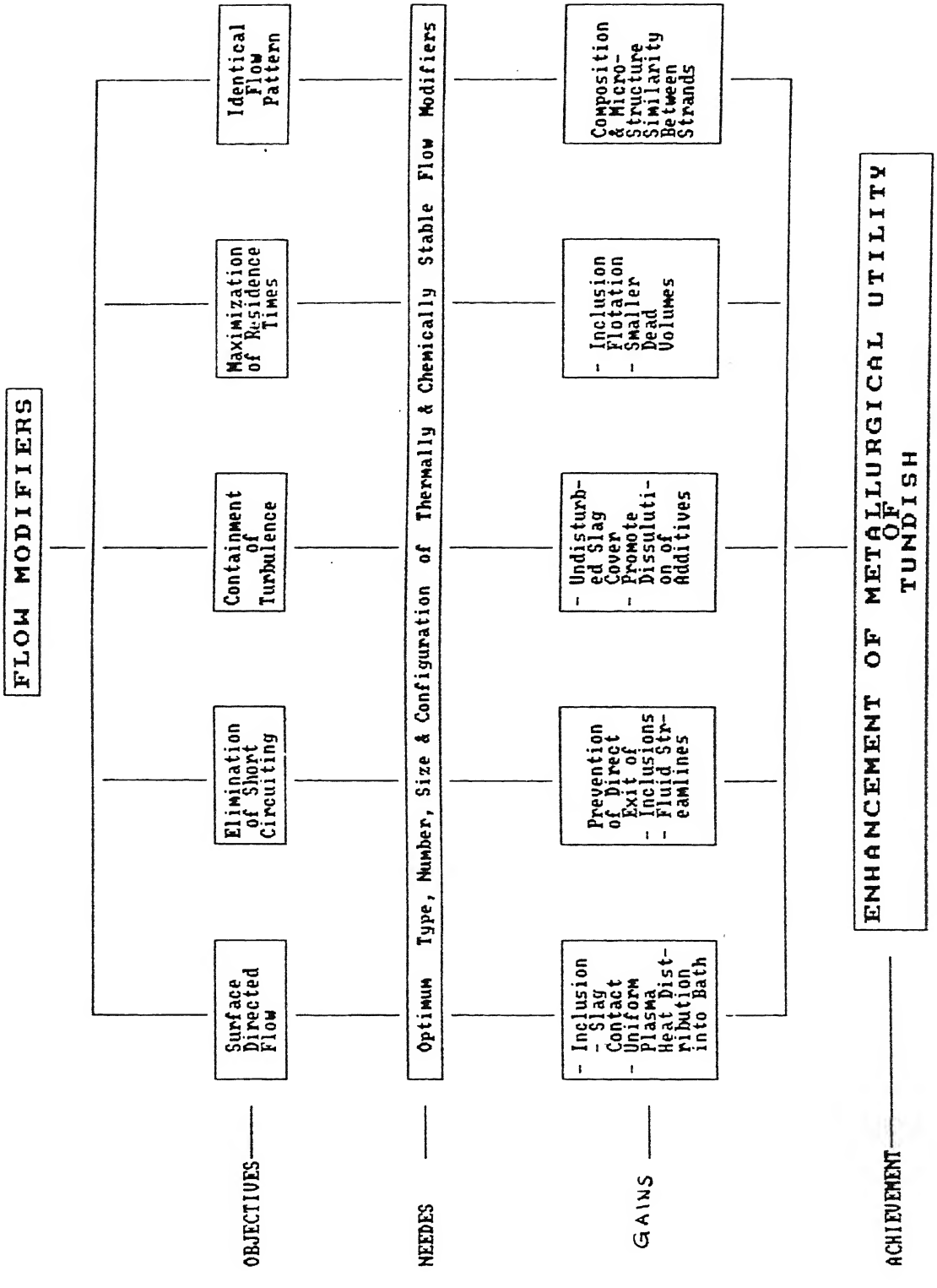

Fig.7.1: Function - objective related flow sheet for the use of FMs in tundish.

Similarly for the new installations of the continuous casting machines it would be desirable to have some guideline for the selection of the tundish dimensions and dimensions and configurations of the FMs. Although tundish design would depend on other factors like strand size, casting speed, number of strands etc. the present correlations may be used to select dimensions of tundish and FMs on the basis of the fluid flow dynamics.

CHAPTER - 8

CONCLUSIONS

The dynamics of steel melt flowing in a tundish without and with FM is studied in a physical model by allowing water to flow in a perspex glass tundish. Flow pattern and residence time distribution are investigated by stimulus response technique as a function of variables like tundish width, inlet-exit distance, type of inlet streams (submerged, open and argon shrouded stream), inlet flow rate, depth of submergence of the inlet shroud, size, number, type and configurations of flow modifiers, bath height and model slag cover. The tundish flow rate is controlled by stopper rod and using appropriate nozzle size. The flow pattern is studied by using methylene blue tracer by means of still and video photography. The RTD is studied by using potassium chloride (KCl) tracer and by recording the electrical conductivity of water continuously at the exit of the tundish. In general, the following conclusions are drawn.

i) It is found that the submerged stream pouring in tundishes without FMs and widths greater than 0.21Lproduces short circuiting of the fluid at all Froude numbers and inlet-exit distances. For tundish widths smaller than 0.21L, no short circuiting is observed.

ii) weir of all sizes placed at any distance could not eliminate short circuiting. However, dam alone or in combination with weir

or slotted dam eliminates completely the short circuited flow. Further, it is observed that the dam produces the surface directed flow and dampens the turbulence of the inlet stream.

iii) The variation of minimum, peak and mean residence times is found to depend among other factors on the tundish width and FMs. In tundishes without FMs the minimum residence time is found to show a maximum value at W = 0.21L for all inlet Froude numbers and inlet-exit distances. The peak and mean residence times decrease with the decrease in the tundish width. However, in presence of dam or weir+dam, the minimum and peak residence times are found to show a minimum value at a particular value of the tundish width at all inlet-exit distances and Froude numbers.

iv) Empirical correlations are obtained to determine the residence times in presence and absence of FMs. By following the mechanism of momentum transfer it is shown that the different values of the Reynolds number within the region of the turbulent flow do not influence the eddy size distribution at the exit of the submerged ladle shroud. From this derivation, it is asserted that the proposed correlations predict a plausible trend with the tundish parameters.

v) For open stream pouring without or with air chamber, it is found that the entrained air on release into the tundish creates surface turbulence. The flow is predominantly towards the surface. Weir is found to restrict the effect of buoyancy on the upward flow within the region upstream of the weir as a result of which the flow downstream the weir is observed to be free from

surface waves. Dam is not found to be effective in controlling the surface waves induced by the rising bubbles.

vi) The axial dispersion due to open stream pouring is found to be similar to that of submerged stream pouring in tundish without FMs. However, weir is found to increase the minimum and peak residence time for open stream pouring when compared with submerged stream pouring.

CHAPTER - 9

SUGGESTIONS FOR FUTURE WORK

1. Industrial tundishes are of wide varieties in design and operating under different conditions. The effect of other designs e.g. δ-shape, T-shape etc. on the fluid flow behaviour could be undertaken.

2. From the literature, the influence of dimensions and configurations of dam alone or weir+dam on the velocity field could not be determined. Such a study would be useful to explain the observed behaviour of the variation of residence times with tundish width in presence of dam or weir+dam.

3. It is worthwhile to investigate the tundish fluid flow behaviour in presence of a liquid slag.

4. It would be desirable to conduct experiments in the actual tundish in order to validate the residence time values calculated by the correlations of the present study.

5. In view of the finding of the present study that fluid flow behaviour is influenced by the tundish width, further work would be desirable to establish the interrelationship between the residence time and the velocity fields in presence and absence of FMs.

REFERENCES

1. L.J. Heaslip and A. McLean: Continuous casting, Iron and Steel Society, AIME, 1(1983), 93.

2. P. Tolve, A. Praitoni and A. Ramacciotti: Steel Times, 3(1987), 128.

3. A. McLean: Steelmaking Conference Proceedings, (1988), 3.

4. F. Schrewe: Continuous Casting of Steel; Fundamental Principles and Practice, Stahl Eisen, (1989), 22.

5. J. Szekely and O.J. Illegbusi: The Physical and Mathematical Modeling of Tundish Operations, Springer-Verlag New York Inc. (1989).

6. A. Chatterjee and S. Govindarajan: Monograph on Continuous Casting of Tata Steel, Tata Steel, (1991), 37.

7. A. McLean: Proceedings Scaninject VI, Lulea, Sweden, 6(1992), 139.

8. B. Mintz, S. Yue and J.J. Jones: Intern. Matls. Reviews, 36(1991)No.5, p.187.

. T. Robertson and A. Perkins: Ironmaking and Steelmaking, 13(1986), 301.

10. J.M. Camplin, J. Herbertson, H. Holl, P. Whitehouse, R.I.L. Guthrie, J.W. Han and M. Hasan: Proceedings of the Sixth International Iron and Steel Congress, ISIJ, Nagoya, (1990), 207.

11. J. Tsubokura, I.D. Sommerville and A. McLean: Iron & Steelmaker, (1985), No. 5, 58, 60 and 62; No. 6, 43-45, No. 7, 48-50 and No. 8, 41, 42, 44, 46.

12. M. Byrne and A.W. Cramb: Steelmaking Proceeding of ISS-AIME, 69(1986), 81.

13. Y. Haba, N. Itoyama, H. Hiroshiawa and Imai: International Conference on Technology and Applications of HSLA Steels, ASM, Metals Park, Ohio (1983), 377.

14. N.A. McPherson: Metallurgical Plant and Technology, 1986(3), 40.

15. T. Debroy and J.A. Sychterz: Metall. Trans. B, 16B(1985), 497.

16. J. Szekely and N. El-Kaddah: SCANINJECT IV, MEFOS, Lulea, Sweden, (1986), 14:1-14:33.

17. K.Y.M. Lai, M. Sacludean, S. Tanaka and R.I.L. Guthrie: Metall. Trans. B, 17B(1986), 449.

18. K.H. Tacke and J.C. Ludwig: Steel Research, 58(1987), 262.

19. Y. He and Y. Sahai: Metall. Trans. B, 18B(1987), 81.

20. O.J. Ilegbusi, J. Szekely, R. Boom, A. van der Heiden and J. Klootwijk: Proceedings of W.O. Philbrook Memorial Symposium Conference, Toronto, Canada, (1988), 185.

21. S. Chakraborty and Y. Sahai: Proceedings of the Sixth International Iron and Steel Congress, ISIJ, Nagoya, 1990, 189.

22. S.M. Lee, Y.S. Koo, T. Kang, I.R. Le and Y.K. Shin: Proceedings of the Sixth International Iron and Steel Congress, ISIJ, Nagoya, (1990), 239.

23. S. Chakraborty and Y. Sahai: Metall. Trans. B, 22B (1991), 429.

24. J. -L. Yeh, W. -S. Hwang and C. -L. Chou: Ironmaking and Steelmaking, 19(1992), 501.

25. L. Xintian, Z. Yaohe, S. Baolu and J. Weiming: Ironmaking and Steelmaking, 19(1992), 221.

26. S. Chakraborty and Y. Sahai: Ironmaking and Steelmaking, 19(1992), 479.

27. S. Chakraborty and Y. Sahai: Ironmaking and Steelmaking, 19(1992), 488.

28. S. Chakraborty and Y. Sahai: Metall. Trans. B, 23B(1992), 135.

29. K. Iwata, T. Shumiya, A. Shriaishi, T. Nagahata and I. Yamasaki: Proceedings of the First European Conference on Continuous Casting, Florence,2(1991), 145.

30. H. Nakajima, F. Sebo, S. Tanaka, L. Dimitru, D.J. Harris and R.I.L. Guthrie: Proceedings of the Fifth International iron and Steel Congress, AIME, Washington, 6(1986), 705

31. J.T. Duncombe, G. Jiang and D.A. Preshaw: Proceedings of the First European Conference on Continuous Casting, Florence, 2(1991),459.

32. M. Maeda, T. Saito, K. Ebato, K. Matsuo and H. Fugimoto: Proceedings of the First European Conference on Continuous Casting, Florence,2(1991), 203

33. A. van der Heiden, P.W. van Hasselt, W.A. de Jong and F. Blass: Proceedings of the Fifth International Iron and Steel Conference, AIME, Washington, 6(1986), 755.

34. S. Joo and R.I.L. Guthrie, Canadian Metallurgical Quarterly, 30 (1991), 261.

35. F. Kemeny, D.J. Haris, A. McLean, T.R. Meadowcraft and J.D. Young: Proceedings of Second Process Technology Conference, ISS-AIME, Chicago (1981), 1-23.

36. D.J. Harris and J.D. Young: Continuous Casting, Iron and Steel Society, AIME, 1(1983),99

37. E. Martinez, M. maeda, L.J. Heaslip, G. Rodriguez and A. McLean: Trans. Iron Steel Inst. Japan, 26(1986), 724.

38. Y. Sahai and R. Ahuja: Ironmaking and Steelmaking, 13(1986), 241.

39. J. Knoepke and J. Mastervich: Steelmaking Conference Proceedings, ISS-AIME, 69(1986), 777.

40. S. Govindarajan, S.K. Ajmani, Amit Chatterjee and T. Mukherjee: Proceedings of the International Symposium on Modern Developments in Continuous Casting, New Delhi, (1988), 153.

41. J. Harris, L.J. Heaslip, K.E. O'Leary, R.W. Pugh and C. Jager: Proceedings International Symposium on Direct Rolling and Hot Charging of Strand Cast Billets, Can. Institute of Min. & Met. Perganian Press, 10(1988), 19.

Q.L. He, J. Herbertson, P.A. Whitehouse and K. Gregory: Proceedings of the First European Conference on Continuous Casting, Florence, 2(1991)163.

43. S. Govindarajan, S.K. Ajmani, A.K. Roy and A. Chatterje: Proc. First European Conference on Continuous Casting, Florence, Italy, 2(1991)223.

44. Hintikka and J. Konttinen: Proceedings of the First European Conference on Continuous Casting, Florence, 2(1991)153

45. P. Tolve, A. Praitoni and A. Ramacciotti: Steelmaking Proceedings,ISS-AIME,69(1986) 689.

46. S. Joo and R.I.L. Guthrie: Met. Trans., 24B(1993) No.5, 755-788.

47. O. Levenspiel: Chemical Reaction Engineering, Wiley Eastern Limited (1986), 296.

48. J.T. Davies: "Turbulence Phenomena", Academic Press Ic., Mew York (1972).

49. S. Singh and S.C. Koria: Ironmaking and steelmaking, 20(1993) 221.

50. S. Singh and S.C. Koria: ISIJ. Inter. 33(1993), 1228.

51. W. Medehall and T. Sincich: Statistics for the Engineering and Computer Sciences, Collier Macmillan Canada Inc. (1988), 499.

52. C.R. Kothari: Quantitative Techniques, Vikas Publishing House Pvt. Ltd., New Delhi (1978).

53. S. Singh and S.C. Koria: Physical modeling of the effects of FMs on the dynamics of steel melt flowing in a tundish, ISIJ Intern, 34(1994)

54. G.F. Froment and K.B. Bischoff: Chemical Reactor Analysis and Design, 2nd Edition, 1990, John Wiley and Sons, Inc.

55. H.S. Fogler: Elements of Chemical Rection Engineering, 1992, Prentice-Hall Inc., Englewood Cliffs, N.J., U.S.A.

56. F. Salvati, P. Tolve, M. Masala, E. Peisino and D. Broglio: Proceedings of the First European Conference on Continuous Casting, AIM, Florence 2(1991), 173.

57. C. Moore, C.P. Heanley, C.O. Chapman and Y. Suguro: Proceedings of the First European Conference on Continuous Casting, AIM, Florence 2(1991), 185.

APPENDIX-1

```
10 REM PROGRAM TO ACTUATE TRACER INJECTION
20 CONTROL CIRCUIT AND TO ACQUIRE DATA
30 REM input values are sampling rate(SMPRT=4 samples/sec),
40 REM trial sampling(TSTM) and experimental sampling(EXTM) time
50 REM in minutes.
60 REM RDATA is the output file
70 REM TSDT is the number of trial samples and EXDT is the
80  REM EXDT     : number of experimental samples
90  REM TDAT%    : Value of trial sample data
100 REM INDATA% : value of experimental sample data
110 OPEN "O", 1, "RDATA"
120 DIM INDATA%(7000)
130 SMPRT = 4
140 TSTM = 15
150 EXTM = 20
160 CNT% = 100/SMPRT
170 TSDT = TSTM*SMPRT*60
180 EXDT = EXTM*SMPRT*60
190 BASE = &H240
200 OUT (BASE+3), &H92
210 OUT (BASE+7), &H36
220 OUT (BASE+4), 80
230 OUT (BASE+4), 195
240 OUT (BASE+7), &H76
250 OUT (BASE+5), 2
260 OUT (BASE+5), 0
270 OUT (BASE+7), &HB4
280 OUT (BASE+6), (CNT% MOD 256)
290 OUT (BASE+6), CNT% / 256
300 K=1: I=1
310 M=60*K-4
320 N=M+4
330 IF (I>M) AND (I<=N) GOTO 360
340 CH=0
350 GOTO 370
360 CH=2
370 OUT (BASE+2), CH * 16
380 R1 = INP (BASE+1)
390 IF (R1 < 128) THEN GOTO 380
400 R1 = INP (BASE+1)
410 IF (R1 >= 128) THEN GOTO 400
420 A = INP (BASE)
430 B = INP (BASE+1) AND &HF
440 TDATA% = (A + 256 * B)
450 PRINT CH,I,TDATA%
460 IF (I=TSDT) GOTO 500
470 IF (I=N) THEN K=K+1
480 I = I+1
490 GOTO 310
500 CLS
510 LOCATE 16,12: PRINT "TRIAL SAMPLING OVER"
520 PRINT "INJECTION START"
530 OUT (&H3BC), 1
540 FOR J = 1 TO 2700
550 NEXT J
560 OUT (&H3BC), 0
570 PRINT "INJECTION ENDS"
580 K=1: I=1
590 M=60*K-4
600 N=M+4
610 IF (I>M) AND (I<=N) GOTO 640
620 CH=0
630 GOTO 650
640 CH=2
```

```
650 OUT (BASE+2), CH * 16
660 R1 = INP (BASE+1)
670 IF (R1 < 128) THEN GOTO 660
680 R1 = INP (BASE+1)
690 IF (R1 >= 128) THEN GOTO 680
700 A = INP (BASE)
710 B = INP (BASE+1) AND &HF
720 INDATA%(I) = (A + 256 * B)
730 PRINT I,INDATA%(I)
740 IF (I=EXDT) GOTO 780
750 IF (I=N) THEN K=K+1
760 I = I+1
770 GOTO 590
780 CLS
790 LOCATE 16,12: PRINT "DATA SAMPLING OVER"
800 I=1
810 PRINT # 1, I,INDATA%(I)
820 I=I+1
830 IF (I<=EXDT) GOTO 810
840 CLOSE
850 SYSTEM
860 STOP
```

APPENDIX-2

```
C       THIS PROGRAM CALCULATES THE FOLLOWING, BY USING
C       THE DATA RECORDED BY THE DATA ACQUISITION PROGRAM
C       1. Tracer concentration as a function of time(CONC vs SEC)
C       2. Mass of tracer out through the tundish exit(GMOUT)
C       3. Mean residence time(TBARE)
C       4. Variance(VAR)
C       5. Normallised values of tracer concentration
C          and time(CONCN vs SECN)
C       RDATA is the input file and the other input values are :
C       ITMIN : value of minimum residence time in seconds
C       MAXDT : total data values recorded by data acquisition program
C       TUNVOL: tundish volume in litres
C       VOLFLT: volumeteric inlet flow rate in litres per minute
C       CONF  : conversion factor for millivolts to grams of tracer
C       RTD.DAT, NRTD.DAT and MB.OUT are output files.
        DIMENSION DTIN(6000),DAMV(1500),AMV(1500)
        DIMENSION SEC(800),VOLT(800),CONC(I)
        DIMENSION SECN(800),CONCN(800)
        OPEN (UNIT=6, FILE ='\BASIC\RDATA')
        OPEN (UNIT=7, FILE ='RTD.DAT')
        OPEN (UNIT=8, FILE ='NRTD.DAT')
        OPEN (UNIT=9, FILE ='MB.OUT')
        ITMIN=50
        MAXDT=4800
        TUNVOL=86.2
        VOLFLT=9.30
        CONF=0.0462
        DO 20 I=1,MAXDT
        READ(6,*)IS,DTIN(I)
20      CONTINUE
        K=1
        JMAX=(MAXDT/4)-3
        DO 40 J=1,JMAX
        I=4*J
        M=15*K
        N=M*4
        IF (N.GE.MAXDT) GO TO 25
        AVRV=(DTIN(N-3)+DTIN(N-2)+DTIN(N-1)+DTIN(N))/4.0
        AVRV=1010.0
25      IF (J.EQ.M) GO TO 30
        DAMV(J)=((DTIN(I-3)+DTIN(I-2)+DTIN(I-1)+DTIN(I))/4.0)-AVRV
        GO TO 40
30      DAMV(J)=((DTIN(I-5)+DTIN(I-4)+DTIN(I+1)+DTIN(I+2))/4.0)-AVRV
        K=K+1
40      CONTINUE
        AMVB=(DAMV(3)+DAMV(4)+DAMV(5))/3.0
        DO 50 I=1,JMAX
        AMV(I+3)=(DAMV(I)-AMVB)/100.0
50      CONTINUE
        DO 60 I=1,ITMIN
        AMV(I)=0.0
60      CONTINUE
        IMAX=MAXDT/8
        DO 70 I=1,IMAX
        J=2*I-1
        SEC(I) = J-1
        VOLT(I) = (AMV(J)+AMV(J+1))/2.0
        CONC(I) = VOLT(I)*CONF
        WRITE(7,80) SEC(I),CONC(I)
70      CONTINUE
80      FORMAT(I4,4X,F5.3)
        TBART=TUNVOL/VOLFLT
        TBARNM=0.0
        TBARDN=0.0
```

```
      VARNM=0.0
      DLT=2.0
      DO 90 I=1,IMAX
      GMT=CONC(I,*DLT
      TBARNM=TBARNM+SEC(I)*GMT
      TBARDN=TBARDN+GMT
      VARNM=VARNM+SEC(I)*SEC(I)*GMT
90    CONTINUE
      TBARE=TBARNM/(TBARDN*60.0)
      VAR=(VARNM/(TBARDN*60.0*60.0))-(TBARE*TBARE)
      GMOUT=TBARDN*VOLFLT/60.0
      WRITE(9,*) TBARE,VAR,GMOUT
      DO 100 I=1,IMP1
      SECN(I)=SEC(I)/(TBART*60.0)
      CONCN(I)=CONC(I)*TUNVOL/GMOUT
      WRITE(8,95) SECN(I),CONCN(I)
95    FORMAT(2X,F6.4,5X,F5.3)
100   CONTINUE
      STOP
      END
```

APPENDIX - 3

INTER-RELATIONSHIP BETWEEN RESIDENCE TIMES AND TUNDISH FLOW VOLUMES

In the tundish design a knowledge of the flow volumes in the tundish is sometimes necessary. Total volume of the fluid is given by

$$v = v_p + v_d + v_m = 1 - v_{sc} \qquad \text{A-1)}$$

In the tundish fluid flow system $t_{min} \neq t_{peak}$ hence it is suitable to define dispersed plug volume rather than v_p. Dividing Eq. A-1 by v we get

$$v_{dp} + v_d + v_m = 1 - v_{sc} \qquad \text{A-2)}$$

In the absence of short circuiting, v_{sc} in Eq. A-2 becomes zero. In the present study the short circuited volume v_{sc} is calculated to be 6-8% for the range of tundish widths, W, varying from 0.21L to 0.31L. Taking 7% as average we get

$$v_{dp} + v_d + v_m = 0.93 \qquad \text{A-3)}$$

$$\text{Now } v_{dp} = \frac{\left(t_{min} + t_{peak}\right)}{2\,\bar{t}} \qquad \text{A-4)}$$

$$\text{and } v_d = 1 - \frac{t_{mean}}{\bar{t}} \qquad \text{A-5)}$$

Substituting A-4 and A-5 into A-2 and in the absence of short circuiting we get,

$$v_m = 1 - \frac{\left(t_{min} + t_{peak}\right)}{2\,\bar{t}} - 1 + \frac{t_{mean}}{\bar{t}}\,, \qquad \text{A-6)}$$

which after simplification gives

$$v_m = \frac{1}{\bar{t}}\left(t_{mean} - \frac{t_{min} + t_{peak}}{2}\right) \qquad \text{A-7)}$$

Thus with the help of Eqs. A-4, A-5 and A-7 the flow volumes can be calculated easily from the residence time values.